5-2012

Forest Fragmentation Patterns in Maine Watersheds and Prediction of Visible Crown Diameter in Recent Undisturbed Forest

Brianne Elizabeth Looze

FOREST FRAGMENTATION PATTERNS IN MAINE WATERSHEDS AND PREDICTION OF VISIBLE CROWN DIAMETER IN RECENT UNDISTURBED FOREST

By

Brianne Elizabeth Looze

B.S. University of Wisconsin-Superior, 2009

A THESIS

Submitted in Partial Fulfillment of the

Requirements for the Degree of

Master of Science

(in Forest Resources)

The Graduate School

The University of Maine

May, 2012

Advisory Committee:

Steven A. Sader, Professor of Forest Resources, Advisor

Cynthia Loftin, Associate Professor of Wildlife Ecology and Unit Leader—Wildlife, Maine Cooperative Fish and Wildlife Research Unit

Jeremy Wilson, Associate Professor of Forest Management

THESIS ACCEPTANCE STATEMENT

On behalf of the Graduate Committee for Brianne Looze, I affirm that this manuscript is the final and accepted thesis. Signatures of all committee members are on file with the Graduate School at the University of Maine, 42 Stodder Hall, Orono, Maine.

Steven A. Sader, Professor of Forest Resources Date

LIBRARY RIGHTS STATEMENT

FOREST FRAGMENTATION PATTERNS IN MAINE WATERSHEDS

AND PREDICTION OF VISIBLE CROWN DIAMETER

IN RECENT UNDISTURBED FOREST

By Brianne E. Looze

Thesis Advisor: Dr. Steven A. Sader

An Abstract of the Thesis Presented
in Partial Fulfillment of the Requirements
for the Degree of Master of Science
(in Forest Resources)
May, 2012

Extensive harvesting practices coupled with major ownership change have led to increasing fragmentation of Maine's forest, a reduction from larger, contiguous mature forest patches into smaller patches. Using Landsat Thematic Mapper (TM) - based forest cover and change maps (1991-2007), fragmentation metrics, and Principal Components Analysis (PCA), this study determined the extent and configuration of forest fragmentation within three ecoregions and 186 level 5 watersheds throughout the state of Maine. Forests in the Northeastern ecoregion had higher harvest rates and more interspersed patches of undisturbed forest. Forests in the South-Central ecoregion are composed of more, smaller patches than their Northeastern and Western counterparts but had the highest proportion of undisturbed forest at the end of the study period. The cover type PCA indicated that softwood has been the most harvested cover type; mixedwood and hardwood were more prevalent in the residual forest stands. Softwood forests showed a marked decrease in size and area in unharvested forests of the Northeastern and

Western ecoregions. The Western ecoregion consisted of small patches of hardwood forest that were closer together, and hardwood forest represented a greater proportion of the landscape. Softwood forest patch shapes were more complex in the South-Central ecoregion. This research provides a numerical assessment of the spatially explicit effects of the 1991-2007 harvesting legacy on the landscape (watershed level) composition of Maine.

With Maine's northern forest being fragmented and patch size decreasing over time, maintaining a distribution of larger trees may be ecologically valuable. There are no spatially explicit maps for Maine showing the distribution of old growth or large diameter forest and ground data is lacking. Therefore, methods using multiple sources of remotely sensed data, topographic and site index data were combined in a modeling application to predict visible crown diameter (VCD) as a proxy for tree size in recent undisturbed forest (RUF), stands that were not harvested between 1972 and 2007. Change detection maps derived from Landsat TM imagery, raw Landsat TM imagery, two sources of aerial photography, and ancillary data were used as input into a random forests model. Results indicated differences in VCD ranges and importance of predictive variables between softwood, mixedwood, and hardwood forest cover. Recent undisturbed softwood and mixedwood VCD decreased with increasing site elevation and slope. Softwood VCD increased with increasing spectral values of Landsat TM 1, the Normalized Difference Moisture Index and Tasseled Cap wetness, suggesting sensitivity to moisture or shadowing in the canopy. Recent undisturbed hardwood forests were found on the best sites at low elevations. Hardwood VCD responded to spectral variables, especially

Tasseled Cap brightness, and the Landsat TM reflected infrared wavebands 4, 5, and 7. This research is repeatable in other regions, provided there is access to historical aerial photography and reliable map information or ground data that could verify the presence of undisturbed forest at earlier dates.

ACKNOWLEDGMENTS

Thanks must first go to my funding sources for making this opportunity possible. This research was funded by a New England Forestry Foundation Pingree Easement Monitoring Grant and a Northeastern States Research Cooperative Theme 3 Grant.

I also wish to express my gratitude to my advisor, Dr. Steve Sader, for planting the seed that became this project, always answering my questions, and providing ample resources for me to complete this research. I also thank my advisory committee members, Dr. Cyndy Loftin and Dr. Jeremy Wilson, for their insight and suggestions throughout my work on this research. I owe a lot to past and present MIAL members. This research would not have been possible without the previous work of Matt Noone and Kasey Legaard. Their data, and the answers to innumerable questions, created a solid foundation for this research to be completed. Thank you to Rei Hayashi for completing a preliminary study for Chapter 2 of this project. Tim Smith and Dave Sandilands, thanks for the good times in the lab. I enjoyed working with all of you.

To my Momma, Jacob, Kelli, Seth, Ainslie, Aubrie, and Heath: thank you for being the best motivators in the world. Everything I do is for you guys. You are all such amazing people, and I am so proud to call myself your daughter and your big sister. Finally, I have to thank this guy I know. Kevin, thank you for believing in me and constantly reassuring me that I can do this. You're the best.

TABLE OF CONTENTS

LIST OF TABLES

LIST OF FIGURES

LIST OF EQUATIONS

CHAPTER 1

CUMULATIVE FOREST FRAGMENTATION PATTERNS IN MAINE: 1991-2007

Introduction

Maine's northern forest has been intensely harvested since the mid-19th century. This removed most large pine and spruce trees from Maine's presettlement forest by the early 1900s (Irland 2000). Subsequent harvests and a devastating spruce budworm (*Choristoneura fumiferana*) outbreak led to understocked forests through the 1930s. By the 1950s, the forest began to enter merchantable size again, and large trees were removed for sawlogs. In the 1970s and 1980s, the northern forest was heavily harvested, often in large clearcuts, to salvage balsam fir (*Abies balsamea*) and red spruce (*Picea rubens*) in response to another extensive spruce budworm infestation (Seymour 1992). In the early 2000s, Maine's forest was composed of many low quality stands, with 40% poletimber and 30% sawtimber size trees statewide (McWilliams et al. 2005). Due to restrictions of the Maine Forest Practices Act of 1989 limiting the size and area of clearcuts, most harvesting in northern Maine is accomplished through partial harvesting methods; thus, the harvest area footprint has increased to maintain relatively stable harvest volume rates (Sader et al. 2003, McWilliams et al. 2005). Significant ownership change occurred in the northern forest beginning in the 1980s and continued through the early 2000s (Irland 2000, Maine Forest Service 1999, Laustsen et al. 2003, Hagan et al. 2005). Over the past decade, these new owners have been harvesting forestland at different rates; Timber Management Investment Organizations (TIMOs) harvest more than other industrial and non-industrial forest owners (Jin and Sader 2006, Noone 2010).

This extensive harvesting history has led to fragmentation of Maine's forest, a reduction from larger, contiguous mature forest patches into smaller, separated patches of younger age classes. Timber harvesting removes a larger amount of biomass from a forest than do most natural disturbances (Harris 1984). The effects of clearcutting and road building on forest fragmentation are well documented; these processes lead to smaller forest patch size, less core area per forest patch, and increased edge habitat (Franklin and Forman 1987, Ripple et al. 1991, Mladenoff et al. 1993, Tinker et al. 1998). Forest fragmentation can have significant effects on species diversity and wildlife habitat. Fragmentation and forest cover loss can lead to population decline of large, wide-ranging species as well as habitat specialists (Hunter 2002). Large forest patches and core areas protect some of the most vulnerable plant and animal species that cannot survive in smaller patches and fragmented forest landscapes. Forest edges are more vulnerable to fire and effects of predators on nests or habitats of interior-dwelling species (Brittingham and Temple 1983, Yahner 1988, Noss and Csuti 1997, Hunter 2002). Loss of connectivity between old growth or late successional forest can limit migration of species (Noss and Csuti 1997).

Several studies have examined the harvesting legacy in northern Maine, but the forests of southern Maine may provide additional information to be considered when studying harvesting effects on the Maine forest landscape. Many forests in southern

Maine have regenerated from abandoned agricultural land over the past several decades (Irland 2000). Forests in southern Maine are interspersed with other land use types, such as agriculture and urban areas; therefore, these forests occur in smaller patches than in the northern part of the state (McWilliams et al. 2005, SWOAM 2005). Like the northern forest, forests in southern Maine are primarily under private ownership, but they tend to be owned by families and other small non-industrial private forest (NIPF) landowners. For these reasons, forests in southern Maine may utilize a different management approach than their northern counterparts (SWOAM 2005).

Geospatial technology and methodologies, such as the integration of remote sensing and Geographic Information Systems (GIS), have been used to quantify changes in forest composition and configuration due to fragmentation (Ripple et al. 1991, Mladenoff et al. 1993, Tinker et al. 1998, Riitters et al. 2002, Wulder et al. 2009). These methods, however, have rarely been employed on a regional or statewide scale. Analysis of statewide spatio-temporal forest trends in Maine may be informative to understand driving forces influencing differences in harvest rates and forest composition observed in watersheds and ecoregions across the state. The availability of free, geo-referenced satellite data, specifically medium resolution imagery (30 m) from the Landsat Thematic Mapper (TM) archive (www.glovis.usgs.gov), makes statewide forest analyses feasible.

Determining the cumulative extent of forest fragmentation in Maine from 1991 to 2007 will provide a visual and numerical assessment of how recent harvesting has affected the composition and structure of forests at the landscape scale (e.g., watershed level). Existing change detection maps from 1991-2000 and 2000-2007 will be used to compile all cumulative harvest activity over the 16-year study period (Sader et al. 2006, Noone et al. 2012). The resulting harvesting extent map will be combined with an existing 2007 cover type map (Noone 2010) to examine the composition of the residual forest cover. Subsequent analysis using Fragstats 3.3 will provide numerical data through measurement of a selected group of fragmentation metrics (McGarigal et al. 2002). Fragstats has limited data capacity for large area analyses; therefore, breaking up the landscape into United States Department of Agriculture (USDA) Natural Resources Conservation Service (NRCS) Level 5 sub-watersheds (www.nrcs.usda.gov) will create an ecologically meaningful and computationally efficient scale for fragmentation analysis. Few studies have examined forest fragmentation for comparison across multiple watersheds (Tinker et al. 1998, Wulder et al. 2009). Broader scale analyses may be performed by the aggregation of watersheds, for example, at the ecoregion level.

Objectives

This research will use previously existing land cover data (Sader et al. 2005, Noone et al. 2012) with the intent to determine the cumulative extent, composition, and spatial configuration of forest fragmentation within watersheds and ecoregions of Maine from 1991 to 2007 following a period of partial harvesting and small, clustered clearcuts. Using fragmentation metrics and statistical analyses, this study will quantify differences in landscape fragmentation pattern between the industrial, corporate-owned northern forest and the more developed family-owned and municipal southern forest landscape of Maine. Variance in landscape change due to geographic location will be examined using a lake categorization map of Maine, derived from analysis of a number of biophysical variables to determine three major ecoregions in the state (Bacon and Bouchard 1997). The location of the Northeastern and South-Central ecoregions coincide roughly with the northern and southern forests of Maine; the Western ecoregion contains the Western Mountains. Quantifying differences in fragmentation metrics at this broader scale may aid in understanding driving forces in landscape pattern and changes in different regions of the state.

Methods

Study area

The scope of the research and scale of analysis covers the entire state of Maine. It is important to note the dichotomy in forest development of Maine, as the northern forest is owned by a variety of mostly corporate investors who manage the land for wood products or conservation purposes (Irland 1996, Hagan et al. 2005). This area includes the unorganized townships of Maine, encompassing Maine's red spruce and balsam fir resource with very little urban development. The southern forest primarily consists of family-owned woodlots and is managed on a more local, independent scale, and with more variable forest management and conservation strategies than in the north (SWOAM 2005). Due to the extent of urban development, along with the small private ownership pattern, the southern forest is broken into smaller parcels. The western area of Maine is very mountainous and contains areas with steep slopes and shallow soils (McWilliams et al. 2005). Both large and small NIPF landowners manage forestland in western Maine.

Initial data set compilation

This study began by processing 3 pre-existing statewide maps: a 1991-2000 forest change map (Sader et al. 2005), a 2000-2004-2007 forest change map, and a 2007 forest cover type map (Noone 2010, Noone et al. 2012). The 1991-2000 map includes two forested classes, undisturbed and harvested forest, and four nonforest classes: agriculture, water, wetlands, and urban. The 2000-2004-2007 forest change map depicts undisturbed and harvested forest in 2000, 2004, and 2007. The 2007 forest cover type map depicts Maine's undisturbed forest in 2007 as softwood (conifer), hardwood (deciduous broadleaf), and mixedwood (conifer and deciduous). Also, the 2007 forest cover type map includes a recently disturbed forest cover type, where the composition into the 3 cover type categories, mentioned above, is unknown. For more specific information on the development and accuracy of these maps, readers are referred to Sader et al. (2005), and Noone et al. (2012). All maps are derived from Landsat TM imagery; they are projected in the North American Datum (NAD) 1983 Universal Transverse Mercator (UTM) coordinate system, Zone 19N, at 30 m ground pixel resolution.

Preprocessing forest harvest maps

The 1991-2000 and the 2000-2004-2007 forest change maps were manipulated using ERDAS Imagine 9.3 (ERDAS 1999) to produce data suitable for fragmentation analysis. These maps have two thematic classes of interest: undisturbed forest and harvested forest. Baseline nonforest data for the three time-series maps were derived from the 1991-2000 change map. The undisturbed and harvested classes were extracted at the chosen dates, resulting in three maps showing the undisturbed and harvested forest cover in 1991, 2000, and 2007. A 3x3 majority filter was applied to remove isolated pixels. A clumping operation was applied to merge patches smaller than 2 ha into surrounding patches. Any patches of land cover smaller than 2 ha can be considered negligible for analysis on a statewide scale (Healey et al. 2008, Noone 2010). The baseline nonforest data extracted from the 1991-2000 change map were merged with the forest harvest maps. This nonforest data contains an aggregation of four classes: water, wetland, agriculture, and urban land cover, derived from the 1993 Maine Gap Analysis Program (MeGAP) map (Hepinstall et al. 1999). The final time-series maps consisted of six classes; two forested (undisturbed and harvested) and four nonforested (urban, agriculture, wetland, and water), each depicting the period of forest harvest (just prior to 1991, 1991-2000, 2000-2007).

Preprocessing forest cover type maps

The 2007 forest cover type map (Noone 2010, Noone et al. 2012) has four classes: softwood, mixedwood, hardwood, and disturbed. The disturbed forest cover type was removed from the cover type map and compared to the 2007 time series forest harvest map for agreement between harvested areas. All pixels from both maps that indicated harvesting were combined to create one common disturbed forest cover map for the year 2007 to ensure continuity between the two final 2007 maps. The nonforest pixels were merged with the forestland pixels, creating a complete statewide forest cover type map. A 3x3 majority filter and clumping operation were applied to smooth patches to a 2 ha minimum mapping unit. Finally, the forest harvest data from the 2007 time series map was overlaid to reveal the forest types distributed in the undisturbed forest. The final cover type map contained five classes: softwood, mixedwood, hardwood, harvested forest, and nonforest.

Preprocessing NRCS Level 5 watershed and ecoregion maps

A map of Level 5 watersheds was obtained from the Natural Resources Conservation Service (NRCS) website (www.nrcs.usda.gov). The four forest change/cover maps (1991 forest change, 2000 forest change, 2007 forest change, 2007 forest cover) were segmented into NRCS Level 5 watersheds. There are 186 Level 5 watersheds in Maine; these range in size from 18,068 to 347,559 acres. The watersheds were used as biophysical units for fragmentation analysis and for comparing results at a landscape scale. Each watershed was extracted from the statewide watershed map and combined with the four statewide forest change/cover maps to create 744 separate watershed maps (Figure 1.1a). A map prepared by the Maine Department of Environmental Protection (DEP) shows three ecoregions in the state: Northeastern, South-Central, and Western (Bacon and Bouchard 1997). These ecoregions were developed based on surficial geology of the state, separating coastal southern Maine from mountainous western Maine. The NRCS Level 5 watersheds were given a value corresponding to the ecoregion that contained the majority of the watershed (Figure 1.1b).

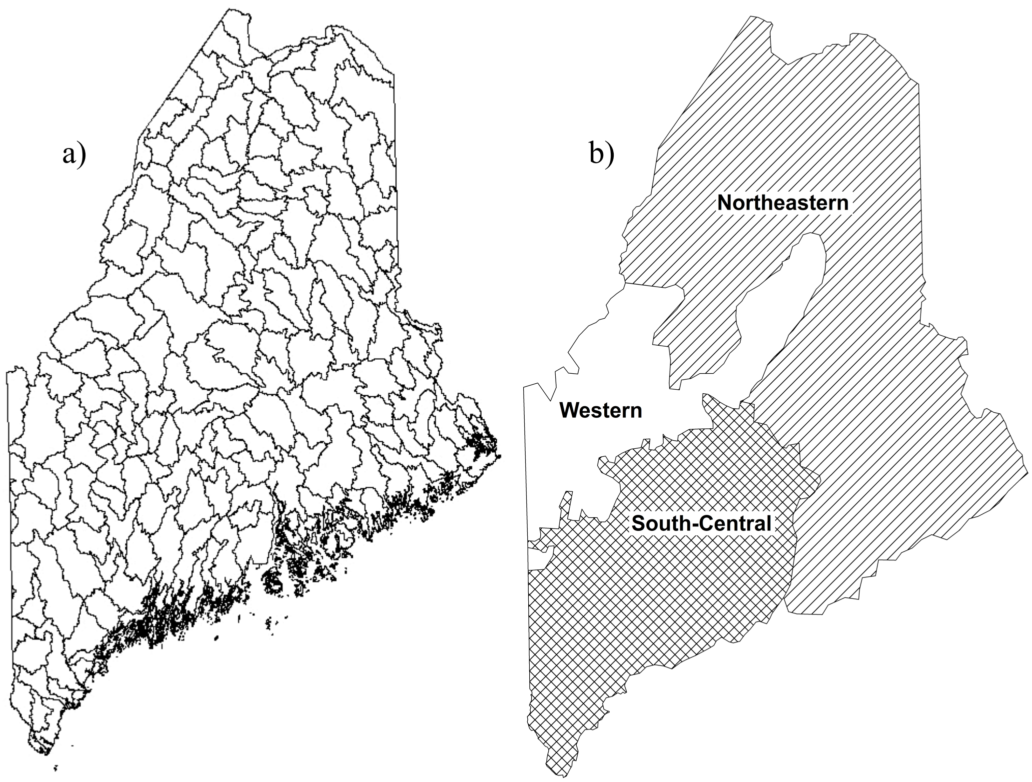

Figure 1.1: Study area. a) Natural Resource Conservation Service Level 5 watersheds and b) Maine Department of Environmental Protection Ecoregions

Preprocessing for fragmentation analysis

Fragstats 3.3 is a free software package used in landscape ecology to calculate fragmentation statistics, which allows analysis of landscape change over time (McGarigal et al. 2002). This computer program has specific requirements for the input datasets. One of these requirements is that the data are signed (values can be both positive and negative), non-zero rasters. To comply with these requirements, all watershed maps were converted from discrete, unsigned rasters. The signed, non-zero rasters were converted to ESRI GRID files using ArcGIS 9.3 (ESRI 1996-2012). ESRI GRID files have a smaller disk space requirement, which increased the efficiency of fragmentation analysis.

Fragmentation analysis

The output from Fragstats consists of data tables with calculated values for all selected metrics along with a patch ID image with a unique identifier for each patch within the image. Fragstats calculates three types of metrics: patch, class, and landscape. Patch metrics measure every patch in all classes within a landscape; their main value is in calculating higher-level metrics, and they have little interpretive value for the purposes of this study. Class metrics are measured for all cover types, or classes, in a landscape by integrating all of the patches of each cover type and presenting values for them. These are the most important metrics in this study, as Fragstats will quantify both the amount and spatial configuration of each class (or land cover type), indicating the extent and fragmentation of these classes over the landscape. Class metrics will determine the effects of harvesting on Maine's forest over the 16-year study period. Landscape metrics integrate all patches and cover types to quantify the overall landscape pattern; the interpretive value of these metrics becomes relevant in the case of unique patch or class metric trends. A selected group of metrics was chosen for calculation within Fragstats 3.3. Statistical analysis requires linear variables; therefore, metrics that are scale independent, relatively linear, and simply interpreted were utilized in this analysis (Neel et al. 2004, Cushman et al. 2008). Metrics that are standardized by area were used to account for varying watershed size (Tinker et al. 1998). Other metrics were chosen for exploratory purposes (Table 1.1). Definitions of all metrics can be found in Appendix A.

Table 1.1: Metrics used for Maine forest fragmentation analysis in Fragstats 3.3

Metric	Level of Analysis
Area*[#]	P, C, L
Core Area*[#]	P, C, L
Disjunct Core Area*[#]	P, C, L
Perimeter	P
Perimeter-Area ratio*[#]	P, C, L
Percentage of Landscape*[#]	C, L
Core Area Percentage of Landscape*[#]	C, L
Radius of Gyration*[#]	P, C, L
Patch Density*[#]	C, L
Edge Density*[#]	C, L
Euclidean Nearest Neighbor*	P, C, L
Landscape Shape Index*[#]	P, C, L
Largest Patch Index	P, C, L
Fractal Dimension Index*[#]	P, C, L
Core Area Index*[#]	P, C, L
Number of Core Areas*	P, C, L
Number of Disjunct Core Areas*	C, L
Clumpiness Index[#]	C, L
Landscape Division Index[#]	C, L
Splitting Index[#]	C, L
Effective Mesh Size[#]	C, L

*indicates that distribution metrics were calculated: mean, area-weighted mean, standard deviation, and coefficient of variation.
[#]indicates inclusion in Principal Components Analysis, class level metrics only.
P = patch, C = class, L = landscape

Some important metrics for this analysis are: Patch Density, Area Weighted Mean Patch Size, Mean Nearest Neighbor Distance, Edge Density, and Core Area. These metrics are relatively scale independent and will provide the most information on landscape response to harvesting (Tinker et al. 1998, Li et al. 2005, Wulder et al. 2009). Due to non-linear behavior, Mean Nearest Neighbor Distance was not used in additional statistical analysis; instead interspersion metrics were used. These metrics, including landscape division index, landscape splitting index, and effective mesh size, measure distance between patches and behave linearly, making them ideal for further statistical analysis (Cushman et al. 2008).

Within Fragstats 3.3, there are multiple components needed to prepare and run a fragmentation analysis. When the class/landscape metrics for edge density and core area are selected, the program asks the investigator to define edge parameters. Edge is the transition between two cover types. For the purpose of this study, a 90 m edge was used, as 90 m from a landscape boundary is a distance suitable for edge effects to take place (Hughes and Bechtel 1997). The other edge parameter chosen by the investigator is background boundary analysis. When a landscape boundary is along the background of the input file in Fragstats, that boundary can be completely counted as edge, proportionally counted as edge, or not counted as edge at all. To prevent overestimation of edge effects, background boundary was not counted as edge (Erin Simons, 2010, personal communication). A text file detailing the class properties of the input file is also required to run a fragmentation analysis. This file consists of an ID number for each class, a description of the cover type, and two true/false values: one to determine if a class is the background, the other to determine if a class should be included in the output of the analysis. The four nonforest classes of the forest harvest time-series maps were eliminated to increase computational efficiency and reduce the amount of data, as this information is not relevant for further statistical analysis to meet the objectives of this study. The nonforest class was included in the cover type analysis since it serves as a valid land cover type.

For efficiency in running the fragmentation analysis, four batch processing files were created, one for each statewide map. Each batch processing file contained information on all 186 NRCS Level 5 watersheds to be analyzed. The chosen metrics were selected for each level of classification. The output from Fragstats 3.3 consists of text files that can be imported into Microsoft Excel for further analysis. All output was converted to Excel comma-delimited files to facilitate reading the data into statistical software.

Statistical analysis

Fragstats is an exploratory tool; therefore further statistical analyses must be done for hypothesis testing. A one-way analysis of variance (ANOVA) was used to determine if the percentage of forest harvested during the study period differed significantly between the three ecoregions. The fragmentation metric used for this analysis was Percentage of Landscape of harvested forest in 2007. This metric was log transformed to meet the normality and constant variance assumptions of ANOVA. Principal Components Analysis (PCA) is a multivariate statistical method that groups correlated variables into components to reduce redundancy. Fragstats metrics are often correlated, and PCA has been shown to be an effective method in removing the correlation while still maintaining the integrity of the original data (Tinker et al. 1998). Meeting the normality assumption of PCA is difficult with Fragstats data, but Neel et al. (2004) have produced a list of metrics that are relatively linear and therefore considered more suitable for this type of analysis. Metrics used in the PCAs are listed in Table 1.1. The harvested forest PCA used the same metrics, but did not include Landscape Division Index or the Clumpiness Index. These metrics measure the effects of the reduction of a land cover type and therefore were counterintuitive to the harvested forest cover type. Data were read into the statistical software R v.13.1 (www.cran.r-project.org), which has powerful utilities for PCA. Loadings from these analyses were examined and interpreted for each of the four maps in this study. Although leniency on meeting the assumption of normality exists for fragmentation data, the data were transformed to be as close to normal as possible. Most transformations reduced the spread of the data, with the logarithmic transformation occurring most often. Square root transformations were also used, and occasionally data were expanded by taking them to some exponential power. When the data had achieved its maximum normality, PCA was run using commands from a number of R libraries. Once the PCA was run, the eigenvalues were displayed and the number of PCs for further analysis was chosen by examining scree plots and the broken stick value for all eigenvalues. When the number of PCs was determined for each analysis, they were interpreted by obtaining the structure correlations and communality values for each metric at each PC. Finally, a series of ordinations were created to visually interpret the PCs and determine the fragmentation patterns of the watersheds throughout the state.

Results

All analyses have simple structure, meaning that most of the variation is explained on the first two principal components (PCs). Ordinations of these analyses were grouped by Maine DEP Ecoregion (Figure 1.1b, Bacon and Bouchard 1997) to display landscape patterns within watersheds for each ecoregion (Figs. 1.2-1.7, 1.9-1.11). The first PC consistently represents area and dispersion metrics. Area metrics have an inverse relationship with the first PC. Negative scores on the first PC axis indicate watersheds that consist of large patches that are closer together on the landscape; positive scores indicate watersheds that consist of small patches that are spread out over the landscape. Northeastern forest watersheds tend to be positioned on the negative side of the PC 1 axis, whereas South-Central forest watersheds tend to be located on the positive side of the PC 1 axis. The second PC explains more variance due to similar metrics. Communality values represent the percentage of a variable's variance that is explained by the retained PCs. These were interpreted to ensure that all metrics were sufficiently represented in each analysis. All results presented focus on the first two PCs, as they explained much of the variance in each analysis.

Undisturbed forest, 1991-2007

The three PCAs of undisturbed forest cover shared many characteristics. Three PCs were chosen for each analysis; the first PC was always strongly correlated with area, core area, interspersion metrics, and patch density. The second PC was most often correlated with percentage of landscape. For all undisturbed forest cover PCAs, a watershed with a low negative score on the first PC will consist of large patches that are near each other across the landscape. A watershed with a high positive score on the first PC will have a large number of small patches that are more dispersed over the landscape. The first PC explains the vast majority of the variance in these analyses; therefore all interpretation focuses heavily on this one axis. The 2007 undisturbed forest cover PCA further indicated that a watershed with a low negative score on the first PC will consist of complexly shaped patches, and a watershed with a high score on the first PC will consist of patches that are more uniform in shape and size. Communality values showed that all metrics were strongly represented in all three analyses (Tables 1.2, 1.3, and 1.4).

Table 1.2: Structure correlations and communality values, 1991 undisturbed forest

	PC1	PC2	PC3	Communality
PLAND	-0.547	0.7	-0.129	0.805
PD	0.797	-0.429	0.008	0.820
ED	0.748	-0.121	0.55	0.877
LPI	-0.694	0.511	0.142	0.763
AREA_AM	-0.843	-0.305	0.404	0.966
AREA_SD	-0.935	0.086	0.263	0.950
GYRATE_AM	-0.753	-0.321	0.459	0.880
GYRATE_SD	-0.743	0.443	0.087	0.756
FRAC_SD	0.629	0.454	0.333	0.713
FRAC_CV	0.612	0.459	0.348	0.706
PARA_SD	0.336	0.528	0.43	0.577
CORE_AM	-0.889	-0.271	0.302	0.956
CORE_SD	-0.957	0.102	0.142	0.946
CORE_CV	-0.194	-0.827	0.35	0.843
CAI_SD	0.15	0.586	-0.567	0.688
CLUMPY	-0.281	-0.66	-0.274	0.590
DIVISION	0.716	-0.539	-0.112	0.816
MESH	-0.876	-0.175	0.328	0.906
SPLIT	0.708	-0.425	-0.19	0.718

Table 1.3: Structure correlations and communality values, 2000 undisturbed forest

	PC1	PC2	PC3	Communality
PLAND	-0.627	-0.669	-0.09	0.849
PD	0.839	0.401	0.045	0.866
ED	0.733	0.23	-0.559	0.904
LPI	-0.794	-0.341	-0.174	0.777
AREA_AM	-0.872	0.323	-0.308	0.960
AREA_SD	-0.953	0.008	-0.224	0.959
GYRATE_AM	-0.803	0.312	-0.388	0.892
GYRATE_SD	-0.752	-0.413	-0.165	0.763
FRAC_SD	0.75	-0.374	-0.218	0.750
FRAC_CV	0.733	-0.394	-0.232	0.747
PARA_SD	0.321	-0.473	-0.458	0.536
CORE_AM	-0.918	0.258	-0.198	0.948
CORE_SD	-0.971	-0.052	-0.085	0.953
CORE_CV	-0.399	0.779	-0.27	0.838
CAI_SD	0.29	-0.523	0.484	0.591
CLUMPY	-0.443	0.443	0.552	0.698
DIVISION	0.812	0.389	0.159	0.836
MESH	-0.906	0.165	-0.252	0.911
SPLIT	0.832	0.332	0.197	0.841

Table 1.4: Structure correlations and communality values, 2007 undisturbed forest

	PC1	PC2	PC3	Communality
PLAND	-0.557	-0.57	-0.445	0.833
PD	0.802	0.128	0.396	0.816
ED	0.606	-0.569	0.461	0.903
LPI	-0.837	-0.341	-0.087	0.824
AREA_AM	-0.902	-0.138	0.353	0.957
AREA_SD	-0.963	-0.185	0.077	0.967
GYRATE_AM	-0.888	-0.183	0.303	0.913
GYRATE_SD	-0.733	-0.299	-0.365	0.760
FRAC_SD	0.648	-0.368	-0.191	0.592
FRAC_CV	0.621	-0.445	-0.183	0.617
PARA_SD	0.179	-0.732	-0.141	0.587
CORE_AM	-0.943	-0.052	0.244	0.952
CORE_SD	-0.981	-0.058	-0.046	0.968
CORE_CV	-0.558	0.089	0.708	0.820
CAI_SD	0.241	0.123	-0.799	0.711
CLUMPY	-0.515	0.735	-0.08	0.811
DIVISION	0.843	0.383	0.112	0.871
MESH	-0.924	-0.19	0.274	0.965
SPLIT	0.829	0.411	0.137	0.874

The ordinations for these analyses visually support what the scores indicate and display landscape patterns of the three ecoregions. Watersheds with high positive values along the first PC axis have smaller and more separated patches of undisturbed forest. The 2007 PCA also indicates that these watersheds have a greater proportion of undisturbed forest over the landscape. Watersheds with low values along the first PC axis contain patches of undisturbed forest that are larger and closer together, and in 2007, these patches are complexly shaped (Figs. 1.2, 1.3, and 1.4). The ordinations demonstrate how the unharvested forest landscape changed over the course of the study period. In 1991, watersheds in the Western ecoregion consist of large patches of undisturbed forest that are closer together on the landscape. The South-Central ecoregion consists of small, interspersed patches of undisturbed forest. There does not appear to be a trend in patch characteristics within the Northeastern ecoregion (Figure 1.2). In 2000, these trends remain the same. By 2007, a noticeable shift occurs in the ordination (Figure 1.3). In 2007, the dichotomy between the Western and South-Central ecoregions becomes more extreme, as there is almost no overlap between watersheds within these areas. Northeastern watersheds show a shift to the left, indicating that undisturbed forest in this ecoregion occurs in smaller, more interspersed patches after 16 years of harvesting. The entire cluster of watersheds has rotated slightly to the right in the 2007 ordination, which can be attributed to one metric, the clumpiness index (CLUMPY). The strength of this metric on the second PC axis increased dramatically between 2000 and 2007 (Tables 1.3 and 1.4). This means that patches of undisturbed forest in the Western and heavily harvested Northeastern ecoregions tend to be clumped together (Figure 1.4).

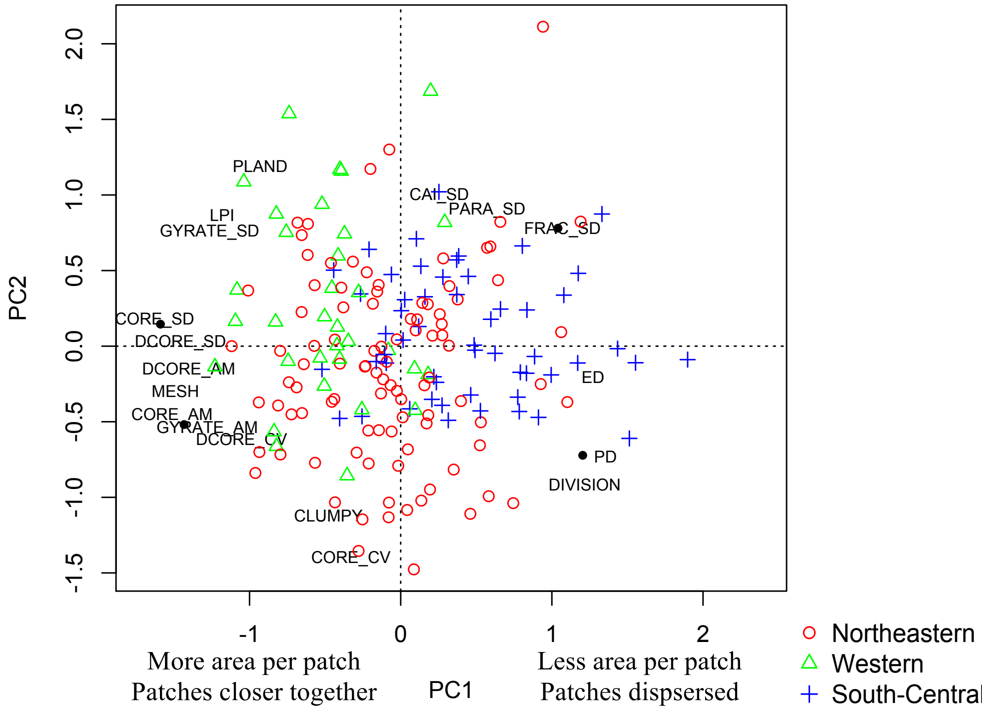

Figure 1.2: PCA ordination, 1991 undisturbed forest for watersheds in 3 ecoregions

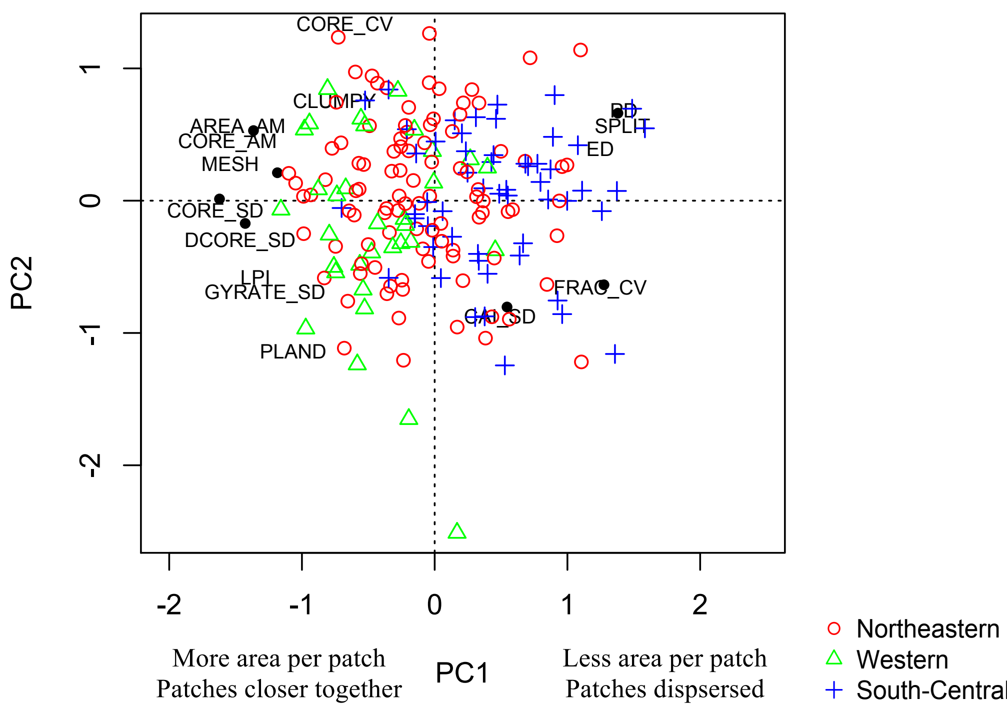

Figure 1.3: PCA ordination, 2000 undisturbed forest for watersheds in 3 ecoregions

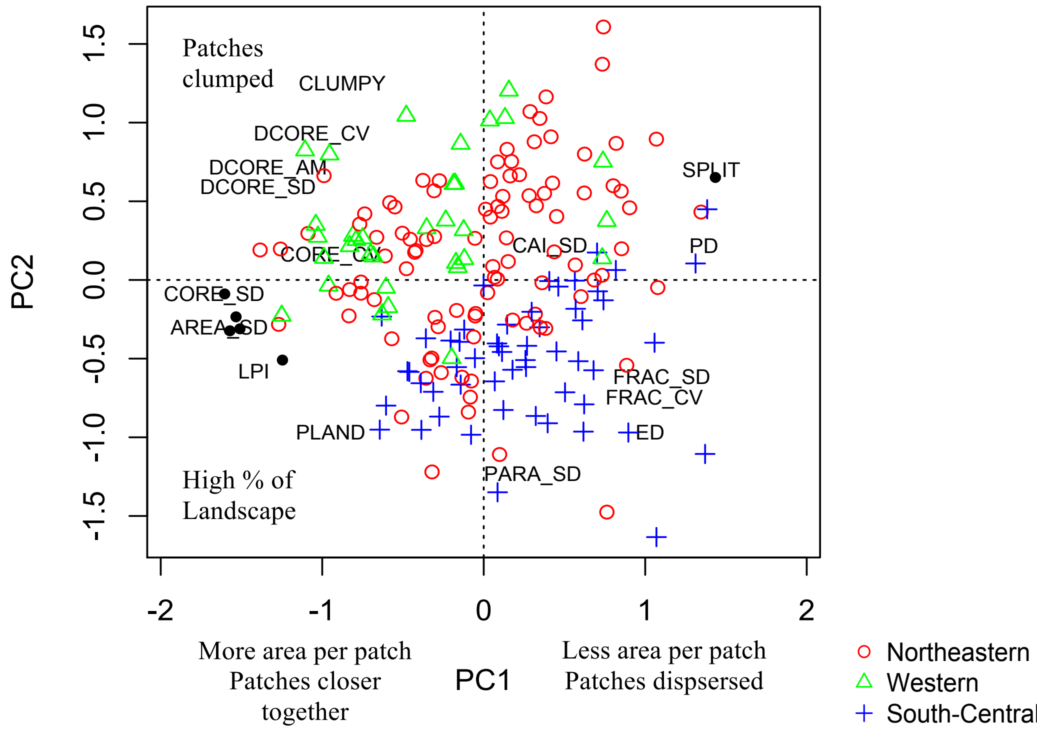

Figure 1.4: PCA ordination, 2007 undisturbed forest for watersheds in 3 ecoregions

Harvested forest, 1991-2007

Three principal components (PCs) were chosen for each of the three PCAs. The first PC was most often strongly correlated with area, core area, radius of gyration, interspersion metrics, patch density, fractal dimension index, and percent of landscape. The second PC was most often strongly correlated with core area. A watershed with a low score on the first PC will consist of large patches that are near each other and more uniform in shape and size across the landscape. These watersheds will also have a greater amount of total harvested forest area. A watershed with a high score on the first PC will have a large number of small, complexly shaped patches that are more dispersed over the landscape. Communality values indicate that all metrics were strongly represented in all of the PCAs (Tables 1.5, 1.6, and 1.7).

Table 1.5: Structure correlations and communality values, 1991 harvested forest

	PC1	PC2	PC3	Communality
PLAND	-0.956	0.027	0.248	0.976
PD	-0.583	-0.348	0.528	0.740
ED	-0.898	-0.077	0.36	0.942
LPI	-0.889	0.127	0.223	0.857
AREA_AM	-0.956	0.057	-0.018	0.918
AREA_SD	-0.975	0.083	-0.036	0.958
GYRATE_AM	-0.955	0.095	0.007	0.920
GYRATE_SD	-0.969	0.141	-0.025	0.959
FRAC_SD	-0.843	0.2	0.041	0.753
FRAC_CV	-0.843	0.2	0.033	0.751
PARA_SD	-0.374	0.501	-0.427	0.572
CORE_AM	-0.966	-0.105	-0.157	0.968
CORE_SD	-0.951	-0.125	-0.189	0.956
CORE_CV	-0.411	-0.812	-0.161	0.854
CAI_SD	-0.837	0.336	-0.122	0.828
MESH	-0.984	0.046	0.093	0.980
SPLIT	0.926	-0.145	-0.241	0.937

Table 1.6: Structure correlations and communality values, 2000 harvested forest

	PC1	PC2	PC3	Communality
PLAND	-0.863	-0.36	0.252	0.938
PD	0.758	-0.217	0.575	0.953
ED	-0.398	-0.576	0.643	0.905
LPI	-0.877	-0.082	0.052	0.778
AREA_AM	-0.981	0.132	0	0.981
AREA_SD	-0.991	0.068	-0.047	0.989
GYRATE_AM	-0.984	0.078	-0.023	0.975
GYRATE_SD	-0.977	-0.068	-0.128	0.976
FRAC_SD	-0.804	-0.459	0.02	0.857
FRAC_CV	-0.811	-0.45	0.01	0.860
PARA_SD	-0.25	-0.604	-0.17	0.457
CORE_AM	-0.972	0.187	-0.014	0.981
CORE_SD	-0.978	0.151	-0.042	0.981
CORE_CV	-0.275	0.624	0.584	0.807
CAI_SD	-0.826	-0.077	-0.385	0.836
MESH	-0.991	0.02	0.06	0.986
SPLIT	0.899	0.189	-0.046	0.847

Table 1.7: Structure correlations and communality values, 2007 harvested forest

	PC1	PC2	PC3	Communality
PLAND	-0.933	-0.264	0.096	0.949
PD	0.867	-0.222	-0.336	0.913
ED	-0.409	-0.701	-0.131	0.676
LPI	-0.923	-0.029	0.045	0.855
AREA_AM	-0.987	0.074	-0.051	0.982
AREA_SD	-0.994	0.045	0.033	0.990
GYRATE_AM	-0.986	0.055	0.004	0.976
GYRATE_SD	-0.97	-0.044	0.203	0.984
FRAC_SD	-0.498	-0.813	-0.012	0.908
FRAC_CV	-0.502	-0.816	-0.045	0.920
PARA_SD	0.1	-0.573	-0.485	0.573
CORE_AM	-0.986	0.096	-0.064	0.986
CORE_SD	-0.99	0.095	-0.003	0.990
CORE_CV	-0.482	0.337	-0.735	0.886
CAI_SD	-0.767	0.035	0.484	0.824
MESH	-0.993	0.01	-0.024	0.987
SPLIT	0.938	0.068	-0.092	0.894

The ordinations for these analyses visually support what the scores indicate and display landscape patterns of the three ecoregions (Figs. 1.5, 1.6, and 1.7). The ordinations consistently show that watersheds with high positive values along the first PC axis have smaller and more separated patches of harvested forest. Watersheds with low negative values along the first PC axis consist of patches of harvested forest that are larger and closer together. In 1991, watersheds in the South-Central (blue crosses) ecoregion are located on the positive end of the first PC axis, meaning that patches of harvested forest are small and highly interspersed. South-Central watersheds are also located on the negative end of the second PC axis, indicating that patch size is widely variable. Watersheds in the Western (green triangles) ecoregion are located toward the negative end of the first PC axis, therefore they consist of patches of harvested forest that are larger and closer together. Western watersheds are located on the positive end of the second PC axis, indicating that patch size is more uniform than in the South-Central ecoregion. Most watersheds in the Northeastern (red circles) ecoregion follow the pattern of the Western ecoregion (Figure 1.5). In 2000, the landscape patterns remain the same, but the second PC axis loses its effect on variability of patch size (Figure 1.6). In 2007, the landscape patterns within the South-Central and Western ecoregion are consistent with those in 2000. Watersheds in the Northeastern ecoregion have shifted farther along the negative end of the first PC axis, indicating that patches of harvested forest have become larger and closer together (Figure 1.7).

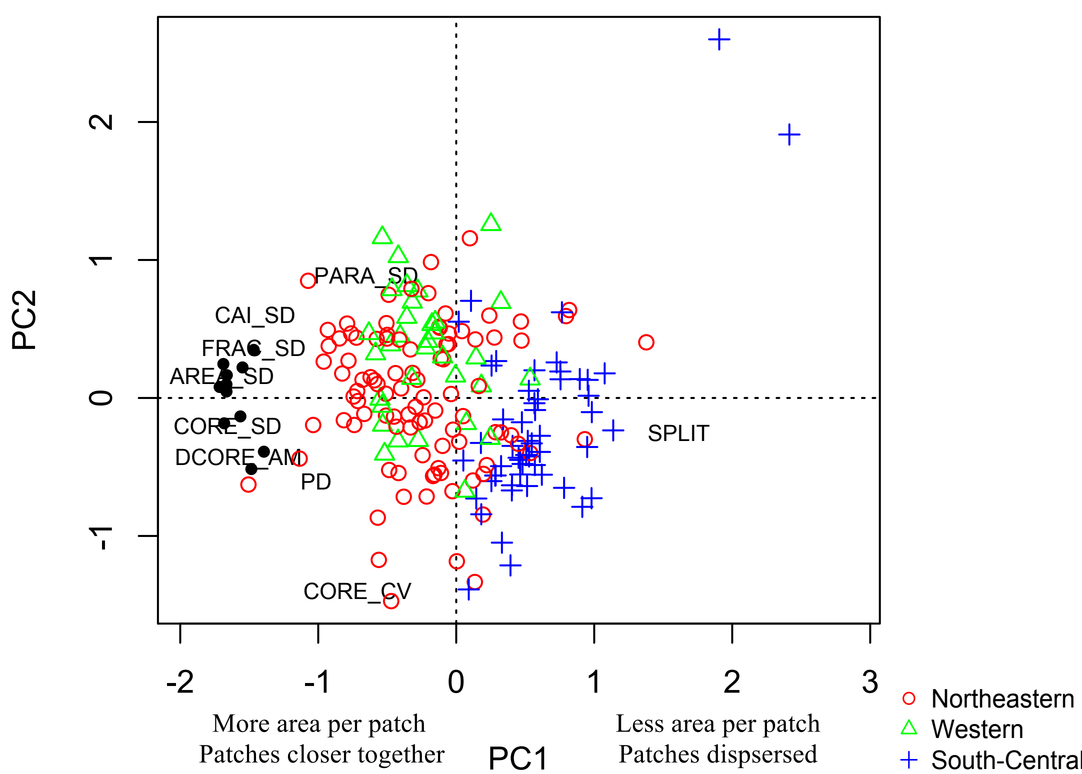

Figure 1.5: PCA ordination, 1991 harvested forest for watersheds in 3 ecoregions

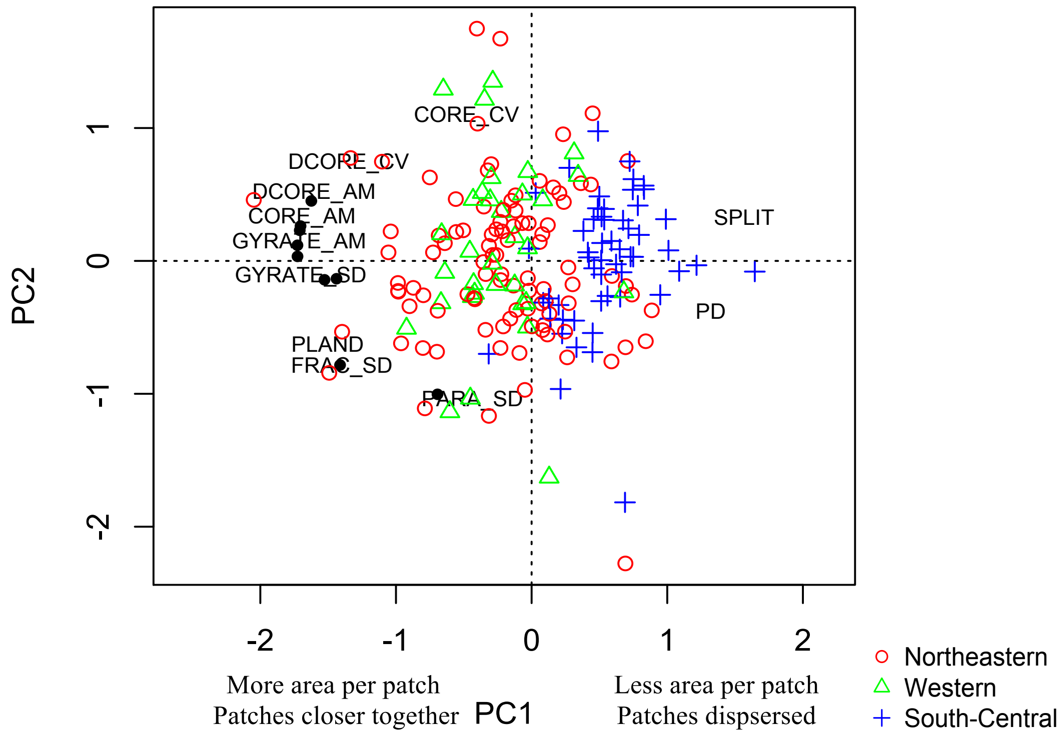

Figure 1.6: PCA ordination, 2000 harvested forest for watersheds in 3 ecoregions

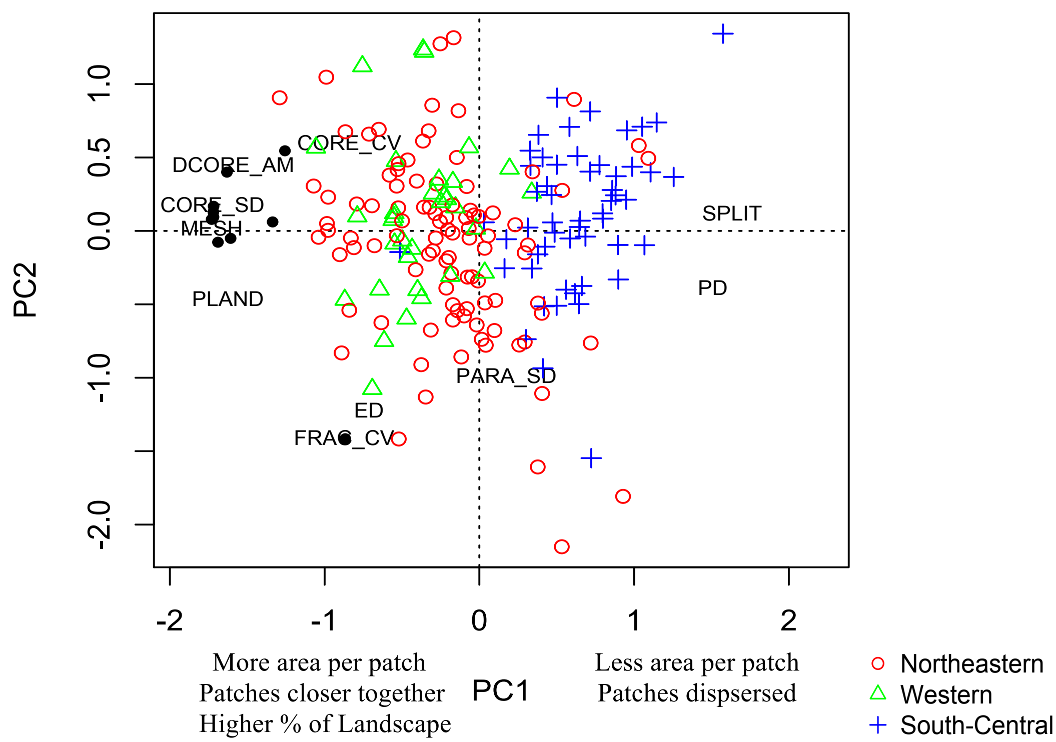

Figure 1.7: PCA ordination, 2007 harvested forest for watersheds in 3 ecoregions

Additionally, analysis of variance results indicate that there was a significant difference in the amount of forest harvested (PLAND of harvested forest; see Appendix A) between the Northeastern and the South-Central ecoregions ($p<0.001$). There was no significant difference in amount of forestland harvested between the Northeastern and the Western ecoregions (Figure 1.1b) ($p=0.456$).

A map depicting the percentage of forest harvested within each of the NRCS Level 5 watersheds provides a visual reference to the trend across the state of Maine (Figure 1.8). An analysis of ownership on 19 NRCS Level 5 watersheds that had more than 42% of forest harvested between 1991 and 2007 shows that most of these heavily harvested watersheds consist of land owned by TIMOs and Real Estate Investment Trusts (REITs) (Figure 1.9, Table 1.8).

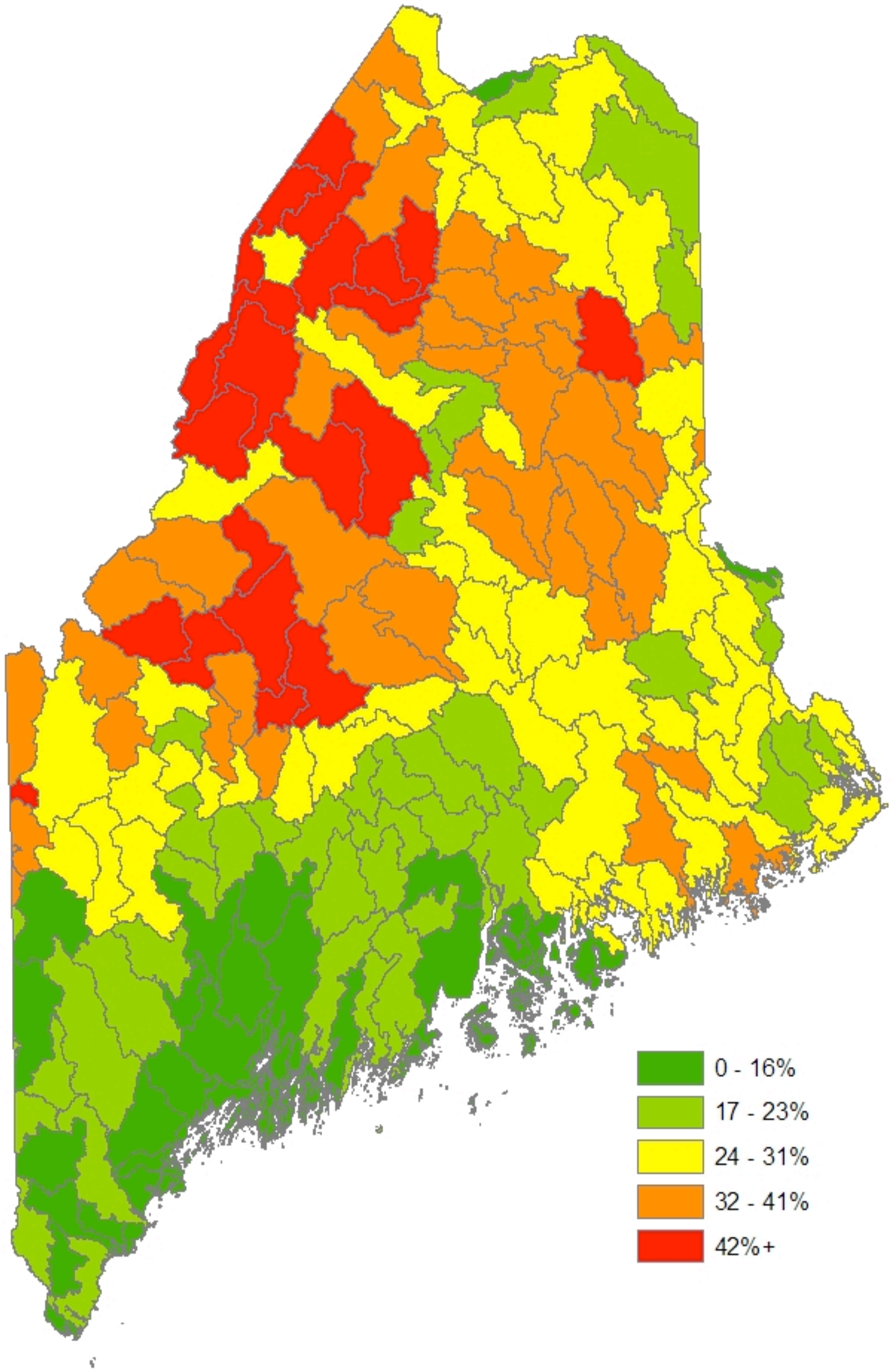

Figure 1.8: Percentage of forestland harvested by NRCS Level 5 watershed, 1991-2007.

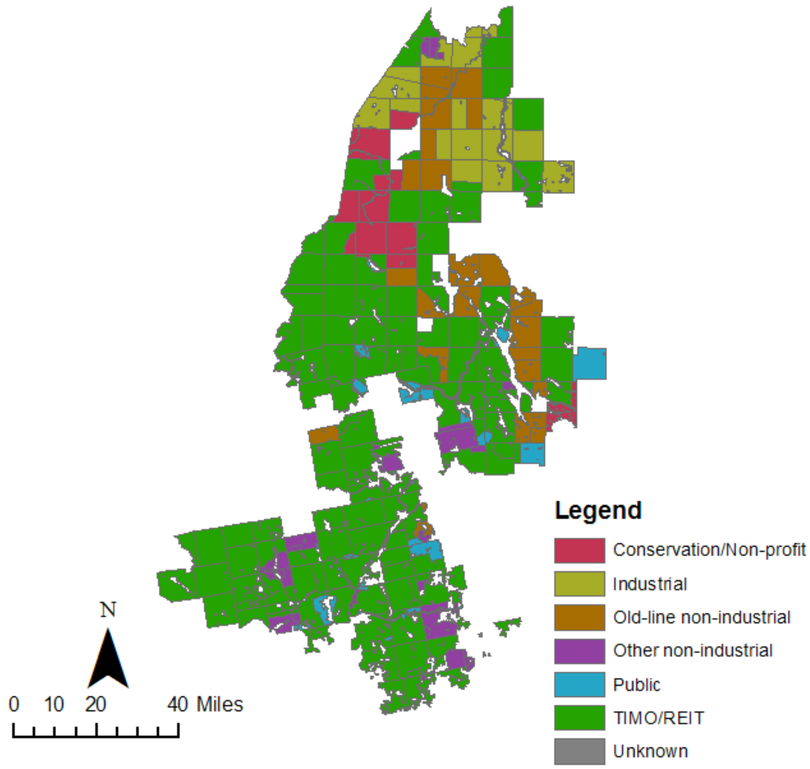

Figure 1.9: Ownership classes for 19 heavily harvested NRCS Level 5 watersheds

Table 1.8: Acreage of 19 heavily harvested NRCS Level 5 watersheds by ownership classes

Class	Total acreage	Percent of total
TIMO/REIT	1911802.3	64.8%
Industrial	281488.4	9.5%
Old-line non-industrial	332452.4	17.3%
Other non-industrial	126509.7	4.3%
Conservation/Non-profit	174498.5	5.9%
Public	118957.5	4.0%
Unknown	1482.2	0.05%
Total	2946515	100%

Cover type analysis, 2007

As with previous PCA results, three principal components (PCs) were chosen for each cover type analysis. All three PCAs had strong correlations with area, core area, radius of gyration, and interspersion metrics on the first PC. Additionally, the first PC of the hardwood forest cover analysis (Table 1.9) was strongly correlated with fractal dimension index, percent of landscape, and edge density. The first PC of the mixedwood forest cover analysis (Table 1.10) was strongly correlated with percent of landscape, clumpiness index, and edge density, and the first PC of the softwood forest cover analysis (Table 1.11) was strongly correlated with largest patch index, patch density, and the clumpiness index. The second PC was strongly correlated with different metrics for each analysis. For hardwood forest cover, the second PC was correlated with core area. For mixedwood forest cover, the second PC was correlated with patch density. For softwood forest cover, the second PC was correlated with fractal dimension index and edge density.

The relationships with various metrics should be acknowledged, but the overall trend of each cover type remains the same. A watershed with a low score on the first PC will consist of large patches of each cover type that are near each other across the landscape. A watershed with a high positive score on the first PC axis will have a large number of small patches of each cover type that are more dispersed over the landscape. Additionally, a watershed with a high positive score on the second PC axis will have patches of softwood forest that are more uniform in shape and size. Communality values showed that all metrics were strongly represented in all three analyses (Tables 1.9, 1.10, and 1.11).

Table 1.9: Structure correlations and communality values, 2007 hardwood cover type

	PC1	PC2	PC3	Communality
PLAND	-0.914	0.021	-0.321	0.939
PD	-0.411	-0.01	-0.849	0.889
ED	-0.798	0.033	-0.571	0.963
LPI	-0.91	0.064	-0.119	0.847
AREA_AM	-0.974	-0.023	0.158	0.974
AREA_SD	-0.976	-0.025	0.179	0.984
GYRATE_AM	-0.973	-0.05	0.14	0.970
GYRATE_SD	-0.931	-0.092	0.158	0.901
FRAC_SD	-0.673	-0.625	-0.19	0.879
FRAC_CV	-0.664	-0.643	-0.182	0.888
PARA_SD	-0.47	-0.664	0.15	0.684
CORE_AM	-0.953	0.23	0.122	0.976
CORE_SD	-0.941	0.281	0.13	0.981
CORE_CV	-0.522	-0.405	0.139	0.456
CAI_SD	-0.342	0.813	-0.119	0.791
CLUMPY	-0.756	-0.039	0.529	0.854
DIVISION	0.489	-0.18	0.166	0.300
MESH	-0.989	-0.024	-0.034	0.979
SPLIT	0.934	-0.008	0.176	0.903

Table 1.10: Structure correlations and communality values, 2007 mixedwood cover type

	PC1	PC2	PC3	Communality
PLAND	-0.905	-0.219	0.251	0.931
PD	-0.25	-0.799	0.184	0.734
ED	-0.747	-0.503	0.305	0.904
LPI	-0.927	-0.008	0.128	0.876
AREA_AM	-0.98	0.11	-0.093	0.981
AREA_SD	-0.981	0.131	-0.022	0.979
GYRATE_AM	-0.975	0.095	-0.085	0.967
GYRATE_SD	-0.943	0.089	0.025	0.897
FRAC_SD	-0.678	-0.638	-0.013	0.868
FRAC_CV	-0.677	-0.641	-0.022	0.870
PARA_SD	-0.641	-0.528	0.01	0.690
CORE_AM	-0.933	0.307	0.031	0.964
CORE_SD	-0.901	0.383	0.128	0.974
CORE_CV	-0.732	-0.176	-0.579	0.902
CAI_SD	0.359	0.585	0.63	0.867
CLUMPY	-0.796	0.444	-0.094	0.840
DIVISION	0.527	-0.083	-0.483	0.518
MESH	-0.991	0.004	0.019	0.982
SPLIT	0.943	0.062	-0.188	0.928

Table 1.11: Structure correlations and communality values, 2007 softwood cover type

	PC1	PC2	PC3	Communality
PLAND	-0.881	-0.234	0.054	0.835
PD	0.728	-0.224	0.388	0.730
ED	-0.471	-0.685	0.208	0.735
LPI	-0.85	0.184	0.109	0.768
AREA_AM	-0.947	0.178	0.226	0.979
AREA_SD	-0.976	0.114	0.124	0.980
GYRATE_AM	-0.947	0.142	0.23	0.969
GYRATE_SD	-0.941	-0.071	0.025	0.892
FRAC_SD	-0.365	-0.829	0.217	0.867
FRAC_CV	-0.387	-0.818	0.244	0.879
PARA_SD	0.545	-0.512	0.114	0.573
CORE_AM	-0.984	0.057	-0.046	0.973
CORE_SD	-0.973	-0.02	-0.19	0.984
CORE_CV	-0.335	0.439	0.713	0.814
CAI_SD	-0.526	-0.4	-0.715	0.948
CLUMPY	-0.715	0.474	-0.231	0.790
DIVISION	0.452	-0.416	-0.122	0.392
MESH	-0.967	0.08	0.209	0.985
SPLIT	0.884	-0.1	-0.064	0.796

The ordinations for these analyses visually support what the scores indicate and display landscape patterns of the three ecoregions (Figures 1.10, 1.11, and 1.12). The hardwood forest cover ordination (Figure 1.10) shows that watersheds with high positive values along the first PC axis have smaller and more separated patches of hardwood forest. Watersheds here tend to be in the Northeastern ecoregion (red circles). Watersheds with low negative values along the first PC axis consist of larger patches of hardwood forest and have a greater proportion of hardwood forest over the landscape. Watersheds that are positioned on the negative end of the first PC axis are located in the Western ecoregion (green triangles). Watersheds with high positive values along the second PC axis consist of widely variable patch sizes with simple edge shapes. These tend to be located in the South-Central ecoregion (blue crosses) (Figure 1.10).

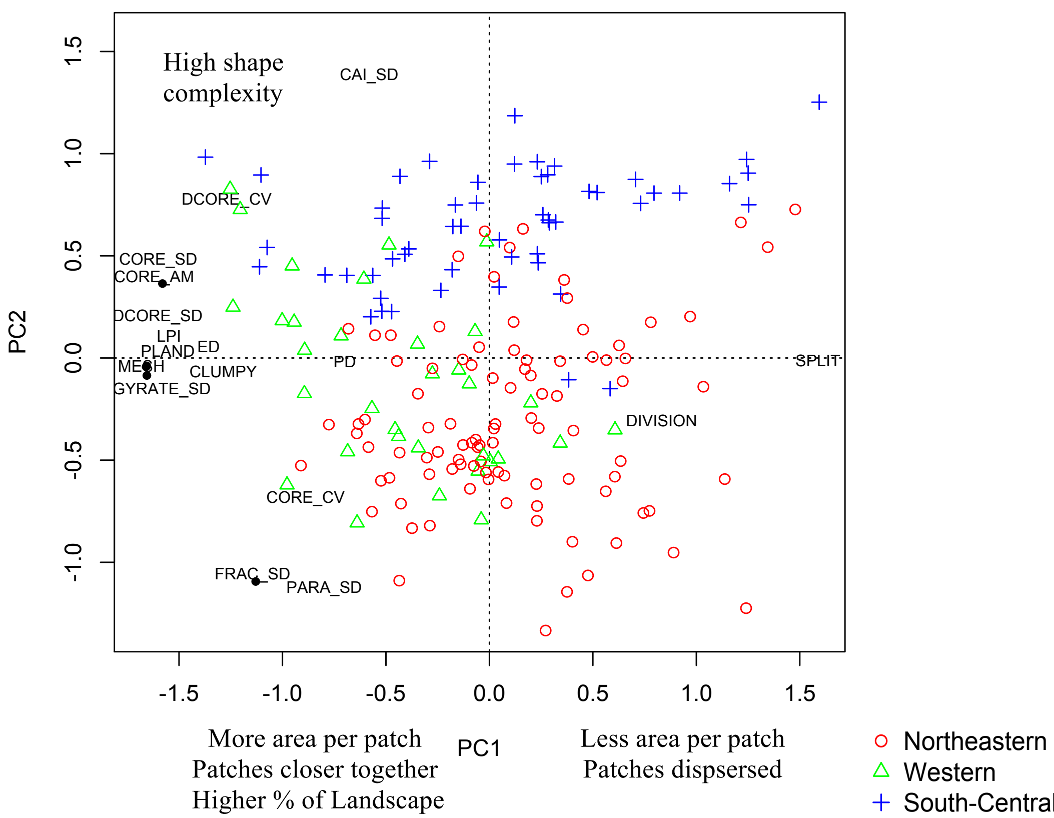

Figure 1.10: PCA ordination, 2007 hardwood forest for watersheds in 3 ecoregions

The mixedwood forest cover ordination (Figure 1.11) shows that watersheds with high values along the first PC axis have smaller and more separated patches of mixedwood forest. Watersheds represented here tend to be in the South-Central ecoregion (blue crosses). Watersheds with low values along the first PC axis consist of larger patches of mixedwood forest that are closer together. Watersheds that are positioned on the negative end of the first PC axis are located in the Northeastern (red circles) and Western (green triangles) ecoregions. Patch density loaded strongly on the second PC axis (Figure 1.11).

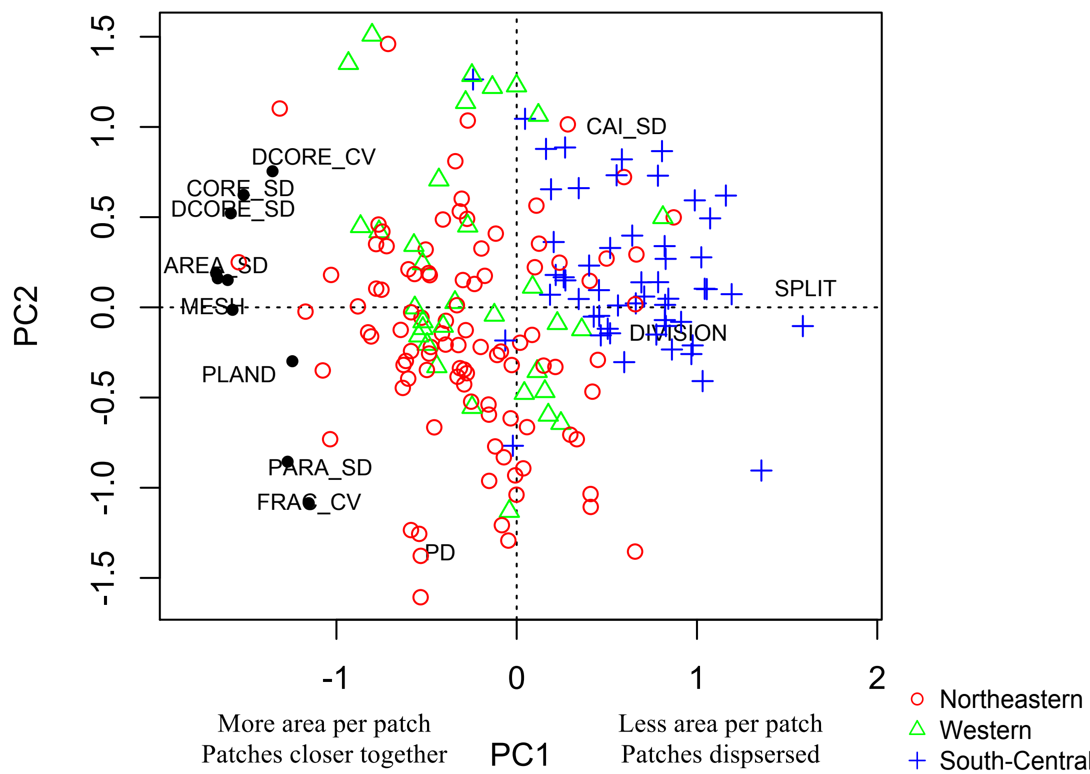

Figure 1.11: PCA ordination, 2007 mixedwood forest for watersheds in 3 ecoregions

The softwood forest cover ordination shows that watersheds with high values along the first PC axis have smaller and more separated patches of softwood forest

(Figure 1.12). Watersheds represented here tend to be in the Western (green triangles) and Northeastern (red circles) ecoregions. Watersheds with low values along the first PC axis consist of patches of softwood forest cover that are larger and closer together. Watersheds that are located on the negative end of the first PC axis are mostly located in the South-Central ecoregion (blue crosses) (Figure 1.12). There is also a strong trend on the second PC axis in this analysis; variability of shape complexity loads strongly on the negative end of the second PC axis. This suggests that softwood forest cover patch shapes are more complex in forests of the South-Central ecoregion.

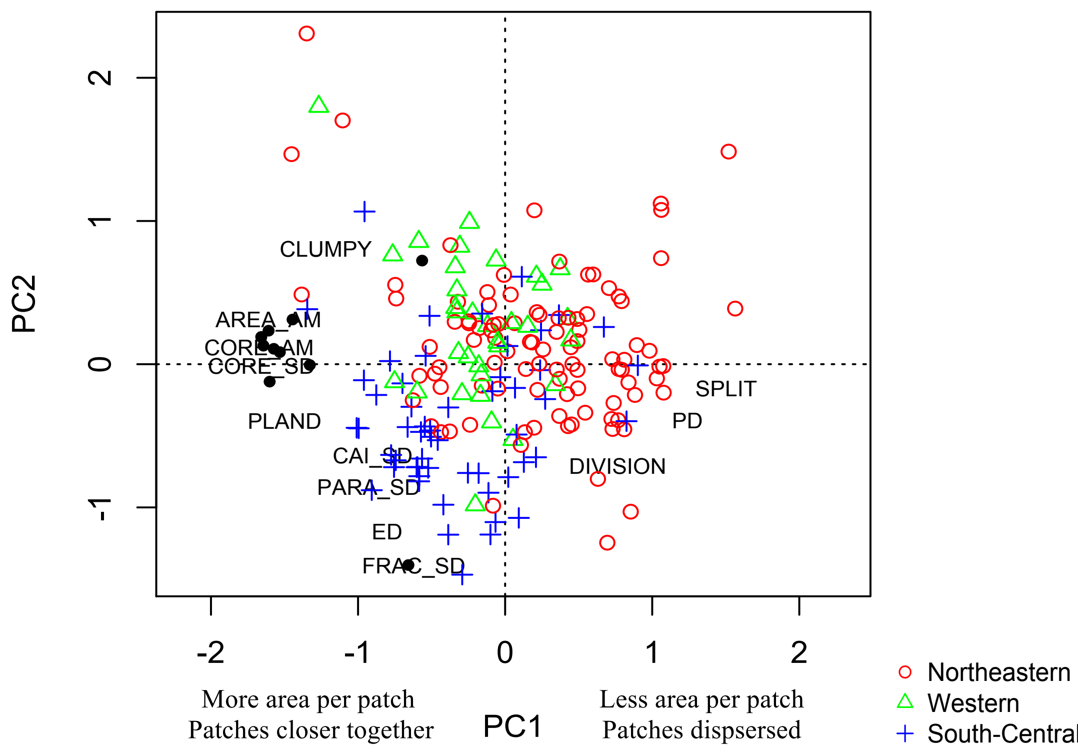

Figure 1.12: PCA ordination, 2007 softwood forest for watersheds in 3 ecoregions

Maps of three watersheds, one from each ecoregion, were created to depict typical harvesting patterns over the study period (Figures 1.13, 1.14, and 1.15). In summary, a greater amount of forestland was harvested within watersheds in the Northeastern ecoregion (depicted by Figure 1.13) than watersheds in the South-Central ecoregion (depicted by Figure 1.15). Watersheds in the Western ecoregion (depicted by Figure 1.14) were harvested in variable amounts; overall they were harvested more than South-Central watersheds, but less than Northeastern watersheds. Hardwood and mixedwood cover types were prevalent in residual forest cover in the Northeastern and Western ecoregions; softwood cover remained relatively stable in the South-Central ecoregion (Figures 1.13, 1.14, and 1.15).

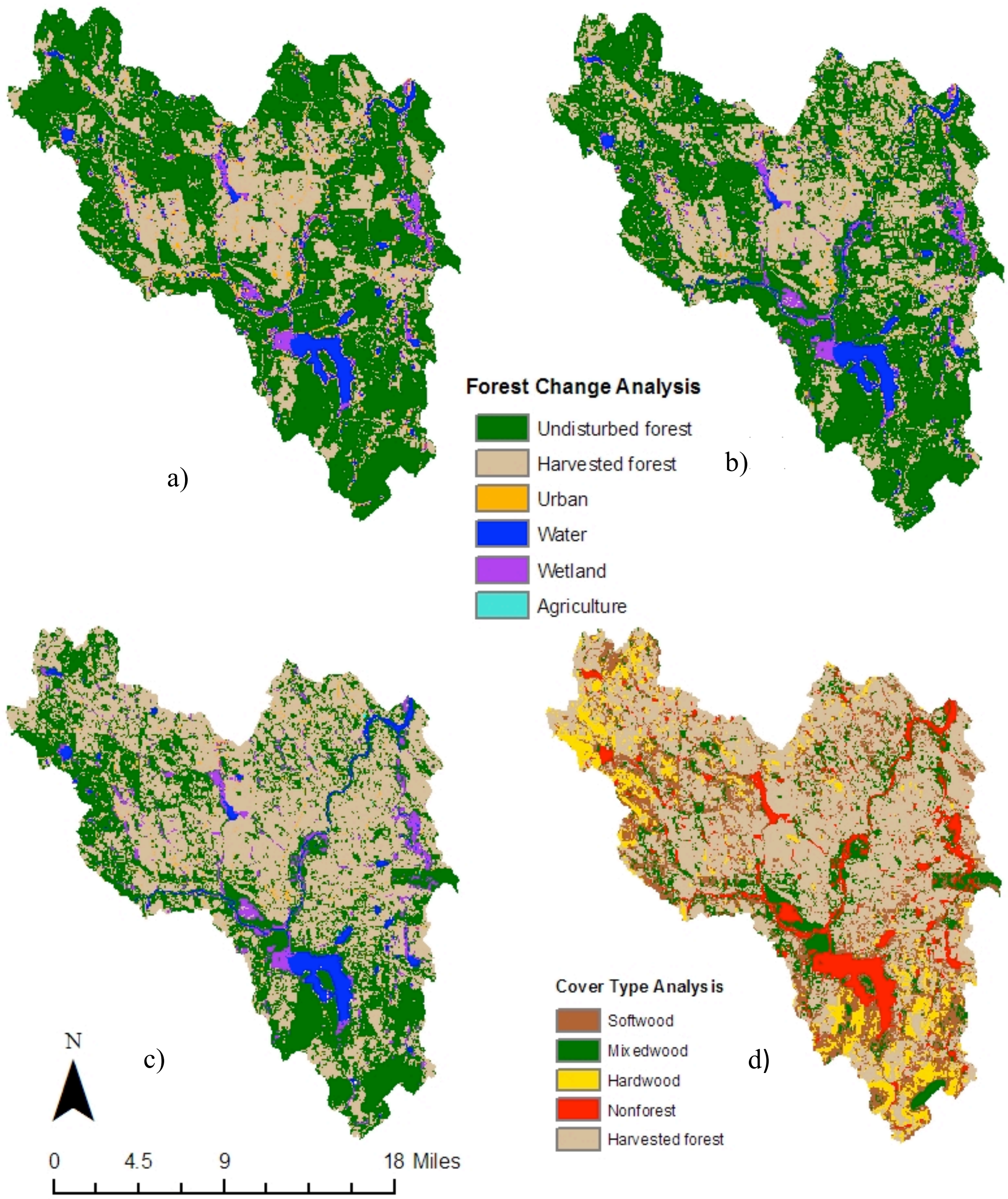

Figure 1.13: Upper West Branch Penobscot River watershed. A typical watershed in the Northeastern ecoregion: a) Forest change, 1991; b) Forest change, 2000; c) Forest change 2007; d) Residual cover type, 2007.

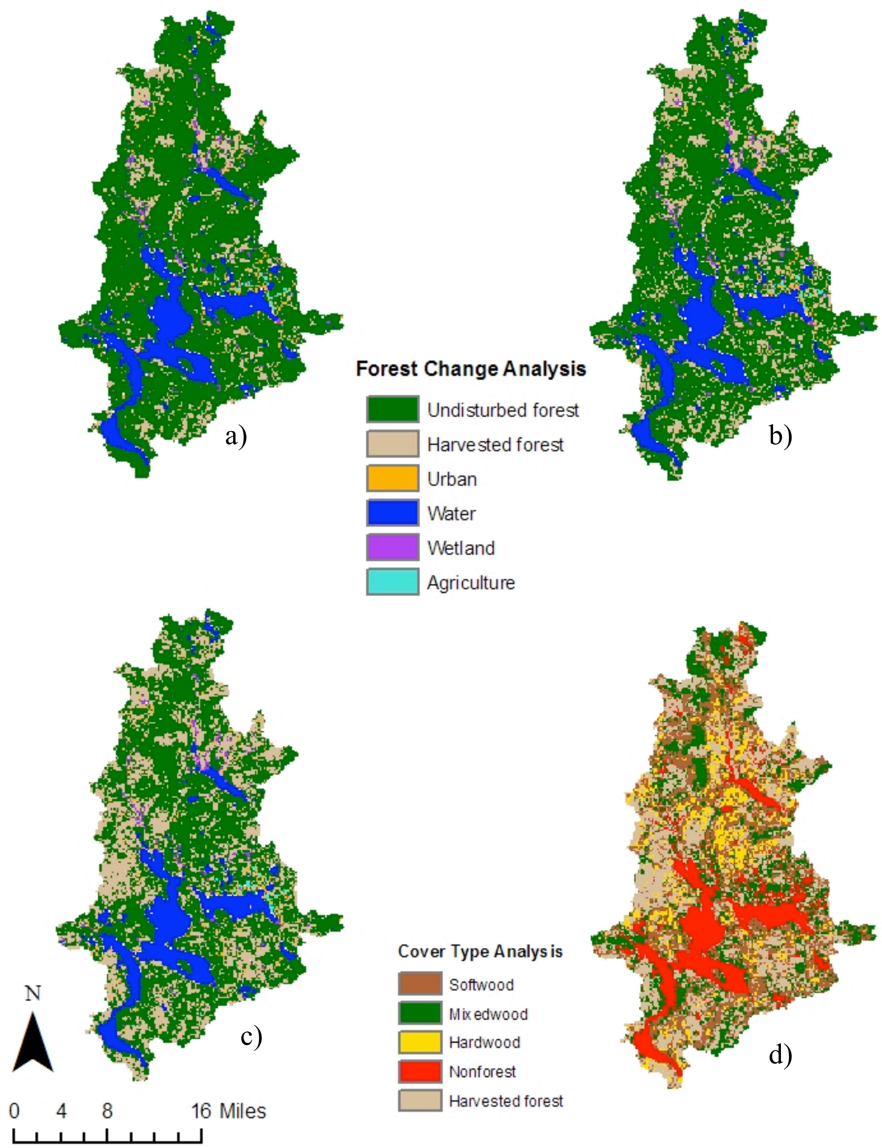

Figure 1.14: Lower Richardson River watershed. A typical watershed in the Western ecoregion: a) Forest change, 1991; b) Forest change, 2000; c) Forest change 2007; d) Residual cover type, 2007.

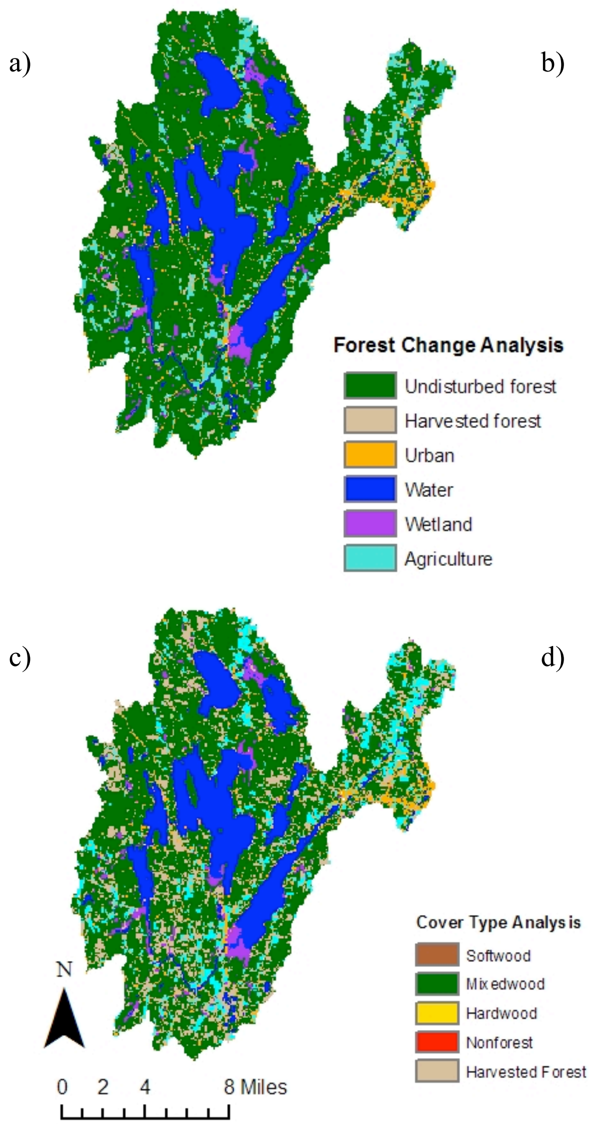

Figure 1.15: Belgrade Lakes-Messalonskee Stream watershed. A typical watershed in the South-Central ecoregion: a) Forest change, 1991; b) Forest change, 2000; c) Forest change 2007; d) Residual cover type, 2007.

Discussion

Ecoregion characteristics

The three ecoregions of Maine (Figure 1.1 b, Bacon and Bouchard 1997) have three distinct landscape compositions. The landscape composition of the Northeastern ecoregion is almost all undeveloped forestland. Timber harvesting is the primary industry in northern Maine, and large harvest sites are commonplace on the heavily forested landscape (Irland 2000, Sader et al. 2006). The landscape composition of the South-Central ecoregion consists of multiple types of land use. Urban and agricultural lands are more prevalent, with smaller areas of undeveloped forest found between properties. Timber harvesting is practiced on a more local scale in this area than in the northern part of the state (Sader et al. 2005, McWilliams et al. 2005). The landscape composition of the Western ecoregion combines attributes of both the Northeastern and South-Central regions, with small towns situated between large tracts of undeveloped forestland. Western Maine is also highly mountainous and contains some steep slopes that are not conducive to harvesting.

Forest fragmentation patterns

In the Northeastern ecoregion, patches of undisturbed forest were larger and more uniform in shape and size in 1991. By 2007, patches of undisturbed forest were smaller and much more complex in shape. This can be attributed to large-scale partial harvesting operations, which cover more area and tend to have more uneven boundaries than clearcuts (Sader et al. 2003, Jin and Sader 2005, Maine Forest Service 2007). The proportion of undisturbed forest in the Northeastern watersheds, by 2007, was much less than in other areas of the state, indicating that continuous harvesting occurred over a large area during the entire study period. The Upper West Branch Penobscot River watershed (Figure 1.13) is representative of the continuous harvesting and significant decrease in undisturbed forest by 2007. The Maine Forest Service maintains an annual inventory on silvicultural practices; the northern counties of Maine consistently had a greater amount of harvesting than the rest of the state (Maine Forest Service 2007). It was interesting that the Northeastern ecoregion PCA ordinations had such a wide spread; perhaps separating the agricultural area of Aroostook County or Downeast Maine from the northern forest would provide more information on landscape pattern in that part of that state.

In the South-Central ecoregion, patches of undisturbed forest were small, complexly shaped, and well dispersed over the watersheds in 1991. These same characteristics remained in 2007. The percentage of undisturbed forest, compared to the northeastern ecoregion, remained relatively steady as less harvesting occurred. Land cover type proportions were also more balanced over time. The Belgrade Lakes-Messalonskee Stream watershed shows a typical South-Central watershed (Figure 1.15). Southern counties of Maine had the highest live-tree growth to removal rate in the state from 1996 to 2003, at 1.4:1 (McWilliams et al. 2005).

The Western ecoregion represented intermediate fragmentation patterns between those observed in the Northeastern and South-Central ecoregions. In 1991, Western watersheds primarily consisted of large patches of undisturbed forest that are close together. There is a shift in landscape pattern in 2007, as the Western watersheds more closely resembled the Northeastern watersheds with a lower proportion of undisturbed forest and complex patch shapes. The harvested forest PCA ordinations show an increase in harvested forest area for the Western ecoregion between 2000 and 2007 (Figures 1.5 and 1.6). This trend suggests that somewhat higher harvesting rates occurred in the most recent time period, from 2000 to 2007. The Richardson Lake watershed (Figure 1.14) is representative of the increased harvesting trend in the Western ecoregion.

Results from the PCAs on harvested forestland complement the findings of the undisturbed forest PCAs; where there is more undisturbed land, there is less harvested land. The amount of forest harvested in the Northeastern ecoregion varied widely over the study period, but overall, more land was harvested in the Northeastern ecoregion than in the Western and South-Central ecoregions (Figure 1.8). Forest harvest area in northern Maine has increased since the 1990s (Maine Forest Service 2007). Recent partial harvesting practices may occur over more land area to maintain the same timber output as former clearcutting practices (Sader et al. 2005, McWilliams et al. 2005, Sader et al. 2006, Maine Forest Service 2007). Forest ownership change in the Northeastern ecoregion may be contributing to increased forest harvest rates. Timber Investment Management Organizations (TIMOs) own significant acreage in the northeastern ecoregion, and they harvest more forest than other landowner types (Figure 1.9, Table 1.8) (Jin and Sader 2006).

Watersheds in the South-Central ecoregion had the lowest percentage of harvested forest over the study period. The South-Central ecoregion had two outliers with high values along both PCs, indicating that there was very little harvested forest in these two watersheds at the beginning of the study period. The outlying South-Central watersheds are Portsmouth Harbor and York County Frontal Drainages, both of which primarily consist of non-forest land cover types (Figure 1.5). These results for South-Central watersheds agree with earlier findings of Sader et al. (2005); harvest blocks in the more populated southern part of Maine were smaller than harvest blocks in other areas of the state.

Watersheds in the Western ecoregion consistently had a greater area of harvested forest than watersheds in the South-Central ecoregion. Some watersheds in the Western ecoregion have experienced ownership change, much like watersheds in the Northeastern ecoregion (Hagan et al. 2005). The Maine Land Use Resource Commission (LURC) has established mountain protection rules that restrict harvest on forestland over 2,700 feet in elevation. Western watersheds have a higher proportion of forest on steeper slope classes and at higher elevations, some of which are “inoperable” for timber harvests (Noone 2010).

Cover type trends

Hardwood forests had less complex patch shapes but ranged widely in size and proportion within the South-Central ecoregion. This reflects the patchiness associated with multiple land uses as well as the lower volume of hardwood trees compared to softwood trees in this ecoregion (McWilliams et al. 2005). The Western ecoregion typically consisted of large patches of hardwood forest that are closer together, and hardwood forest makes up a greater proportion of the landscape in the Western ecoregion than in the other ecoregions (McWilliams et al. 2005). The Northeastern ecoregion had small patches of hardwood forest that are more interspersed. Softwood species were heavily harvested over the study period. This trend was reported earlier by Jin and Sader (2006).

Mixedwood forest proportions show a similar outcome to the overall trends observed in the forest change analysis. In the South-Central ecoregion, mixedwood forest occurred in small, interspersed patches with complex shapes. The patch density is low compared to the Northeastern and Western ecoregions, and the percent of landscape as mixedwood forest is also low in this regard. Very little harvesting occurred within mixedwood forests in the South-Central ecoregion over the study period. The Northeastern and Western ecoregions show similar landscape patterns with mixedwood forest. Both ecoregions had large mixedwood patch sizes that are closer together, and they also had a higher proportion of mixedwood forest over their landscapes, compared to the South-Central ecoregion. Noone (2010) found that biophysical regions as described by McMahon (1990) in the northern and western parts of Maine had a substantial increase in mixedwood forest cover from 1993-2007. Mixedwood forest cover is becoming more prevalent in Maine and other areas in New England, which may be due to extensive selective harvesting (McWilliams et al. 2005, Saunders et al. 2011).

Softwood forests show a marked trend of decreasing size and area in undisturbed forests in the Northeastern and Western ecoregions. Softwood species, such as balsam fir and red spruce, dominate the northern forest, and they were harvested at higher rates until recently, as the availability of mature softwood has declined (Seymour 1992, McWilliams et al. 2005). There are three notable outlier watersheds in the Northeastern ecoregion that contain a large amount of softwood forest cover in 2007 (Figure 1.12). Upon further exploration, it was discovered that Baxter State Park intersects all three of the outlying watersheds. Baxter State Park is under permanent conservation where harvesting is strictly prohibited, with the exception of the Scientific Forest Management Area in the northwest corner of the park. Other conservation lands, owned by a variety of landowners, border Baxter State Park in the adjoining watersheds.

Jin and Sader (2006) reported landowner harvesting preference by cover type in northern Maine from 1991-2004 and found that in the 1990s, softwood was overwhelmingly preferred. In the 2000s, other cover types were harvested at a more equal rate with softwoods, possibly as hardwood and mixedwood regeneration stands following the spruce budworm salvage logging became marketable (Rice 2003). Markets for hardwood products in Maine were unfavorable for many years, but demand for hardwood products increased in the 1990s, leading to more managed hardwood forests in the state

(Rice 2003, McWilliams et al 2005). The South-Central ecoregion had a higher percentage of softwood forest, associated with the goals and practices of smaller, more family-based landowners with less emphasis on harvesting softwood to supply mills that existed in the earlier period of the study (SWOAM 2005). Softwood forest cover may remain more stable over time in areas experiencing less frequent forest harvest (Olson and Wagner 2010).

Conclusions

The forest harvest PCA ordinations (Figs. 1.2-1.7) consistently show that forests in South-Central Maine are smaller and made up of more patches than their Northeastern and Western counterparts. As harvesting activity progressed over the study period, undisturbed forests in Northeastern watersheds, and to a lesser degree in Western watersheds, were split into more, smaller patches due to the expanse of partial harvesting. Undisturbed forest cover in watersheds of South-Central Maine remained relatively stable due to lower harvesting rates. In watersheds of the Western ecoregion, undisturbed forest area experienced varying rates of loss. This could be related to the higher proportion of steep, mountainous terrain found in that part of the state, where harvesting is restricted. The cover type PCA ordinations (Figures 1.10-1.12) indicate that softwood has been the most harvested cover type over time. Mixedwood and hardwood represent higher proportions in the 2007 residual undisturbed forest, and likely are increasing as regenerating forest cover types, as reported by other authors (McWilliams et al. 2005, Saunders et al. 2011, Noone et al. 2012). It is important to note that the forest disturbance measured is cumulative over the study period, but it is not permanent. These forests will eventually regenerate into marketable timberlands that could be measured as undisturbed forest in a future analysis similar to this one.

This research is the first to provide a statewide numerical assessment of the spatially explicit effects of harvesting on the landscape (watershed level) composition of Maine. This study confirms results of previous studies concerning the harvesting rates and trends and the effects of land ownership changes (McWilliams et al. 2005, Hagan et al. 2005, Jin and Sader 2006). The TIMO/REIT landowner group owned a higher percentage of heavily harvested watersheds in the Northeastern ecoregion. These investment landowners appear to harvest forestland at higher rates to maximize the shorter-term return on their timberland assets (Hagan et al. 2005).

This study demonstrates the usefulness of Landsat TM data as a cost-effective and spatially explicit statewide forest monitoring tool. Analyzing time-series Landsat TM data integrated with existing GIS data allows analysis at user-selected scales, as in the case of this fragmentation analysis by NRCS Level 5 watershed and Maine DEP ecoregion (Bacon and Bouchard 1997). Fragmentation analysis has become a crucial tool for determining how land cover change affects landscapes (Mladenoff et al. 1993, Riitters et al. 2000, Wulder et al. 2009); studies similar to this one can be conducted in other states or regions using existing data sets and fragmentation analysis software (McGarigal et al. 2002).

Future Work

The database created in this research could be used as a stratification tool to determine possible locations of older, undisturbed forest as part of a statewide assessment of plant or animal biodiversity. Knowing the locations of older undisturbed forest can facilitate studies of habitat connectivity for Maine's forest-dependent wildlife species, such as American marten (*Martes americana*) (Fuller and Harrison 2005, Simons 2009). Spatially-explicit forest cover type and age class data could aid in determining larger, connected tracts of forestland suitable for future conservation protection areas, which are becoming more important with the onset of urban sprawl in South-Central Maine (Colby Environmental Policy Group 2007). Future studies of forest fragmentation in the northern forest states may only need to focus on a few well-represented metrics to obtain an accurate assessment of landscape change pattern. As demonstrated in this study, patch area, patch core area, radius of gyration, and effective mesh size together provide a suitable explanation for landscape change across the varying landscape patterns of Maine.

CHAPTER 2

PREDICTING VISIBLE CROWN DIAMETER ON RECENT UNHARVESTED FOREST STANDS IN NORTHERN MAINE

Introduction

In Maine's presettlement forest, large, old red spruce dominated the overstory (Seymour 1992). Lorimer (1977) described an all-aged climax forest in northern Maine; 32% of the forest was mature even-aged and 27% was all aged. Cary (1894) reported that 60% of spruce trees harvested in the early 1890s were between 150-225 years old. Over the last 160 years, a series of historical exploitations has led to a completely different forest than the presettlement forest. Initially, only the largest trees were cut—eastern white pine first, then red spruce. Immediately after these initial harvests, large red spruce began to be heavily harvested; these large trees were removed over a very short period of time, thus the sawlog era of Maine was short-lived (Cary 1896). Very little virgin timber remained at the turn of the 20th century, and what remained was likely to occur in remote, inaccessible areas (Hosmer 1902). The last major spruce budworm epidemic of the early 1970s initiated a period of major road building and salvage logging that extended throughout the 1980s (Seymour 1992). Much of the remaining pockets of sawtimber on unprotected private land were harvested, including older hardwood and mixed forest stands that became more valuable as new markets for hardwood developed in the 1990s and early 2000s (Rice 2003). By 2003, only 9 percent of timberland was large sawtimber, which included all hardwood stems greater than 11 inches in diameter at breast height and all softwood stems greater than 9 inches at breast height (McWilliams et al. 2005).

Large trees tend to be found in older stands; however, locating older stands in Maine's heavily harvested forest is difficult. This study uses remote sensing data to predict visible crown diameter on recent unharvested forest (RUF), which is defined in this study as forest stands in northern Maine that have not been harvested for at least 35 years. Visible crown diameter (VCD) is an individual tree characteristic that can be directly measured on aerial photography, and has been used by photo interpreters for decades in forest inventory applications (Avery 1967, Paine and Kiser 2002). VCD measures the part of the tree crown that is visible on an aerial photo, which may eliminate long branches that extend past the area occupied by the crown. Trees measured for VCD are typically in the forest canopy. For many species, crown diameter is related to stem diameter at breast height (dbh), especially when combined with tree height measurements. VCD has been used with statistical models, tied to ground plot measurements, to estimate tree dbh, individual tree volume, or stand-size class (Paine and Kiser 2002). It is important to note that large tree crowns do not directly indicate tree age; it is only assumed that the trees measured in this study have had at least 35 years to grow. These stands could fall in many places along the forest succession spectrum.

In a study that examined the landscape characteristics of older stands in the Pacific Northwest, Healey et al. (2008) described large diameter forests as stands with a quadratic mean diameter (QMD) greater than 20 inches. The term refers solely to trees in the upper canopy (dominant and co-dominants). Quadratic mean diameter was predicted in Pacific Northwest forests using regression-based methods with input variables including Landsat Thematic Mapper (TM) imagery, field-collected dbh data, VCD data from aerial photography, and topographic variables (Weyermann and Fassnacht 2000, Moeur et al. 2005). Using this methodology as a template, a similar analysis of Maine's forest was conducted; however, as Maine's trees are smaller and there are fewer older forest stands remaining, some modifications to the approach were necessary. Without field-collected data to determine QMD, the study presented here relies on VCD measurements on high-resolution digital orthophotography. VCD was measured on Recent Undisturbed Forest. These stands were not harvested between 1972 and 2007. RUF may range from mid- to late- successional stands containing shade tolerant species to mature old growth stands containing large trees. Late successional and old growth stands do exist in Maine but are widely dispersed throughout the state and are relatively uncommon (Tyrrell et al. 1998, Whitman and Hagan 2007). Due to the rarity of late successional and old growth forests in Maine, this analysis requires a modeling approach that is robust to low sample size and is able to handle a large number of variables. A regression tree model, such as random forests, meets these criteria (Breiman 2001, Liaw and Wiener 2002, Powell et al. 2010).

Random forests (RF) is a non-parametric regression tree method that can process a large number of variables through a series of small regression trees to determine the most important variables while being robust to over-fitting and bias (Breiman 2001, Liaw and Wiener 2002). RF has been increasingly used in forest ecology to predict forest structural attributes including biomass, successional stage, crown damage due to fire, and tree species distribution (Prasad et al. 2006, Falkowski et al. 2009, Thompson and Spies 2009, Powell et al. 2010). Powell et al. (2010) used the R (www.cran-r-project.org) package ModelMap (Freeman and Frescino 2009) to implement RF analysis on a group of spectral and biophysical variables to predict biomass using a 20 year Landsat Thematic Mapper (TM) time series. They found that RF had a lower residual mean square error (RMSE) than reduced major axis (RMA) regression or Gradient Nearest Neighbor (GNN) analysis, two commonly used classification methods for this type of analysis. While searching for a rare high biomass hardwood forest type, they discovered that the "RF model…was robust to the lack of reference data for these rare forests because of its ability to identify complex non-parametric relationships among a broad set of spectral and biophysical variables" (Powell et al. 2010). The ability to detect rare forest types makes RF analysis an appropriate model to determine if VCD can be predicted in RUF within Maine's northern forest.

An added utility of the ModelMap package is predictive mapping. A specified response variable over a large area can be mapped using spatially explicit explanatory variables. Predictive mapping techniques have been used with remotely sensed data to estimate forest composition, structure, quadratic mean diameter, and successional stage (Cohen et al. 1995, Weyermann and Fassnacht 2000, Cohen et al. 2001, Ohmann and Gregory 2002); most of these derive predictive models from regression-based classification methods. Cohen et al. (2001) utilized Tasseled Cap spectral indices derived from Landsat TM data (Crist and Cicone 1984) and a digital elevation model (DEM) to increase the accuracy of models used to predict VCD and other forest characteristics.

According to Whitman and Hagan (2007), field measurements of late successional and old growth stands in northern New England require eight or more large diameter trees greater than 16 inches dbh in a 0.06 ac (0.2 ha) forest plot. Old growth forests in Maine generally consist of small tracts 2-20 ha each of single forest types (Maine Critical Areas Program 1983). The spatial pattern of these forests throughout the state may be influenced by life history characteristics, recent disturbance patterns, and structural characteristics such as tree size (Chokkalingam and White 2000). Old growth forests have experienced little or no human disturbance and contain dominant canopy trees that are >125-150 years in age. Forests that are younger than old growth but still over 100 years old are termed late successional stands. Late successional stands possess a variety of ecological conditions and stand ages and may contain large trees (Whitman and Hagan 2007). Locating older forests with larger trees is important for forest management and planning because the stocking and distribution of large trees greatly affect wildlife habitat, biodiversity, stand structure and carbon stocks (McWilliams et al. 2005). Identifying these stands may facilitate management regimes that would allow larger trees to optimize their role in Maine's forest. With Maine's forest being so intensively harvested, maintaining a distribution of larger trees may be ecologically valuable (Brown et al. 1997). Wildlife species such as white tailed deer depend on larger softwood (coniferous) trees for thermal cover through the winter, thus promoting development and wider distribution of larger trees could boost Maine's deer population (Boer 1978), as well as protect populations of other keystone species, such as American marten (*Martes americana*) that depend on forests with mature canopy structure (Fuller and Harrison 2005). There are multiple programs in Maine with a mission to educate the public about conserving Maine's forests. Keeping Maine's Forests and Forests for Maine's Future are two collaborative groups that focus on conservation-based outreach. The Maine Natural Areas Program monitors over 100,000 acres of state-owned ecoreserves (Maine Natural Areas Program 2011). Locations of recent undisturbed forest may be of interest to these groups.

Visible crown diameter has been predicted in multiple forest types (Cohen et al. 2001 [Oregon—Willamette National Forest], Wulder et al. 2000 [Victoria, BC, Canada], Gering and May 1995 [Tennessee], Woodcock et al. 1994 [N. California—Stanislaus National Forest]). Maine's climate and harvesting history have led to a unique forest, therefore a tailored approach is used to predict VCD in RUF in northern Maine. Statewide interpretation of aerial photography is not feasible or cost-effective. No spatially explicit maps showing the location of older forest or visible crown diameter of older forests exist for Maine. A very dense forest harvest Landsat image time series has been compiled (2-3 years between Landsat scene acquisitions) between 1972 and 2007 (Legaard et al., manuscript in preparation). Forest change detection maps derived from these data will provide a first level stratification of RUF. Visual photo interpretation of 1972 National Aeronautics and Space Administration (NASA) U-2 aerial photography will verify that RUF sample plots contained unharvested forest at the beginning of the Landsat time series. 2009 high spatial resolution digital orthophotography (1m ground resolution) from the National Agriculture Imagery Program (NAIP) will provide a detailed look at the forest canopy, showing individual trees where VCD can be measured on stratified sample photo plots using software tools on a computer monitor screen. Exploratory variables, such as spectral indices derived from Landsat imagery, biophysical variables, and ownership data will be examined to determine the landscape characteristics of the RUF. The assumption is that if there are larger diameter trees in Maine under natural regeneration conditions, they would likely be found in the forests that have not been harvested or disturbed for many years. These exploratory variables will be input into a random forests model that will predict average VCD on RUF within the study region. Additional statistical methods will be utilized to further explain model output.

Objectives

This research will test the feasibility of using change detection maps derived from Landsat TM imagery, raw Landsat TM imagery, two sources of aerial photography, and ancillary data to predict VCD in northern Maine. Previous studies have used aerial photo or orthophoto interpretation for validation of Landsat-based forest mapping or change detection studies (Cohen et al. 2001, Briggs and Sader 2008). This is a practical and applied approach that does not rely on extensive field methods. Each remote sensing visual interpretation or digital analysis method applied in this study is well known. The combination of methods, however, is novel and appropriate for Maine forest conditions, where similar studies have not been attempted. The methods are repeatable and transferable to other forest regions, as all of the data types are generally available for free.

Results of this study could support statewide land conservation initiatives, biodiversity analysis, wildlife habitat research, and forestland acquisition programs in Maine.

Methods

Study area

The VCD predictive map was created over the northern two-thirds of the state, which in addition to the study area covers the agricultural fields of Aroostook County, the unorganized townships of Washington County, and some coastal lands. The study area primarily consists of Spruce/Fir, Sugar Maple/Ash, and Cedar/Black Spruce cover types (McWilliams et al. 2005). The map was created in four pieces to accommodate computer memory limitations. The southern part of the state was not included in this analysis because its forest is drastically different from the northern part of the state. Southern Maine encompasses the Oak/White Pine, Beech/Red Maple, and Hemlock/Red Spruce forest cover types. Southern Maine has much higher urban land use and smaller forest parcels than northern Maine (McWilliams et al. 2005). The dense harvest history dataset needed for validation exists only for the area of northwestern Maine that corresponds with the Landsat 5 satellite path 12, row 28; therefore the predictive maps were subset to cover this one Landsat scene. Data for the RF model were collected from this smaller study area. This area is approximately 1.8 million hectares in size and encompasses about 217 townships (Figure 2.1b). Topography in this area is typically flat or rolling, with occasional mountains and associated alpine terrain. The landscape contains an extensive network of lakes, river, and wetlands. Forest cover types remain the same for the area covered by the predictive map. Urban and residential development is minimal; existing development occurs mostly in the southeastern corner of the study region. Forest harvesting is the primary disturbance agent (Hepinstall et al. 1999, Sader and Legaard 2008).

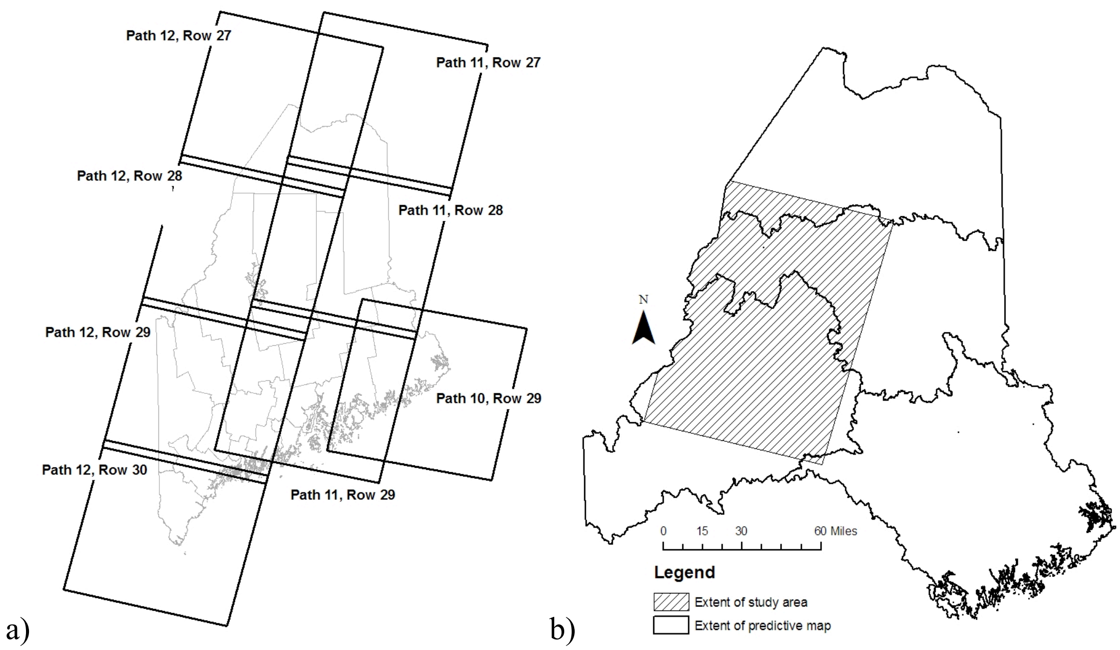

Figure 2.1: Study area. a) Landsat TM scene locations covering the state of Maine, b) extent of the VCD predictive map, split into four parts to accommodate computer memory, and the RUF and VCD validation study area.

Initial data sets

The 35-year harvest time series map used in this study (Legaard et al., manuscript in preparation) was created using forest change detection methodology based on the

Normalized Difference Vegetation Index (NDVI) derived from Landsat Multispectral Scanner imagery from the 1970s and the Normalized Difference Moisture Index (NDMI) from Landsat TM imagery of the 1980s, 1990s, and 2000s. The map detects heavy disturbances, such as the spruce budworm clearcuts of the 1970s, and light disturbances, such as partial harvests that became commonplace after the enactment of the Maine Forest Practices Act of 1989 (Seymour 1992, Sader et al. 2003). The map provides an initial stratification of RUF, representing all forest where no disturbance was detected between 1972 and 2007. In Maine, Sader and others found that NDMI produced accurate maps for detecting major forest types and partial harvests, the prevalent harvesting method used in the state (Wilson and Sader 2002, Sader et al. 2003, Jin and Sader 2005). Two sources of aerial photography were interpreted in this study: 1972 color infrared NASA U2 aerial photography and 2009 true color National Agriculture Imagery Program (NAIP) digital orthophotography. The NASA U2 imagery was collected statewide at a scale of 1:120,000. The Maine Image Analysis Laboratory at the University of Maine archives the only collection of hard copy 9x9 inch NASA U-2 photos available for Maine. The MIAL has a digital archive of 2009 NAIP imagery for the state of Maine. NAIP imagery has a 1 m ground pixel resolution.

Determining plot locations

Six hundred sample plots were randomly located within the RUF derived from the 35-year time series map (Legaard et al., manuscript in preparation). The plots were 10x10 Landsat TM pixels, or 300 m^2 in area. This plot size was selected due to the small scale of the NASA U2 aerial photography used to determine the condition of the forest in 1972 (Figure 2.2).

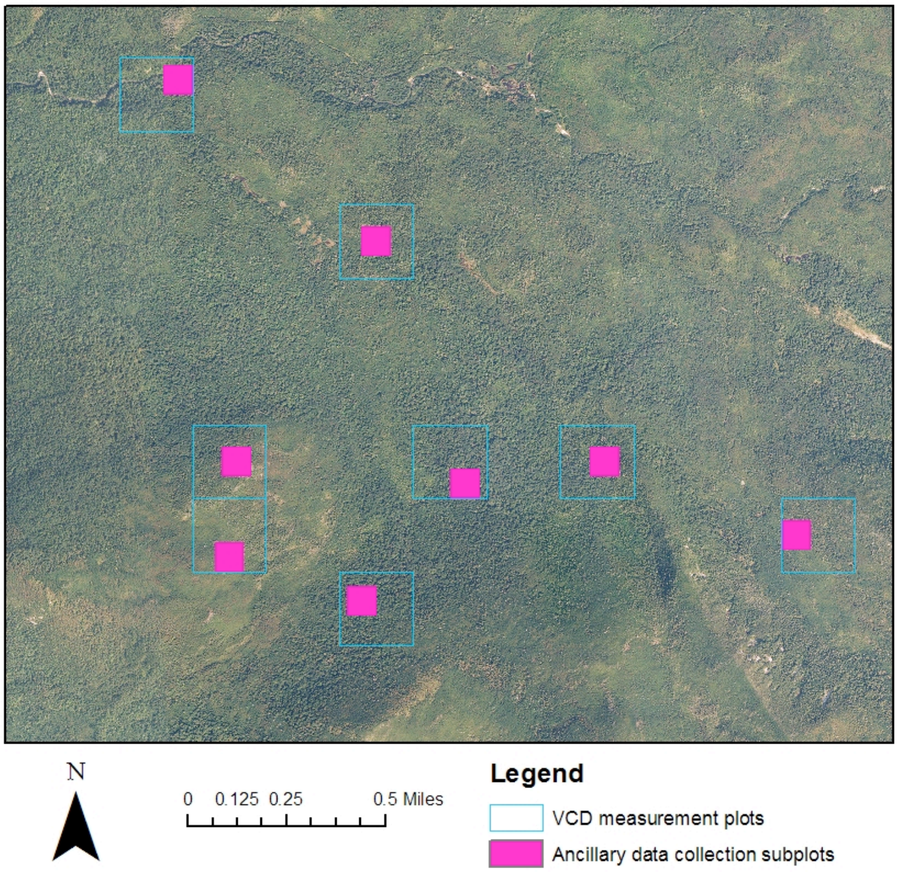

Figure 2.2: Plot scheme for data collection. Plots are displayed on 2009 NAIP true color digital imagery. VCD measurement plots were 10x10 pixels; ancillary data collection subplots were 4x4 pixels.

Aerial photo interpretation

To determine if RUF existed on each sample plot location in 1972, NASA U2 stereo photos were interpreted on a light table with a lupe magnifier (8x) and a stereoscope with 3x magnification (Figure 2.3). Each sample plot was assessed for cover type (hardwood, softwood, or mixedwood), percent of canopy closure, and approximate harvest stage. Harvest stage was classified as recent cut, including cut type information (light/heavy partial cut or clearcut), or as unharvested. Plots that were recently harvested on the 1972 imagery or in the stages of early regeneration were eliminated; 386 RUF plots remained for VCD measurement.

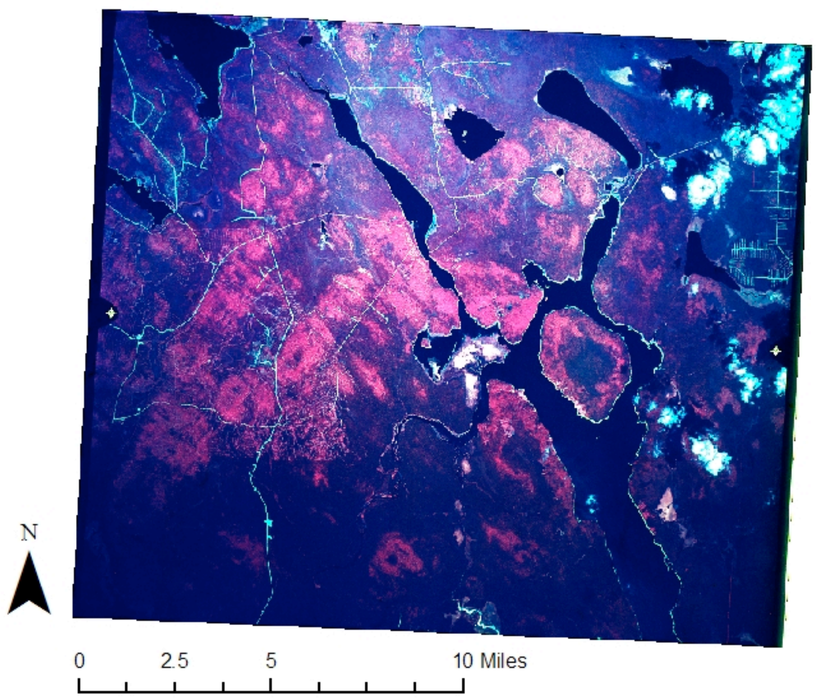

Figure 2.3: 1972 color infrared NASA U2 aerial photo. Light pink areas represent hardwood forest, dark purple areas represent softwood forest.

To determine stand condition and measure VCD at the end of the study period, NAIP imagery was displayed in ArcMap 9.3 (ESRI 1991-2012) (Figure 2.4). Images were arranged on a computer monitor so that photo plots were interpreted at a scale of

1:2,000. This scale was adequate to see and measure individual tree VCD and to contain the entire plot area within the display. Cover type, percent of canopy closure, and approximate harvest stage were recorded and VCD was measured on 10 canopy trees per plot using the Measure tool in ArcMap 9.3 (ESRI 1996-2012). Trees were selected to cover a range of crown diameters and were spatially distributed throughout each plot. VCD measurements were averaged for the 10 trees to provide a single measurement for each plot. Measuring VCD directly from high resolution aerial photography by a trained interpreter without field measurements is an effective and accurate data source (Lillesand and Kiefer 1987, Cohen et al. 2001, Paine and Kiser 2002).

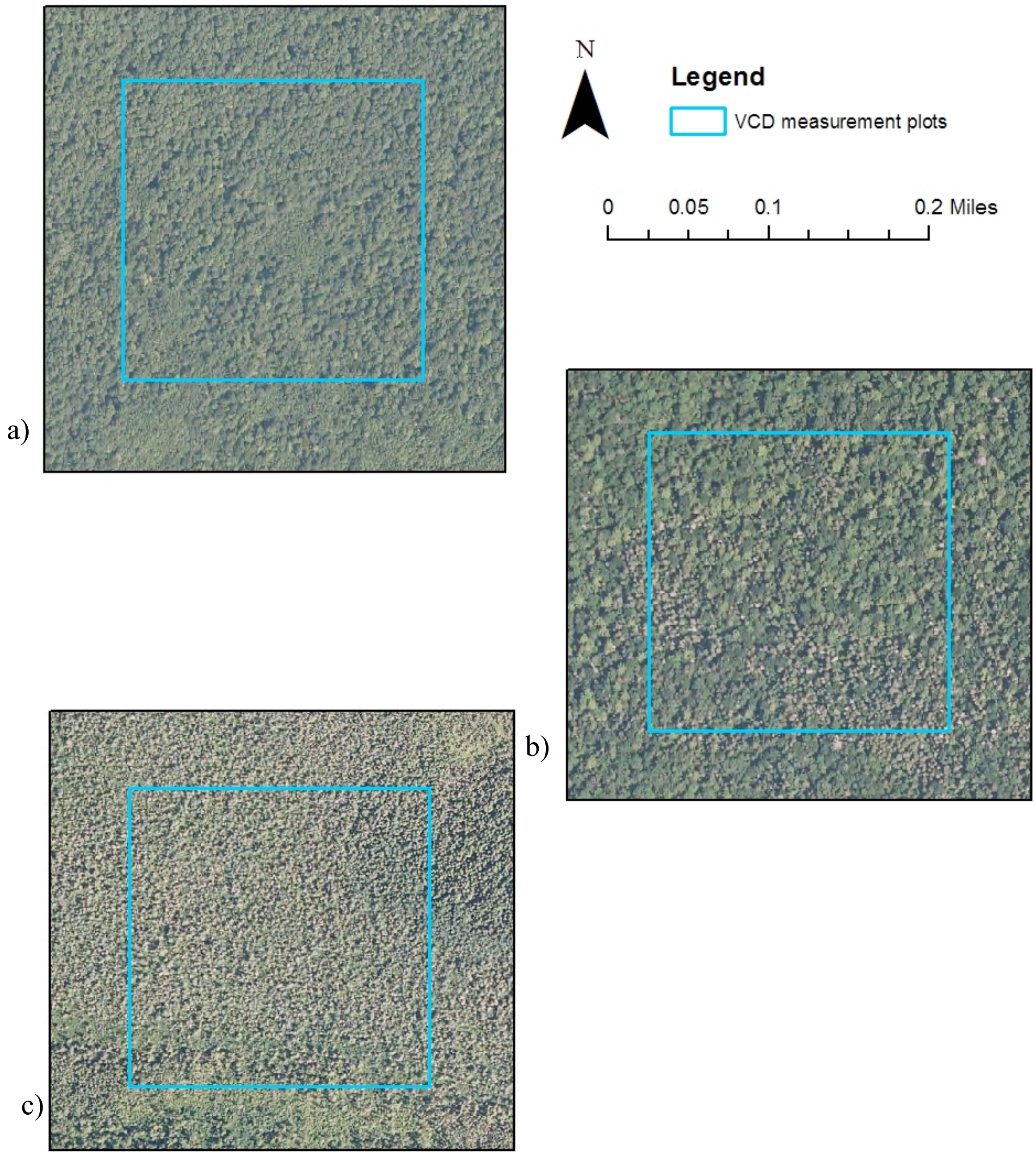

Figure 2.4: 2009 True color NAIP digital aerial imagery. All three cover types examined in this study are displayed: a) hardwood, b) mixedwood, and c) softwood forest cover.

Ancillary data collection

A 30 m digital elevation model (DEM) served as the data source for the calculation of the elevation, slope, and aspect variables of the predictive model. ArcMap 9.3 Spatial Analyst was used to convert the DEM to slope and aspect measurements. The University of Maine Cooperative Forestry Research Unit provided a copy of a statewide 10 m Depth to Water Table map, which was used to measure site index (CFRU 2006). The map was resampled to 30 m and continuous depth to water table measurements were converted to categorical site index measurements, following Briggs Site Index recommendations for Maine (Briggs 1994). Ownership data from the James W. Sewall Company of Old Town, Maine was used to compile landowner type as of 2007. All ancillary data variables (Table 2.4) were collected in a 4x4 pixel subplot. Studies that have incorporated biophysical and spectral variables often collect this data in a 3x3 pixel window to reduce variation; the 4x4 pixel window used in the study presented here does the same (Fiorella and Ripple 1993, Powell et al. 2009). Data were collected using the Zonal Statistics tool in ERDAS Imagine 9.3 (ERDAS 1999). These data were placed into Microsoft Excel for statistical analysis.

Spectral data development

To create the VCD predictive map, Landsat TM imagery was downloaded (www.glovis.usgs.gov) to cover the entire state. Eight Landsat TM scenes cover the state of Maine (Figure 2.1a). Six bands of imagery were downloaded; bands 1-5 and 7 were of interest to this study. Band 6 is a thermal band that was not used in vegetation analysis (Table 2.1).

Table 2.1: Landsat TM wavelengths, spectral band region and spectral response to surface vegetation and moisture conditions

Band	Wavelength (µm)	Spectral Region	Spectral Response
1	0.45-0.52	Blue	Water, soil/vegetation discrimination
2	0.52-0.60	Green	Chlorophyll reflection band
3	0.63-0.69	Red	Chlorophyll absorption band
4	0.76-0.90	Near IR	Veg. types, soil moisture, biomass
5	1.55-1.75	Mid IR	Soil and vegetation moisture
6	10.4-12.5	Thermal IR	Thermal mapping, vegetation stress
7	2.08-2.35	Mid IR	Vegetation moisture content

The optimal time to collect satellite imagery is late spring and early summer, when trees are in full leaf. Due to cloud cover, most scenes collected are from mid to late summer, and five additional secondary scenes were required to fill in gaps due to cloud cover and shadows. In some locations, scenes from 2007 were of poor quality (excessive clouds). In those cases, an acceptable scene from the closest date was used. In total, twelve scenes were used to create the statewide six band Landsat TM image (Table 2.2).

Table 2.2: Landsat TM scenes used in 2007 statewide mosaic

	10-29	11-27	11-28	11-29	12-27	12-28	12-29	12-30
Primary	9/22/06	7/8/05	7/8/05	9/13/06	8/22/07	6/19/07	6/19/07	9/23/07
Secondary			5/27/07	6/14/08		8/22/07	9/23/07	

Preprocessing is required to make raw Landsat TM imagery suitable for spectral analysis. All manipulation of Landsat TM imagery was completed using ERDAS Imagine

9.3 (ERDAS 1999). The six reflective spectral bands were combined to form twelve six-band Landsat TM images. These images were then projected to the North American Datum (NAD) 1983 Universal Transverse Mercator (UTM) coordinate system, Zone 19N. Once projected, the raw spectral values (digital numbers, or DNs) of the images were converted to at sensor reflectance using a model available in ERDAS Imagine that converted the digital numbers first to radiance, then to at sensor reflectance (http://earth.gis.usu.edu/imagestd/) (Equation 2.1).

$$\rho_{BandN} = \frac{\pi(L_{BandN} * Gain_{BandN} + Bias_{BandN} * D^2)}{E_{BandN} * (COS((90-\theta) * \pi / 180))} \text{ [Eq. 2.1]}$$

Equation 2.1: Digital number to at-sensor reflectance conversion. r_{BandN} is the reflectance for Band N, L_{BandN} is the Digital number for Band N, Gain and Bias are band-specific rescaling factors, D is the normalized Earth-Sun Distance, and E_{BandN} is the solar irradiance for Band N.

Calibration coefficients for this model came from Chander et al. (2009). Full size Landsat scenes were reduced to Maine's borders to simplify further data processing. Overlapping areas between Landsat scenes were mostly removed to eliminate redundancy in data processing. A small amount of overlap between scenes was retained to perform radiometric normalization. Clouds were masked out of the primary images using visual interpretation and screen digitizing methods.

Radiometric normalization reduces the variation in reflectance values between Landsat TM images, which assists in creating a seamless statewide mosaic (Beaty et al. 2008). Reduced Major Axis (RMA) regression was used to calibrate the distribution of pixel values of the Landsat images used to resemble that of a reference image (Cohen et al. 2003, Schroeder et al. 2006). The initial reference image was a Landsat TM image of path 12, row 28 taken on June 22, 2007. Pixel values used in the RMA regression model came from a common usable area (CUA) between the two images, which consists of overlapping pixels without cloud cover, water, or agricultural areas. Forested areas were sufficient CUAs because they do not contain areas of drastic contrast (Beaty et al. 2008). This method has demonstrated very low percent difference between a reference image and calibrated images (Beaty et al. 2008). An RMA regression model was applied that normalized pairs of images and mosaicked them together. This was done sequentially until the statewide mosaic was completed (Equation 2.2). Primary and secondary images for each scene were mosaicked before the final mosaic of all eight scenes of the state was created.

$$y_{calib} = y * \frac{\sigma_X}{\sigma_Y} + \left(\overline{X} - \left(\frac{\sigma_X}{\sigma_Y} \right) * \overline{Y} \right) \text{ [Eq. 2.2]}$$

Equation 2.2: RMA regression model for radiometric normalization. y_{calib} is the value of a pixel in the calibrated scene, y is the value of a pixel in the target scene, X is the set of pixels of the reference scene that are common to the target scene, and Y is the set of pixels of the target scene that are common to the reference scene.

The statewide image mosaic was masked to the extent of the predictive map (Figure 2.1b) to create the final six band Landsat TM mosaic as input to the predictive model. The Tasseled Cap Indices, wetness, greenness, and brightness (Crist and Cicone 1984) were calculated by transforming the six band image by a series of coefficients. NDMI and NDVI were calculated using band ratios. NDVI was developed as an alternative to Tasseled Cap greenness as a means of detecting vegetation in satellite imagery, using pixel values from Landsat TM band 3, the visible red band, and Landsat TM band 4, a near-infrared (NIR) band (Franklin et al. 2000) (Table 2.3). NDMI was developed as an alternative to NDVI that has been demonstrated to highlight vegetation more effectively in Maine, using the NIR Landsat TM band 4 and Landsat TM band 5, a mid-infrared (MIR) band (Wilson and Sader 2002, Sader et al. 2003, Jin and Sader 2005) (Table 2.3). All of these spectral indices have been studied for use in predictive models (Cohen et al. 1995, Cohen et al. 2001, Sader and Legaard 2008, Powell et al. 2010).

Table 2.3: Equations to calculate spectral indices

Spectral index	**Equation**
NDVI	$NDVI = \frac{(NIR - VIS)}{(NIR + VIS)}$
NDMI	$NDMI = \frac{(NIR - MIR)}{(NIR + MIR)}$

Spectral data were extracted from the imagery as follows: Landsat TM Bands 1-5, 7, Tasseled Cap Brightness, Greenness, and Wetness, NDVI, and NDMI (Table 2.4). All spectral data variables were collected in 4x4 pixel subplots to reduce variation. Data were collected using the Zonal Statistics tool in ERDAS Imagine and placed into Microsoft Excel for statistical analysis.

Table 2.4: Variables used to predict visible crown diameter

Variable Type	**Name**
Landsat TM Bands	1
	2
	3
	4
	5
	7
Spectral Indices	Tasseled Cap Brightness
	Tasseled Cap Greenness
	Tasseled Cap Wetness
	Normalized Difference Vegetation Index
	Normalized Difference Moisture Index
Biophysical Values	Elevation (m)
	Slope (degrees)
	Aspect (degrees)
Other ancillary data	Site index
	Ownership

Final data formatting

All imagery containing data for the predictive RF model was set to the same extent to facilitate input into the predictive model. To save memory, a no data value of -9999 was applied to all imagery. ModelMap does not assign predictive values to pixels with value -9999. The imagery was then split into four parts to accommodate computer memory limits (Figure 2.1b). Numeric data extracted from the images were sorted by cover type: Hardwood (> 75% broadleaf), Mixed (>25 <75% broadleaf or coniferous), and Softwood (>75% coniferous). A raster Look Up Table was created in Microsoft

Excel that recorded the file locations of imagery used in the predictive model. This table is required for predictive mapping. All variables in the predictive model are displayed in Table 2.4.

Statistical analysis

Random forest analysis is robust to overfitting; therefore variable reduction techniques such as stepwise regression were unnecessary. All model variables (Table 2.4) were placed into an RF model using the ModelMap package in R v. 14.1, 64 bit version (Freeman and Frescino 2009, www.cran-r-project.org). Three models were run, one for each cover type (see above). RF models create a series of trees; each is constructed using a different bootstrap sample of the data. Within the trees, each node is split using the best subset of predictors randomly chosen at that node (Breiman 2001, Liaw and Weiner 2002). For this study, 500 trees were created for each model with five variables randomly chosen at each node. Only these five variables are searched at each node for the best split. The largest tree possible is grown and is not pruned (Breiman 2001).

Each model was tested on "out of bag" (OOB) predictors, which eliminated the need for an additional test set. Bagging constructs predictors using bootstrap samples then aggregates those predictors to form bagged predictors. Each bootstrap sample run leaves out about 37% of the examples; these left out examples (the out of bag predictors) can be used to form accurate estimates of error rates (Breiman 1996, Liaw and Weiner 2002). Output from testing models includes a variable importance plot and an observed vs. predicted plot. Variable importance plots depict two measurements of variable importance. The first is based on mean square error and relates to the prediction accuracy of the OOB examples after permuting each predictor variable. In the second measurement, all importance variables are averaged for an overall measure of importance (Prasad et al. 2006). Only the first measurement is presented in the results of this study. Partial dependence plots were created using the randomForests package in R (Liaw and Wiener 2002) to show the effects of changing individual predictors while holding all other predictors at their average (Thompson and Spies 2009). Two separate models were run for each cover type: one containing ownership and site index, both categorical variables, the other containing only continuous variables. This was done because the categorical data could not be used for predictive mapping. In addition to RF analysis, conditional inference trees, an implementation of regression tree analysis, were created. Conditional inference trees require a statistically significant difference as determined by Monte Carlo randomization to partition the data. This minimizes bias and prevents both overfitting and the need for pruning (Hothorn et al. 2006, Thompson and Spies 2009).

Predictive mapping

ModelMap handles predictive mapping by reading ERDAS Imagine image files into R then producing a series of ASCII grids that contain the predictions. The R package rgdal was used to read image files into R. After each predictive model was created in ModelMap, the predictive mapping function was carried out on the four pieces of the predictive map (Figure 2.1b) for all three models using the raster Look Up Table to locate and read in the explanatory variables. This created 12 output ASCII grids; four pieces for each of the three cover types. The output ASCII grids were imported into ERDAS Imagine for post processing.

Post processing of predictive maps

Output maps from ModelMap do not have a coordinate system; therefore they must be manually georeferenced. Before the pieces of the predictive maps could be mosaicked together, all maps needed to be georeferenced to the Landsat TM imagery used to create the predictive maps. The imagery was projected in the North American Datum (NAD) 1983 Universal Transverse Mercator (UTM) coordinate system, Zone 19N. For each map, 19-20 tie points were created that corresponded to locations on both the target and reference image. Ideal tie points are manmade locations such as road intersections that can clearly be seen on the target and reference images. The final root mean squared (RMS) error for three maps was below 0.5 pixel; the fourth map could not be rectified below an RMS error of 0.9 pixel after multiple tries. Nearest neighbor resampling was run to project the predictive maps into UTM Zone 19N, NAD 1983, with pixels snapped to the reference images to achieve the best fit. Georeferenced maps were mosaicked to create three final maps, one for each cover type.

The predictive maps have pixel values assigned to the entire extent of the input imagery. Since not all of the input imagery represented forest cover, existing data depicting harvest history and forest cover type were used to determine true locations of hardwood, softwood, and mixedwood forests that have not been harvested since 1972 (Legaard et al., manuscript in preparation, Noone et al. 2012). The harvest history and cover type data sets were masked over the predictive maps to create three final predictive maps of the study area that show average VCD on recent unharvested forest (Figure 2.1b).

Validation of predictive maps

Each final predictive map was validated using 2009 NAIP aerial photography (see above for more details on this dataset). Fifty additional validation plots were created for each predictive map; these plots were 10 x 10 Landsat TM pixels, or 300 m^2 in size. VCD was measured as previously described on five trees per plot, then an average crown diameter was calculated for each plot and compared to the average predicted crown diameter.

Results

Hardwood forest cover

Recent unharvested hardwood forest cover comprises 2.3% of the study area in 2007, or roughly 41,400 ha (Figure 2.5). Average predicted VCD of hardwood forest cover ranged from 8 to 10 m (Table 2.5). The random forests model explained 10.2% of the variance in hardwood visible crown diameter, with the five most important predictors being Tasseled Cap brightness, Landsat band 4, Landsat band 7, Landsat band 5, and Tasseled Cap greenness, respectively. Predictor importance was determined by the increase in mean square error in a model with that variable removed (Figure 2.6a). The model had a high RMSE (0.98 m) and a relatively low Spearman's correlation coefficient (rho=0.44). The model over-predicted low VCD values and under-predicted high VCD values (Figure 2.6b). The model correctly predicted average stand visible crown diameter in 82% of validation plots. The predictive model is presented in Table 2.6.

Table 2.5: VCD measurement details for the RF models

	Sample Size	**Minimum**	**Maximum**	**Mean**	**St. Dev.**
Hardwood	32	5.34 m	10.21 m	8.33 m	1.03 m
Mixedwood	297	4.7 m	9.94 m	7.06 m	1.13 m
Softwood	43	4.23 m	7.03 m	5.48 m	0.68 m

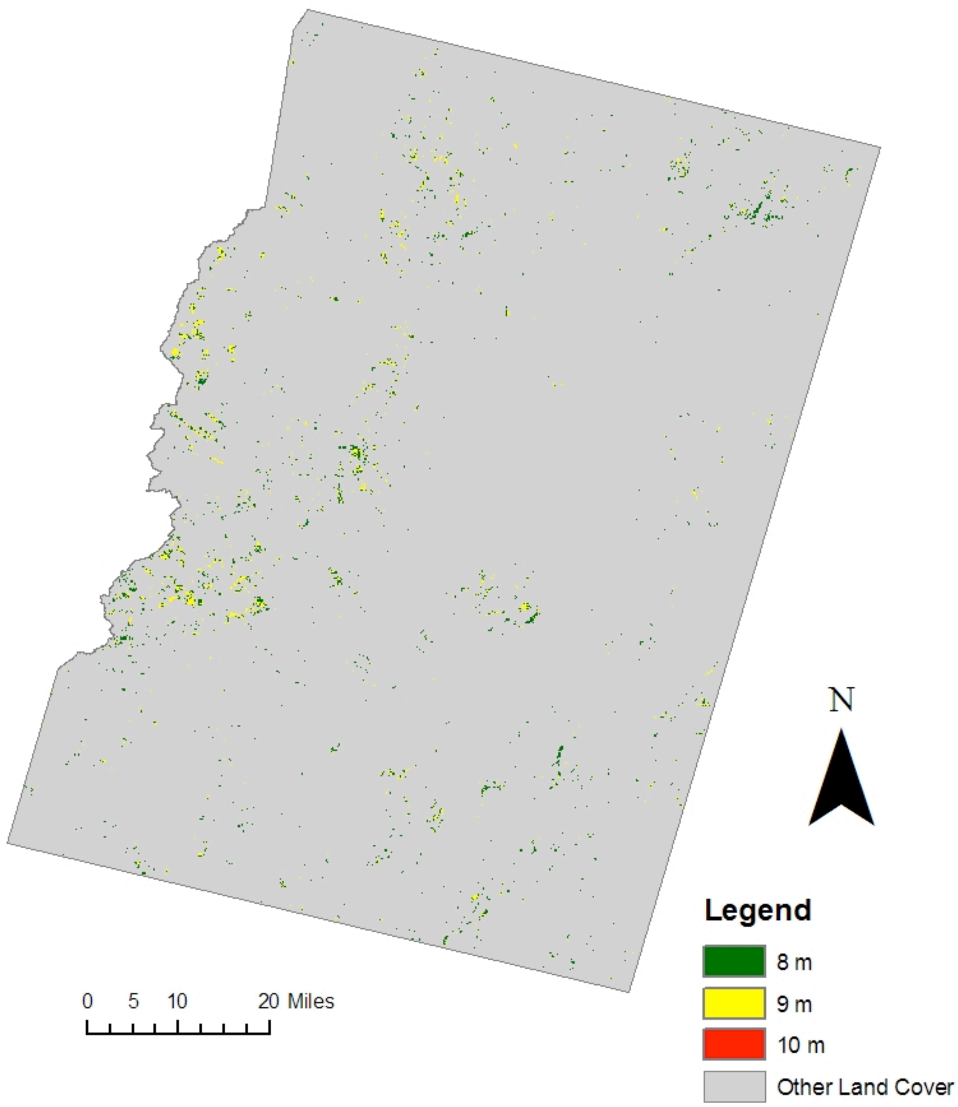

Figure 2.5: Map of predicted visible crown diameter of recent unharvested hardwood forest cover

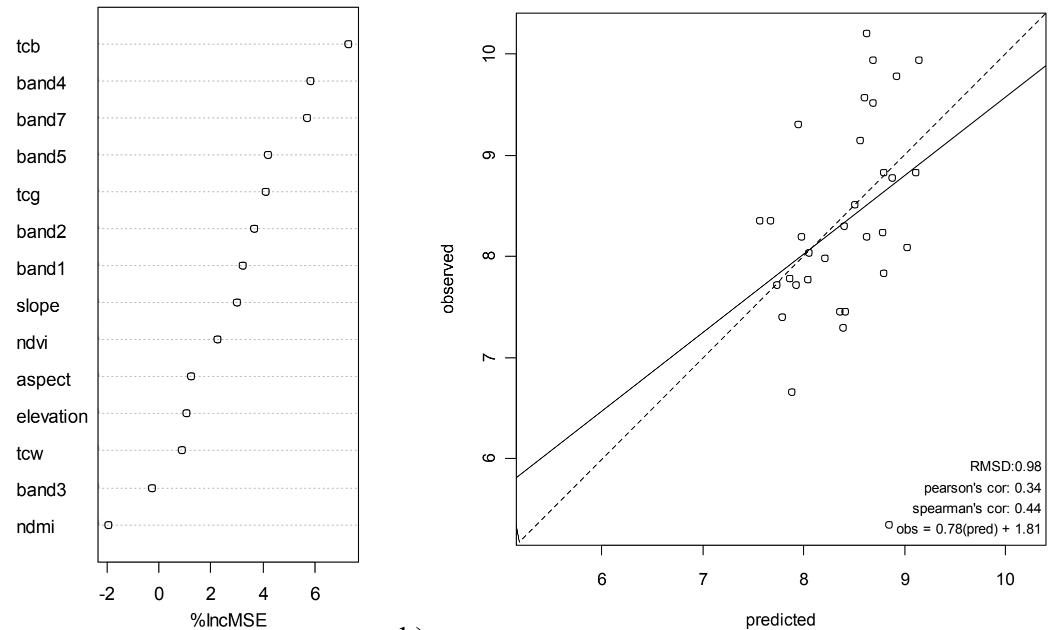

a) b)

Figure 2.6: a) Variable importance plot and b) scatterplot for hardwood forest cover random forests model

Table 2.6: Predictive models for recent unharvested hardwood, mixedwood, and softwood visible crown diameter

Forest Cover Type	**Equation**
Hardwood	y=0.78x+1.81
Mixedwood	y=0.98x+0.1
Softwood	y=0.95x+0.27

Partial dependence plots of the five most important variables in the model indicate the effect each variable has on hardwood VCD. All five variables are from TM spectral bands or derived indices. Average visible crown diameter increases with increasing spectral values for all five of the most important variables to a unique threshold value before tapering off and dropping steeply (Figure 2.7).

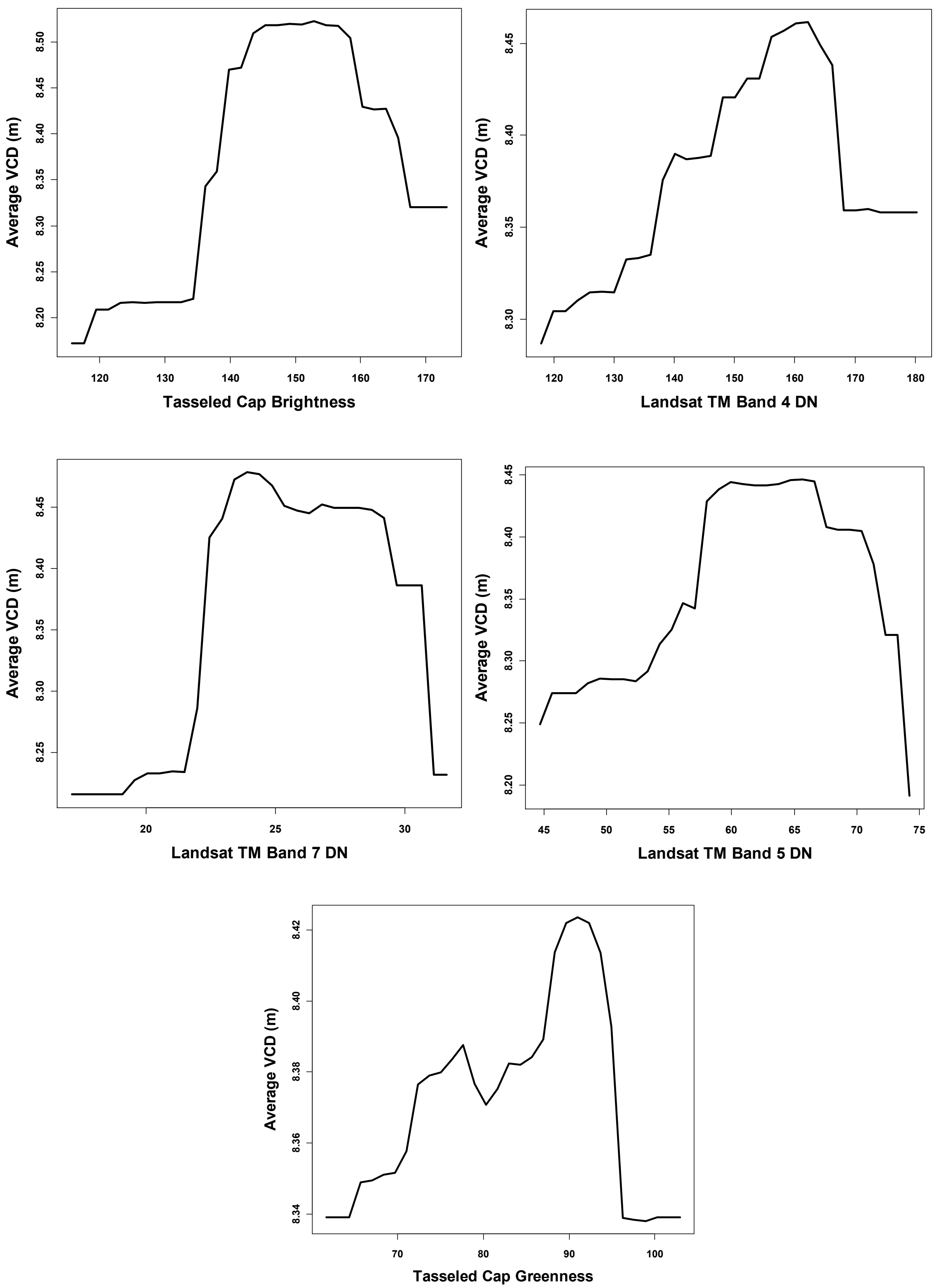

Figure 2.7: Partial dependence plots for the hardwood forest cover random forests model

The conditional inference tree for this model shows that none of the important variables in the random forests model are significant (Figure 2.8).

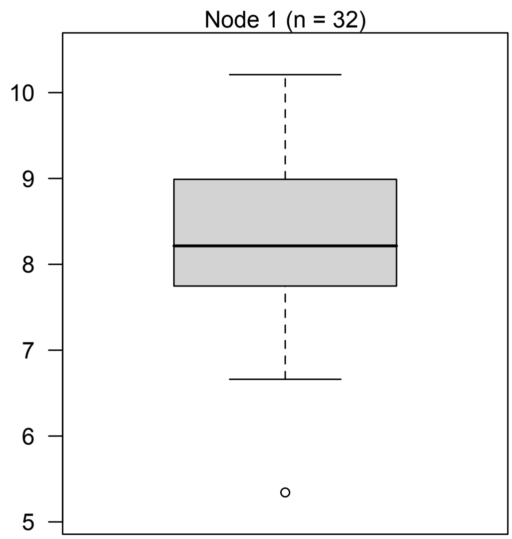

Figure 2.8: Conditional inference tree for the hardwood forest cover random forests model

Mixedwood forest cover

Recent unharvested mixedwood forest cover comprises 5.6% of the study area in 2007, or roughly 100,800 ha (Figure 2.9). Average visible crown diameter ranges from 7-9 m. The random forests model explained 42.75% in variance in mixedwood visible crown diameter, with the five most important variables being elevation, Landsat band 5, Tasseled Cap brightness, Tasseled Cap greenness, and slope, respectively. Predictor importance was determined by the increase in mean square error in a model with that variable removed (Figure 2.10a). The model had a high RMSE (0.86 m) but a satisfactory

Spearman's correlation coefficient (rho=0.65). This model also over predicted low values of VCD and under predicted high values of VCD (Figure 2.10b). The model correctly predicted average stand visible crown diameter in 74% of validation plots. The predictive model is presented in Table 2.5.

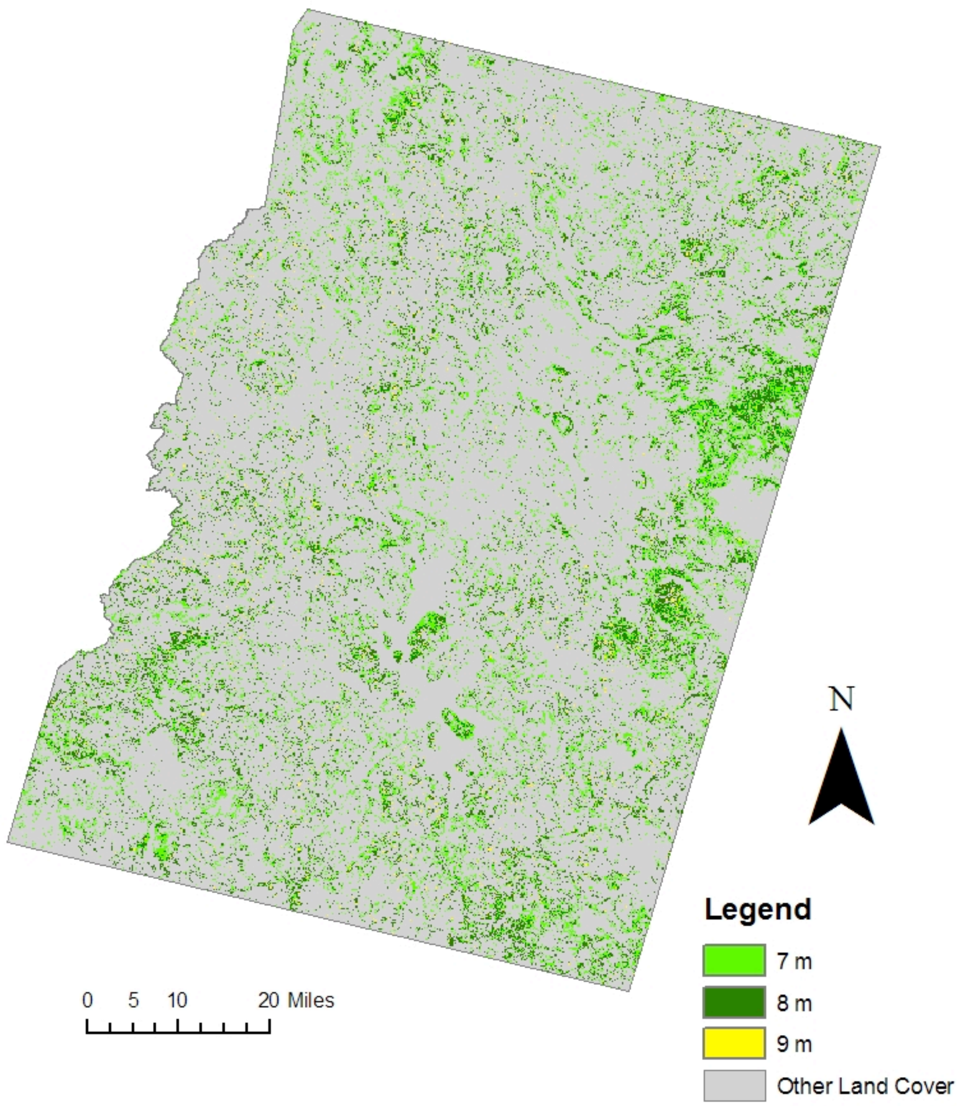

Figure 2.9: Map of predicted visible crown diameter of recent unharvested mixedwood forest cover

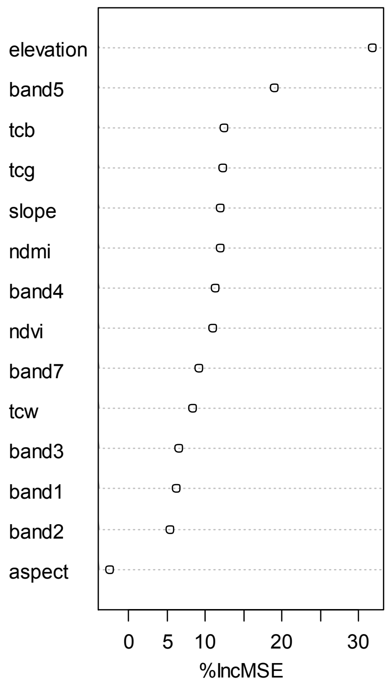

a)

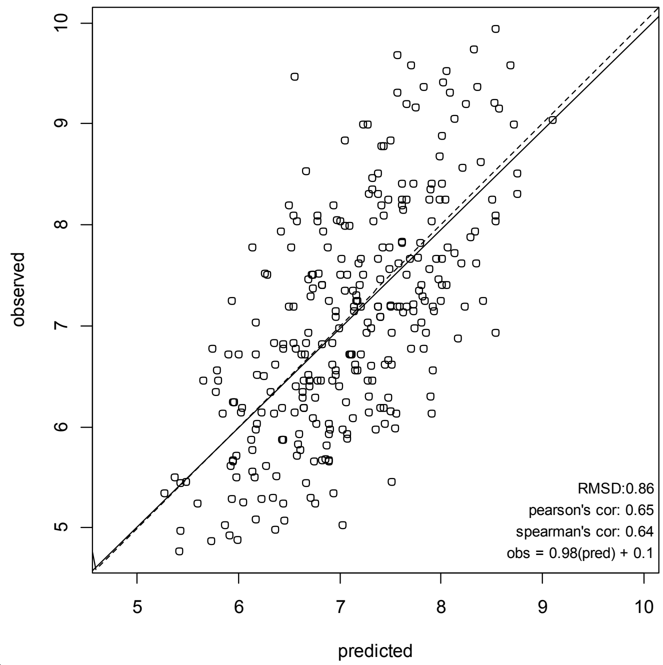

b)

Figure 2.10: a) Variable importance plot and b) scatterplot for the mixedwood forest cover random forests model

Partial dependence plots of the five most important variables show that average mixedwood forest VCD steadily decreases with increasing elevation and slope. Trees at higher elevations or on steeper slopes tend to be smaller than trees at lower elevations or gentle slopes. Digital numbers of the important spectral variables in the model increase with increasing visible crown diameter. This means that an increase in average VCD produces higher spectral values for Landsat TM band 5, Tasseled Cap brightness, and Tasseled Cap greenness (Figure 2.11).

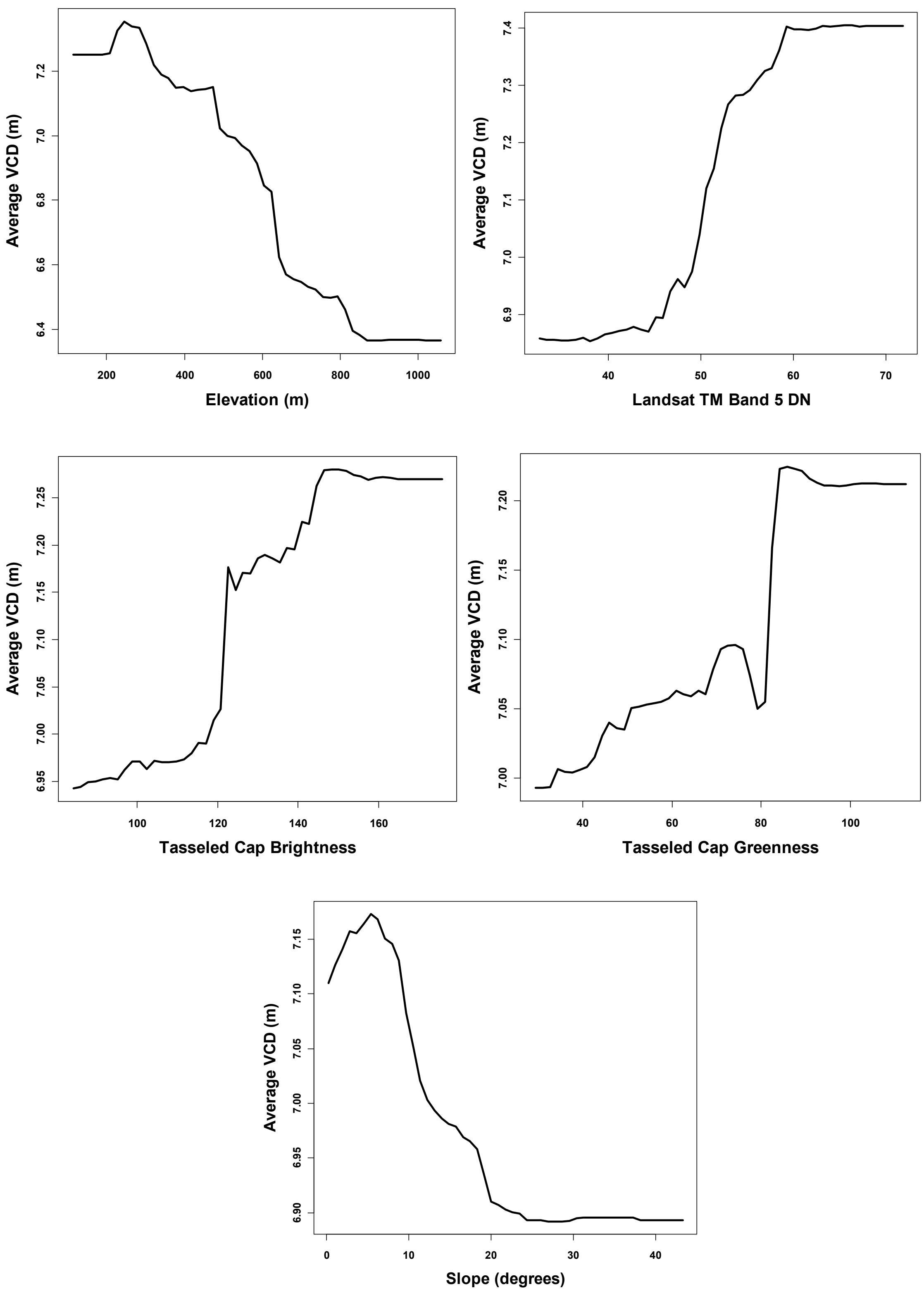

Figure 2.11: Partial dependence plots for the mixedwood forest cover random forests model

The conditional inference tree for this model shows that two of the variables, Landsat TM band 5 and elevation, have statistical significance. Landsat TM band 5 is the initial split of the conditional inference tree (p<0.001). It splits at a DN of 49.68, indicating a spectral difference between softwood dominant stands, which are darker on Landsat TM band 5 imagery and hardwood dominant stands. It splits again at a DN of 57.84, indicating hardwood dominant stands, which are brighter on Landsat TM band 5 imagery. Stands with larger average VCD were found at lower elevations and had higher Landsat TM band 5 reflectance values (Figure 2.12).

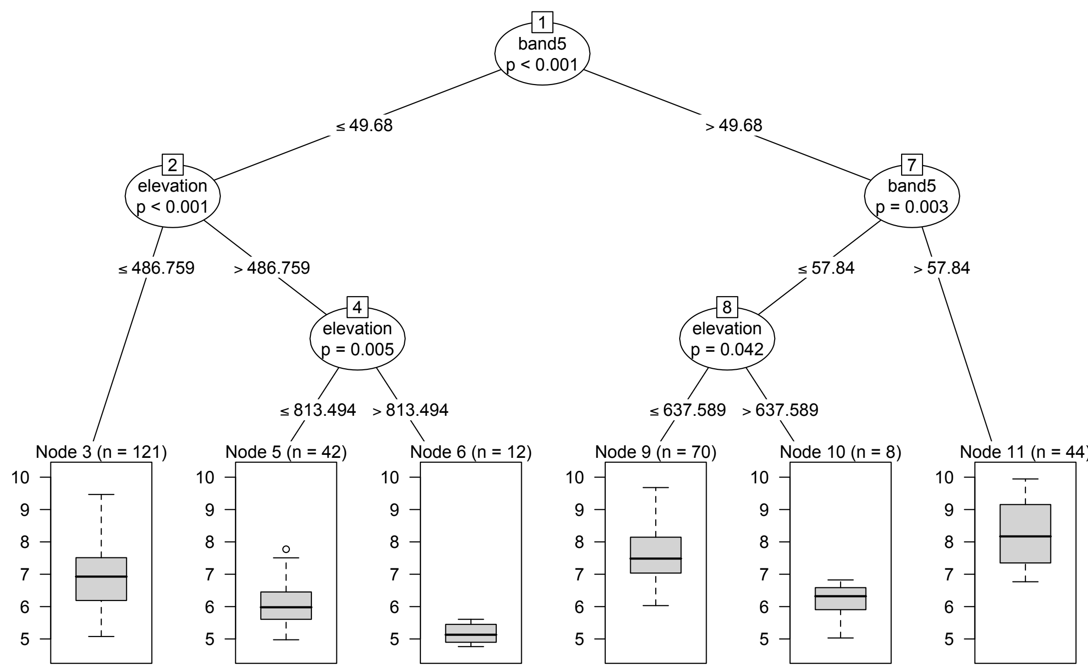

Figure 2.12: Conditional inference tree for the mixedwood forest cover random forests model.

Softwood forest cover

Softwood forest cover comprises 2.1% of the study area in 2007, or roughly 37,800 ha (Figure 2.13). Average visible crown diameter was 6 m. The random forests model explained 21.2% in variance in softwood visible crown diameter, with the five most important variables being elevation, slope, Landsat band 1, Normalized Difference Moisture Index (NDMI), and Tasseled Cap wetness, respectively. Elevation was by far the most important predictor in this model. Predictor importance was determined by the increase in mean square error in a model with that variable removed (Figure 2.14a). The model had a low RMSE (0.59 m) but a relatively low Spearman's correlation coefficient (rho=0.55). As with the hardwood model, the softwood model tends to under predict high VCD and over predict low VCD values (Figure 2.14b). The model correctly predicted average stand visible crown diameter in 84% of the validation plots. The predictive model is presented in Table 2.5.

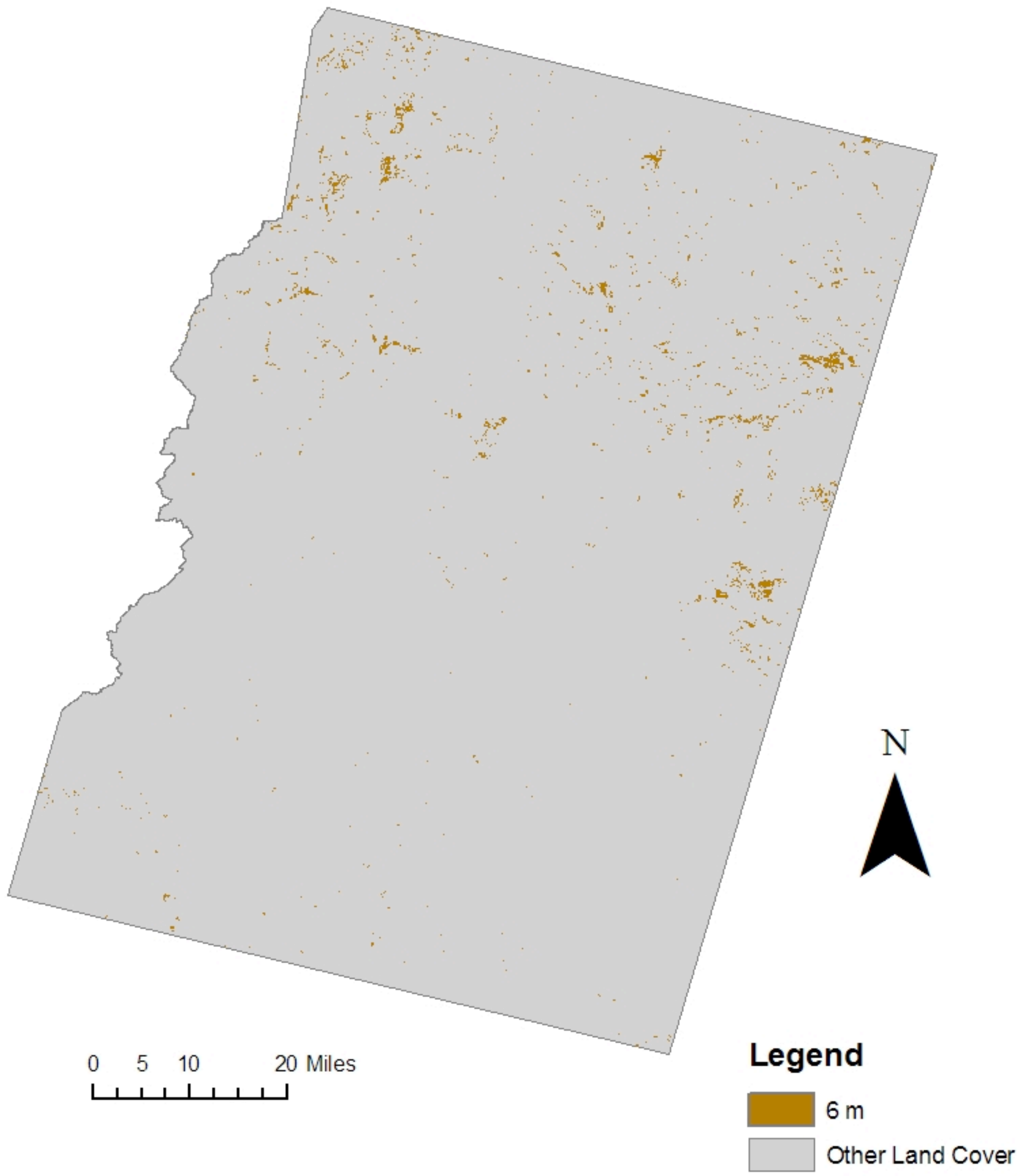

Figure 2.13: Map of predicted visible crown diameter of recent unharvested softwood forest cover

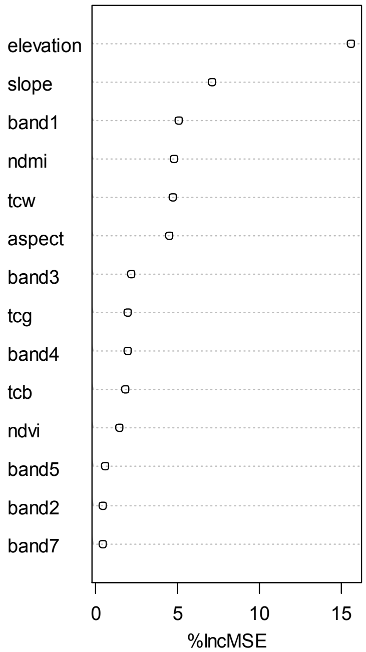

a)

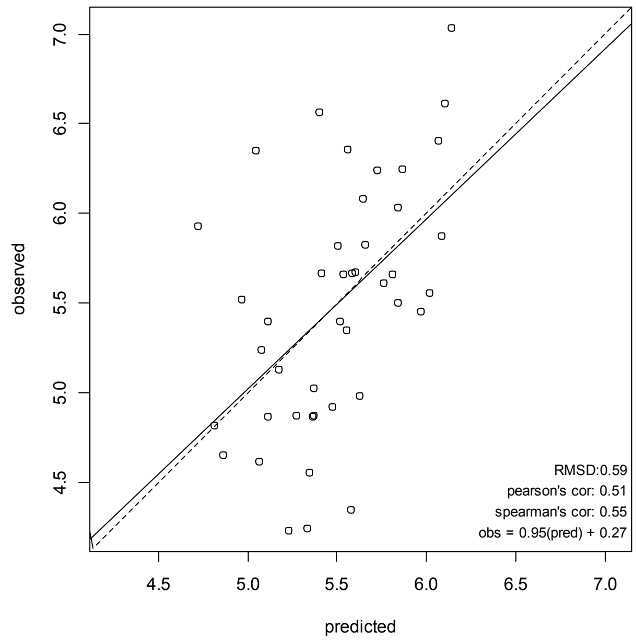

b)

Figure 2.14: a) Variable importance plot and b) scatterplot for the softwood forest cover random forests model.

Partial dependence plots of the five most important variables show that average softwood forest visible crown diameter decreases with increasing elevation and slope. As with mixedwood forest, tree crowns at higher elevations or on steeper slopes tend to be smaller than tree crowns at lower elevations or gentle slopes. Landsat band 1 DN values steadily increase with increasing softwood visible crown diameter, whereas the spectral indices NDMI and Tasseled Cap wetness increase with visible crown diameter to a threshold value before tapering off (Figure 2.15).

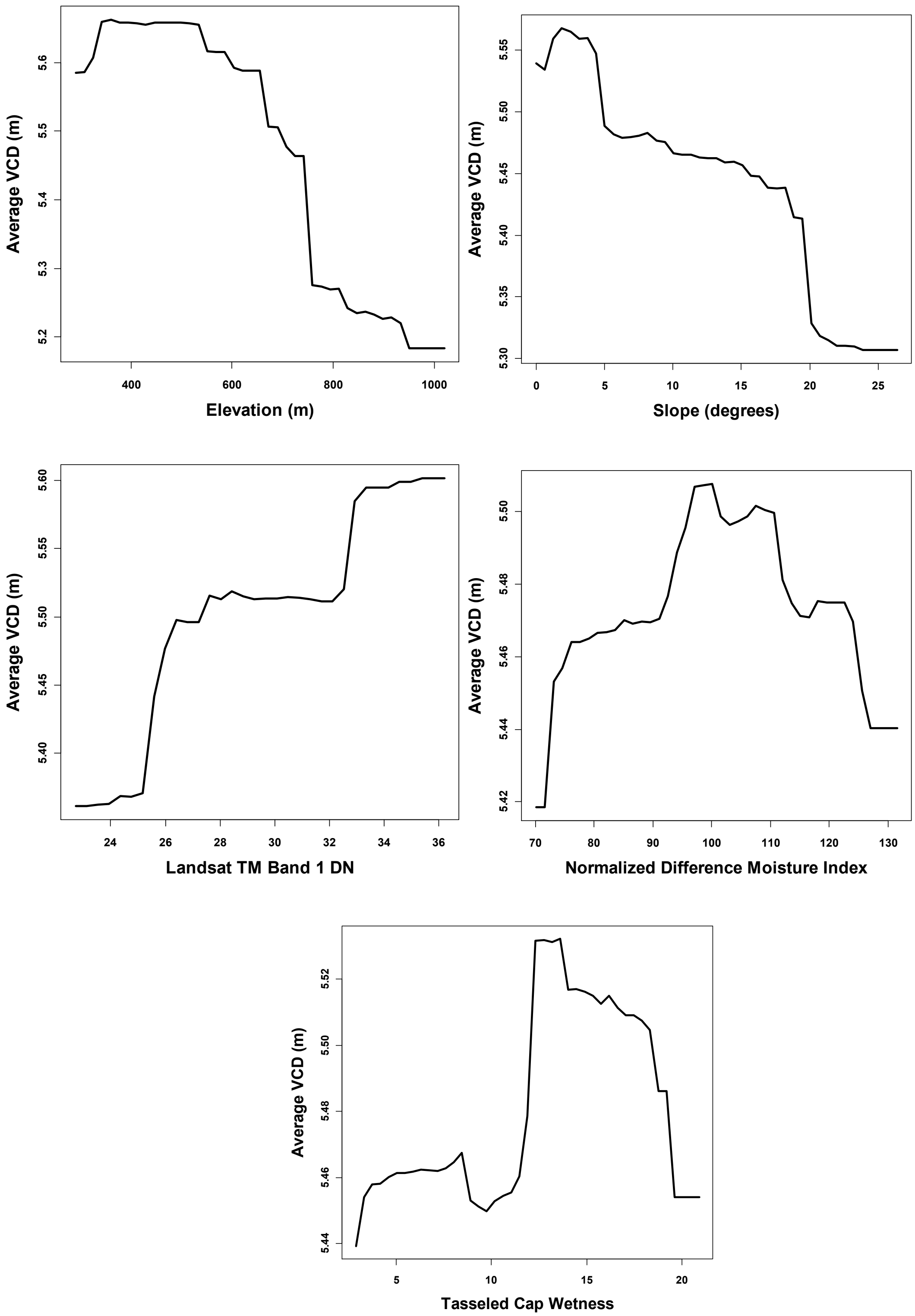

Figure 2.15: Partial dependence plots for the softwood forest cover random forests model.

The conditional inference tree for this model shows that only elevation is statistically significant in this model (p=0.006). Softwood trees above 728 m have smaller visible crown diameters than trees below 728 m (Figure 2.16).

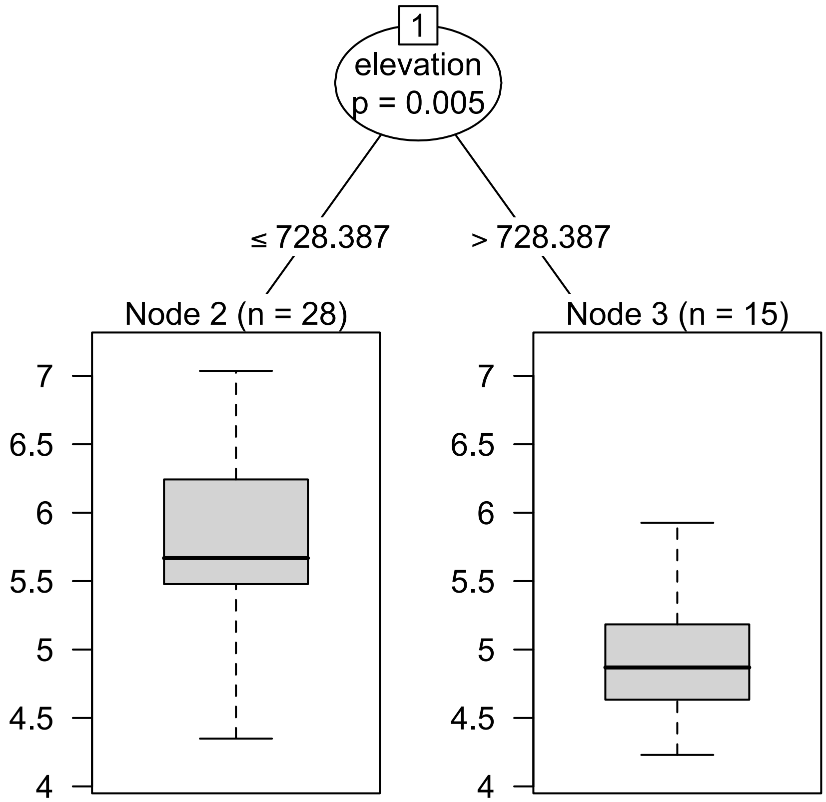

Figure 2.16: Conditional inference tree for the softwood forest cover random forests model.

Discussion

Variable relationships

All three cover types responded best to different combinations of spectral variables. Hardwood visible crown diameter corresponded most strongly with Tasseled

Cap brightness and greenness and Landsat TM bands 4, 5, and 7 (Figure 2.6a). These five variables all indicate the amount of vegetation on a landscape, lending an explanation to these results. Larger crowns will have more vegetation and thus higher spectral values (Crist and Cicone 1984, Wilson and Sader 2002, Li et al. 2009). Landsat TM band 7 has been found to correspond with hardwood biomass (Li et al. 2009), and it has been suggested that Tasseled Cap brightness may be more important in distinguishing between hardwood and softwood cover than Tasseled Cap greenness (Cohen et al. 2001). Landsat TM bands 5 and 7 and Tasseled Cap brightness are also positively correlated with vegetation density (Horler and Ahern 1986). Hardwood forests did not respond strongly to biophysical variables. There were no significant variables in the model (Figure 8) and the variance explained by the model was 10.2%. Although not included in the final predictive model, an exploratory partial dependence plot of the site index variable demonstrated that all hardwood plots had a Briggs site index of 1. This indicates that hardwood forests were only found on the best sites at low elevation in this study.

Mixedwood visible crown diameter had the strongest spectral response from Landsat TM band 5, Tasseled Cap brightness, and Tasseled Cap greenness. Li et al. (2009) found that Landsat TM band 5 corresponds with mixedwood forest biomass. Mixedwood visible crown diameter was significantly influenced by site elevation, and site slope also influenced VCD (Figs. 2.10, 2.11, and 2.12). These results suggest a basic ecological relationship; site quality declines rapidly at high elevations or on steep slopes, which is demonstrated in a site quality map derived from digital depth to water table data for Maine (CFRU 2006). When Cohen et al. (2001) used Tasseled Cap indices to predict visible crown diameter, they found that Tasseled Cap brightness had a stronger effect on VCD than on other stand variables, including vegetation cover and stand age. Tasseled Cap brightness had a strong response with hardwood and mixedwood forest cover; both indices increased with increasing VCD.

As in the mixedwood model, elevation and slope appear in the softwood VCD model as two of the most important variables. Elevation is the most important and only significant variable (Figs. 2.14a and 2.16). Higher elevations and steeper slopes produced smaller crown trees on shallow and less productive soils. The recent undisturbed softwood forests have lower average VCD and less variation compared to recent undisturbed hardwood and mixedwood forests. However, softwood VCD had a very different spectral response than recent undisturbed hardwood or mixedwood forest cover. Landsat TM band 1 was the third most important variable in the softwood VCD model, but it was not one of the important variables in the hardwood or mixedwood VCD models. Additionally, neither NDMI nor Tasseled Cap wetness are important variables in the other two models. NDMI and Tasseled Cap Wetness correlate with the amount of moisture in foliage and soil; Landsat TM band 1 is useful in softwood discrimination and may be sensitive to the amount of shadows in the canopy (Crist and Cicone 1984, Horler and Ahern 1986, Wilson and Sader 2002, Li et al. 2009). Landsat TM band 1 has been found to correlate with softwood biomass (Horler and Ahern 1986, Li et al. 2009). Several studies in western Oregon have found that Tasseled Cap wetness is the most effective spectral index for mapping age class information in closed canopy conifer stands. In these studies, Tasseled Cap wetness values remained steady with stand age, whereas Tasseled Cap greenness and brightness values declined (Cohen and Spies 1992, Fiorella and Ripple 1993, Cohen et al. 1995, Song et al. 2007). Perhaps the spectral response of recent unharvested softwood forest in Maine's northern forest is less of an effect of visible crown diameter as it is influenced by shadows in the canopy. Stand age could have an effect, as these softwood stands should be at least 35 years old. However, the trees in northern Maine are less likely to be old growth, and their size and structure is not directly comparable to the forests in Oregon.

Ecological implications

Forest harvest patterns have been extensively studied in Maine using Landsat time series imagery, even more so since the enactment of the Maine Forest Practices Act of 1989 (Fuller and Harrison 2000, Wilson and Sader 2002, Sader et al. 2003, Jin and Sader 2006). Comparatively, there have been few studies on recent unharvested forest in the state. The relatively long historical data archive of Landsat, dating back to 1972, provided an opportunity to narrow down where the distribution of older forests in Maine might be found. This study shows that 35+ year old forest covers 10.6% of the total study area, or roughly 190,800 ha in northwestern Maine. Whitman and Hagan (2007) described late successional forest as at least 100 years old; however, it is unknown how much of the RUF described in the current study is represented by late successional forest or old growth. Late successional forest is described based on ground measurements and floristic observations, such as the presence of certain lichen species. Late successional forests in Maine may not attain large stature compared to western forests due to differences in climate, site quality, and tree species. It is difficult to estimate how much of what is currently RUF in Maine will remain undisturbed into the future, and it is not possible to estimate the actual age of the RUF forest with the data sets available.

Recent changes in the forest ownership patterns in northern Maine may not bode well for the maintenance of the remaining older forest stands and their biodiversity (Hagan et al. 2005). Significant ownership change occurred within the study area throughout the 1990s and early 2000s. Major forestland owners in northwestern Maine today are Timber Investment Management Organizations (TIMOs) and Real Estate Investment Trusts (REITs) that are known to have different investment strategies and shorter-term forest management planning horizons, compared to the previous large industrial forest owners of the 20th century (Irland 2000, Hagan et al. 2005). These landowner groups have significantly higher harvest rates compared to other major Maine landowner types, including family-owned and longer-term non industrial private forest owners, conservation organizations, and state land holders (Jin and Sader 2006, Noone et al. 2012). Losing late successional and old growth forests may represent a major global threat to biodiversity (Noss 1999, Whitman and Hagan 2007).

Maine has an extensive network of ecological reserves throughout the state. These ecoreserves are mostly located on state lands owned by the Bureau of Public Lands (BPL) and the Department of Inland Fisheries and Wildlife (IFW). The Maine Natural Areas Program (MNAP) monitors these ecoreserves along with some private reserves owned by The Nature Conservancy and the Appalachian Mountain Club. Ecoreserve monitoring reports indicated that on average, these lands have higher stocking, more large trees, and older trees than the average Maine acre (MNAP 2005, 2009, and 2011). Average tree age in ecoreserves is still much younger than in late successional/old growth forests in the state. The size class distribution of the ecoreserves is closer to the idealized distribution for wildlife species proposed by DeGraaf et al. (1992) than the average Maine acre (MNAP 2009). However, most ecoreserves have evidence of harvesting activity, and variation in forest structure means that the ability to represent unmanaged forest is not consistent. The Maine Natural Areas Program is actively exploring the use of Landsat TM satellite imagery to monitor their lands, and the information gathered from this study may be beneficial to them as they look to expand their conservation efforts (MNAP 2011).

The residual RUF matrix consists primarily of smaller patches that are widely spread apart, indicating that there may be a loss of connectivity between these somewhat older stands (Mladenoff et al. 1993). This study supports the findings on forest fragmentation patterns from the first chapter of this thesis. The first chapter demonstrated that after 16 years of recent harvest, patches of unharvested forests in northern Maine were small and widely dispersed. Although no fragmentation metrics were measured for this chapter, a visual assessment shows that recent unharvested forest patches are also small and widely dispersed after 35 years of harvest (Figs. 2.5, 2.9, and 2.13). The first chapter demonstrated that mixedwood cover type was prevalent in the 16-year recent unharvested forests, a finding that can also be confirmed by visual assessment in this chapter (Figs. 1.13, 1.14, and 1.15), and quantitatively by the most area represented after 35 years of harvest (5.6%) compared to the other two forest types.

Management implications

Extensive harvesting practices break up the forest matrix into many small, separated patches (Mladenoff et al. 1993). A landscape scenario model in British Columbia, Canada demonstrated that in absence of natural disturbances, old growth habitat and large patches of forest of similar age and tree species composition decreased unless special management practices were applied. Multiple scenarios indicated complete loss of very large patches of older forest (>1000 ha) after 125 years of harvest, while the number of patches 0-80 ha in size markedly increased (Klenner et al. 2000). Potential management practices include establishing reserves on existing old growth forest, utilizing extended rotation zones, and aggregating harvesting blocks to preserve and maintain large patch sizes (Klenner et al. 2000).

Limitations

Recent undisturbed forest served as the primary source of information on visible crown diameter in this study. Using only RUF may leave out some large trees, such as seed trees left on partial harvesting sites. VCD predictions made in this study only apply to the RUF; a similar analysis on all forestland in northern Maine would require a new study. There are still unknown factors that affect the variance in VCD measurements.

These could include ecological variables, measurement procedures, or how foresters select land for harvesting.

Conclusions

Evaluation of models

The error rates for all three RF models were relatively high; all models predicted visible crown diameter within 1 m of measured VCD. The hardwood model had the highest error rate (RMSE=0.98 m) and the most variability in VCD measurements; the softwood model had the lowest error rate (RMSE=0.58 m) and the least variability in VCD measurements. The variability in VCD measurements can be attributed to crown shape; hardwood trees have crown shapes that are highly visible on aerial photography, whereas the conical crowns of softwood trees are more difficult to distinguish on aerial photography. This makes the hardwood crowns easier to measure and hence, more variable because there can be many different crown sizes measured. Softwood trees appear more uniform in size on aerial photography due to their crown shape (Paine and Kiser 2002).

Correlation coefficients for the three models indicate that there may be a better model to fit this data. Variance explained by all three models was low, meaning that there may be untested variables that could explain more of the variance in visible crown diameter in Maine’s older forests. Statistical significance occurred in two of the three models. Data collection methods may have affected the outcome of the models. Partial dependence plots (Figs 2.7, 2.11, and 2.15) have a stepped appearance, possibly indicating a high number of tree crowns measured in the median range and a low number of tree crowns measured at the extremes of VCD distributions. RF methods may not be as robust to over-fitting and bias when the sample size is less than 100, which occurred in both the hardwood and softwood models (Table 2.5) (Aaron Weiskittel, 2012, personal communication). Further research is required to determine if different modeling methods could produce a better fitting model for visible crown diameter prediction of recently unharvested forests in Maine.

Evaluation of methodology

The unique combination of methods used in this study achieved the objective of predicting visible crown diameter on recent undisturbed forests in Maine. The addition of the NASA U2 photography provided a look at unharvested stands in 1972, which verified forest presence at the beginning of the 35-year Landsat time series and allowed approximate harvest stage to be determined so that only the oldest stands would be included in the sample plots. The digitized NAIP 2009 aerial photography simplified the process of measuring visible crown diameter. The random forests statistical framework was successfully utilized in this study. The combination of spectral indices and Landsat TM bands in an RF model led to the detection of unique spectral relationships based on cover type in recent undisturbed forest and the addition of biophysical variables proved important for predicting mixedwood and softwood visible crown diameter. The

ModelMap package (Freeman and Frescino 2009) predicted visible crown diameter across the study area, and the results indicated differences in VCD ranges among the three cover types. This methodology is repeatable in other regions, provided there is access to historical aerial photography and reliable map information or ground data that could verify the presence of undisturbed forest at earlier dates. Harvest history and land cover type data of the study area are needed to refine ModelMap output. Biophysical variables derived from available geographic information system archives may improve the models depending on the particular regions and topography where the research is conducted.

The inherent weakness of this methodology is that there are no ground-based measurements involved for validation of model development. Only one study that was reviewed for this project did not include ground-based measurements (Cohen et al. 2001). However, both this study and the work of Cohen et al. (2001) were able to produce satisfactory results using the model predictions and validation based on traditional photo interpretation and photogrammetric measurements on high-resolution aerial photography. VCD measurements are usually not taken on the ground in most inventory programs. Ground-based measurements are both time consuming and costly, but the U.S. Forest Service's Forest Inventory and Analysis (FIA) program collects measurements such as stand age and bole diameter at breast height (dbh) annually on 20% of total sample plots (each plot is measured once every 5 years) for the state of Maine. Only one plot is represented every 6000 acres and the plot size is 1/10 acre, much smaller than one Landsat pixel, making spatial comparisons difficult (Noone et al. 2012). FIA diameter data was the basis for the studies of the Northwest Forest Plan that inspired this project (Weyermann and Fassnacht 2000, Moeur et al. 2005, Healey et al. 2008). There is a strict confidentiality agreement with respect to plot locations; therefore, FIA data were not available for this study. Using these data might provide adequate ground truthing, but it could do so at the expense of efficiency, time, and money (Weyermann and Fassnacht 2000) compared to the traditional image interpretation and digital plot measurement methods presented in this study.

Future Work

The methodology presented in this study is promising, but it will require modifications before it can be utilized easily and effectively. Stand age information from FIA data would ensure that older stands are being tested, and stand diameter information from FIA data would provide a validation source for model predictions. Tree height measurements taken either from the ground or from aerial photography could provide insight to the structure of recent undisturbed forests; however, recent public domain sources of high resolution digital imagery are not available with stereo coverage, which is needed for height measurements. Incorporating field work may aid in discovering truly old growth stands by using a field-based assessment to determine if a stand is old growth or late successional in Maine (Whitman and Hagan 2007). If crown diameter is to be measured in the field, measurements should focus on dominant or codominant trees; these are often the trees visible in aerial imagery (Cohen et al. 1995). If field work is cost-prohibitive, Fiorella and Ripple (1993) have described old growth and late successional forest characteristics in Oregon on Landsat TM imagery. These characteristics, including a strong spectral response to Tasseled Cap Wetness for coniferous forests, could be used to refine the predictive model. TCW exhibited a strong response in softwood cover in the RUF. Expanding the existing harvest time series to cover the entire state would provide a record of older, unharvested forests throughout Maine, but such a project would be very time consuming.

LITERATURE CITED

Avery, T.E., 1967. Forest Measurements. New York: McGraw-Hill.

Bacon, L., and Bouchard, R. 1997. Geographic analysis and categorization of Maine lakes: a trial of the draft lake bioassessment and biocriteria technical guidance. Maine Department of Environmental Protection, Augusta, ME: 26 pp.

Beaty, M., Finco, M., Morrison, M., and Maiersperger, T. 2008. Using model II regression for radiometrically matching landsat images over very large areas. In: McWilliams, W., Moisen, G., and Czaplewski, R. (Eds.), Forest Inventory and Analysis Annual Symposium [CD-ROM], October 21-23, 2008, Park City, UT.

Boer, A. 1978. Management of deer wintering areas in New Brunswick. Wildlife Society Bulletin 6: 200-205.

Breiman, L. 1996. Bagging predictors. Technical Report No. 421. Department of Statistics, Univeristy of California, Berkeley, CA. 19 pp.

Breiman, L. 2001. Random forests. Machine Learning 45: 5-12.

Briggs, R.D. 1994. Site Classification Field Guide. Maine Agriculture and Forest Experiment Station Miscellaneous Publication 724. University of Maine, Orono.

Briggs, N.A., and Sader, S.A. 2009. Tracking forest change and development using low cost remote sensing imagery and GIS integration. Northern Journal of Applied Forestry 26: 148-155.

Brittingham, M.C. and Temple, S.A. 1983. Have cowbirds caused forest songbirds to decline? Bioscience 33:31-35.

Brown, S. Schroeder, P., and Birdsey, R. 1997. Aboveground biomass distribution of US eastern hardwood forests and the use of large trees as an indicator of forest development. Forest Ecology and Management 96: 37-47.

Cary, A. 1894. On the growth of spruce. p. 20-36 in Second annual report, Maine Forest Commissioner, Augusta, ME.

Cary, A, 1986. Report of Austin Cary. p. 15-203 in Third annual report, Maine Forest Commissioner, Augusta, ME.

Chander, G., Markham, B.L., and Helder, D.L. 2009. Summary of current radiometric calibration coefficients for Landsat MSS, TM, ETM+, and EO-1 ALI sensors. Remote Sensing of Environment 113: 893-903.

Chokkalingam, U., and White, A.S. 2000. Structure and spatial patterns of trees in old growth northern hardwood and mixed forests of northern Maine. Plant Ecology 00: 1-22.

Cohen, W.B., Spies, T.A., and Fiorella, M. 1995. Estimating the age and structure of forests in a multi-ownership landscape of western Oregon, USA. International Journal of Remote Sensing 16: 721-746.

Cohen, W.B., Maiersperger, T.K., Spies, T.A., and Oetter, D.R. 2001. Modelling forest cover attributes as continuous variables in a regional context with Thematic Mapper data. International Journal of Remote Sensing 22: 2279-2310.

Cohen, W.B., Maiersperger, T.K., Gower, S.T., and Turner, D.P. 2003. An improved strategy for regression of biophysical variables and Landsat ETM+ data. Remote Sensing of Environment 84: 561-571.

Colby Environmental Policy Group. 2007. State of Maine's Environment 2007. Colby College Environmental Studies Program, Waterville, ME: 171 pp.

Cooperative Forestry Research Unit. 2006. Digital Depth to Ground Water Data Layer. The University of Maine, http://www.umaine.edu/cfru/index.htm

Crist, E.P., and Cicone, R.C. 1984. A physically-based transformation of thematic mapper data the TM tasseled cap. IEEE Transactions on Geoscience and Remote Sensing 22: 256-263.

Cushman, S.A., McGarigal, K., and Neel, M.C. 2004. Parsimony in landscape metrics: strength, universality, and consistency. Ecological Indicators 8: 691-703.

DeGraaf, R.M., Yamasaki, M., Leak, W.B., and Lanier, J.W. 1992. New England wildlife: management of forested habitats. Gen. Tech. Rep. NE-144. Radnor, PA: U.S. Department of Agriculture, Forest Service, Northeastern Forest Experiment Station. 271 p.

Falkowski, M.J., Evans, J.S., Martinuzzi, S., Gessler, P.E., and Hudak, A.T. 2009. Characterizing forest succession with lidar data: an evaluation for the Inland Northwest, USA. Remote Sensing of Environment 113: 946-956.

Fiorella, M., and Ripple, W.J. 1993. Determining successional stage of temperate coniferous forests with Landsat satellite data. Photogrammetric Engineering and Remote Sensing 59: 239-246.

Franklin, J.F., and Forman, R.T.T. 1987. Creating landscape patterns by forest cutting: ecological consequences and principles. Landscape Ecology 1: 5-18.

Franklin, S., Moskal, L., Lavigne, M., and Pugh, K. 2000. Interpretation and classification of partially harvested forest stands in the Fundy model forest using multitemporal Landsat TM digital data. *Canadian Journal of Remote Sensing* 26:318-333.

Freeman, E.A., and Frescino. T.A. 2009. ModelMap: an R package for modeling and map production using random forest and stochastic gradient boosting. USDA Forest Service, Rocky Mountain Research Station, 507 25th St., Ogden, UT, USA. eafreeman@fs.fed.us, URL: http://cran.rproject.org/web/packages/ModelMap/index.html.

Fuller, A.K, and Harrison, D.J. 2005. Influence of partial timber harvesting on American martens in north-central Maine. Journal of Wildlife Management 69: 710-722.

Gering, L.R., and May, D.M. 1995. The relationship of diameter at breast height and crown diameter for four species groups in Hardin County, Tennessee. Southern Journal of Applied Forestry 19: 177-181.

Hagan, J. M., Irland, L.C., and Whitman, A.A. 2005. Changing timberland ownership in the northern forest and implications for biodiversity. Manomet Center for Conservation Sciences, Report# MCCS-FSP-2005-1, Brunswick, ME. 34 pp.

Harris, L.D. 1984. The fragmented forest: island biogeography theory and the preservation of biotic diversity. University of Chicago Press, 287 pp.

Healey, S.P., Cohen, W.B., Spies, T.A, Moeur, M., Pflugmacher, D., German Whitley, M., and Lefsky, M. 2008. The relative impact of harvest and fire upon landscape level dynamics of older forests: lessons from the northwest forest plan. Ecosystems 11: 1106-1119.

Hepinstall, J.A., Sader, S.A., Krohn, W.B., Boone, R.B., and Bartlett, R.I. 1999. Development and testing of a vegetation and land cover map of Maine. Maine Agricultural and Forest Experimentation Station. University of Maine. Technical Bulletin 173. p 104.

Horler, D., and Ahern, F. 1986. Forestry information content of Thematic Mapper data. *International Journal of Remote Sensing* 7: 405-428.

Hosmer, R.S. 1902. A study of the Maine spruce. In: 4th Rept. Maine Forest Commissioner, Augusta, ME.

Hothorn, T., Hornik, K., Zeileis, A. 2006. Unbiased recursive partitioning: a conditional inference framework. Journal of Computational and Graphic Statistics 15: 651-674.

Hughes, J.W., and Bechtel, D.A. 1997. Effect of distance from forest edge on regeneration of red spruce and balsam fir in clearcuts. Can. J. For. Res. 27: 2088-2096.

Hunter, M.L. 2002. Fundamentals of Conservation Biology 2nd Ed. Blackwell Science Ltd, Oxford, UK

Irland, L. 1996. Land, timber, and recreation in Maine's northwoods. Maine Agriculture and Forest Experiment Station Miscellaneous Publication 730. University of Maine, Orono.

Irland, L., 2000. Maine forests: a century of change, 1900–2000 and elements of policy change for a new century. In: Maine Policy Review, Winter, 2000, University of Maine, Orono, ME, pp. 66–77.

Jin, S., and Sader, S.A. 2005. Comparison of time-series tasseled cap wetness and the normalized difference moisture index in detecting forest disturbances. Rem. Sens. Environ. 94: 364–372.

Jin, S., and Sader, S.A. 2006. Effects of forest ownership and change on forest harvest rates, types, and trends in Northern Maine. Forest Ecology and Management 228: 177–186.

Klenner, W., Kurz, W., and Beukema, S. 2000. Habitat patterns in forested landscapes: management practices and the uncertainty associated with natural disturbances. Computers and Electronics in Agriculture 27: 243-262.

Laustsen, K.M., Griffith, D.M., and Steinmann, J.R. 2003. Fourth annual inventory on Maine's forests. Augusta, ME: Maine Forest Service, Department of Conservation, 48 pp.

Li, M., Qu, J.J., and Hao, X. 2009. Estimating aboveground biomass for different forest types based on Landsat TM measurements. In Geoinformatics, 17th international conference on. August 12-14, 2009, Fairfax, VA. pp. 1-6.

Li, X., He, H.S., Bu, R.,Wen, Q., Chang, Y., Hu, Y., Li, Y., 2005. The adequacy of different landscape metrics for various landscape patterns. Pattern Recognition 38: 2626–2638.

Liaw, A., Wiener, M. 2002. Classification and regression by random forest. R News 2: 18-22.

Lillesand T. M. & Kiefer R. W., 2000. Remote Sensing and Image Interpretation, 4th ed. Wiley & Sons, Hoboken, NJ.

Lorimer, C.G. 1977. The presettlement forest and natural disturbance cycle of northeastern Maine. Ecology 58: 139-148.

Maine Forest Service, 1999. State of the Forest and Recommendations for Forest Sustainability Standards. http://www.state.me.us/doc/mfs/sofjun12. PDF.

Maine Forest Service, 2007. Silvicultural Activities Report. http://www.maine.gov/doc/mfs/pubs/pdf/silvi/07silvi.pdf. PDF.

Maine Critical Areas Program 1983. Natural old-growth forest stands in Maine and its relevance to the Critical Areas program. Planning report No. 77, Maine Critical Areas Program of the State Planning Office, Augusta, ME. 248 pp.

Maine Natural Areas Program. 2005. Ecological reserve monitoring project update. Maine Department of Conservation, Augusta, ME. 24 pp.

Maine Natural Areas Program. 2009. Ecological reserve monitoring summary report. Maine Department of Conservation, Augusta, ME. 14 pp.

Maine Natural Areas Program. 2011. Ecological monitoring in the 21st century: harnessing emerging technologies for tracking changes in Maine's ecological reserves. Maine Department of Conservation, Augusta, ME. 13 pp.

McGarigal, K., Cushman, S.A., Neel, M.C., and Ene, E.. 2002. FRAGSTATS: Spatial Pattern Analysis Program for Categorical Maps. Computer software program produced by the authors at the University of Massachusetts, Amherst. Available at the following web site: http://www.umass.edu/landeco/research/fragstats/fragstats.html

McMahon, J. 1990. The biophysical regions of Maine: patterns in the landscape and vegetation. University of Maine, Thesis (M.S.).

McWilliams, W.H., Butler, B.J., Caldwell, L.E., Griffith, D.M., Hoppus, M.L., Laustsen, K.M., Lister, A.J., Lister, T.W., Metzler, J.W., Morin, R.S., Sader, S.A., Stewart, L.B., Steinman, J.R., Westfall, J.A., Williams, D.A., Whitman, A., Woodall, C.W., 2005. The forests of Maine: 2003. Resource Bull. NE-164. U.S. Department of Agriculture, Forest Service, Northeastern Research Station, Newtown Square, PA. 188 p.

Mladenoff, D.J., White, M.A., and Pastor, J. 1993. Comparing spatial pattern in unaltered old growth and disturbed forest landscapes. Ecological Applications 3: 294-306.

Moeur, M., Spies, T.A., Hemstrom, M., Martin, J.R., Alegria, J., Browning, J., Cissel, J., Cohen, W.B., Demeo, T.E., Healey, S., Warbington, R. 2005. Northwest forest plan—the first 10 years (1994-2003): status and trend of late successional and old growth forest. General Technical Report PNW-GTR-646. Portland, OR: U.S. Department of Agriculture, Forest Service, Pacific Northwest Research Station. 142 pp.

Montgomery, D.R., Grant, G.E., and Sullivan, K. 1995. Watershed analysis as a framework for implementing ecosystem management. Water Resources Bulletin 31:369-386.

Neel, M.C., McGarigal, K., and Cushman, S.A. 2004. Behavior of class-level landscape metrics across gradients of class aggregation and area. Landscape Ecology 19: 435-455.

Noone, M.D. 2010. Forest change and cover type monitoring and evaluation of disturbance influences in Maine: 1991-2007. University of Maine, Thesis (M.S.).

Noone, M.D. Sader, S.A., and Legaard. K.R. 2012. Are forest disturbances influenced by ownership change conservation easement status and land certification? Forest Science 28: 119-129.

Noss, R.F. and Csuti, B. 1997. Habitat Fragmentation. In Principles of Conservation Biology (2nd ed.) eds. G.K. Meffe and R.C. Carroll, 269-304, Sunderland, MA, Sinauer Associates.

Ohmann, J.L., and Gregory, M.J. 2002. Predictive mapping of forest composition and structure with direct gradient analysis and nearest neighbor imputation in coastal Oregon, USA. Canadian Journal of Forest Resources 32: 725-741.

Olson, M.G. and Wagner, R.G. 2010. Long term compositional dynamics of Acadian mixedwood stands under different silvicultural regimes. Canadian Journal of Forest Resources 40: 1993-2002.

Paine, D.P., and Kiser, J.D. 2002. Aerial Photography and Image Interpretation (2nd ed.). John Wiley & Sons, Hoboken, NJ. pp. 481-508.

Powell, S.L., Cohen, W.B., Healey, S.P., Kennedy, R.E., Moisen, G.G., Pierce, K.B., Ohmann, J.L. 2010. Quantification of live aboveground biomass dynamics with Landsat time-series and field inventory data: a comparison of empirical modeling approaches. Remote Sensing of Environment 114: 1053-1068.

Prasad, A.M., Iverson, L.R., and Liaw, A., 2006. Newer classification and regression tree techniques: bagging and random forests for ecological prediction. Ecosystems 9: 181-199.

Price, J.C. 1981. The contribution of thermal data in Landsat multispectral classification. Photogrammetric Engineering and Remote Sensing 47: 229-236.

Rice, R. 2003. Issues in Maine's Natural Resources Industries—A Brief Review of the Pulp and Paper Industry, College of Nautral Sciences, Forestry, and Agriculture White Papers, University of Maine, Orono. 2 pp.

Riitters, K.H., Wickham, J.D., O'Neill, R.V., Jones, J.B., Smith, E.R., Coulston, J.W., Wade, T.G., and Smith, J.H. 2000. Fragmentation of continental United States forests. Ecosystems 5: 815-822.

Ripple, W.J., G.A. Bradshaw, and Spies, T.A. 1991. Measuring Forest Landscape Patterns in the Cascade Range of Oregon, USA. Biological Conservation. 57:73-88.

Sader, S.A., Bertrand, M., and Hoffhine Wilson, E. 2003. Satellite Change Detection of Forest Harvest Patterns on an Industrial Forest Landscape. Forest Science 49: 341-353.

Sader, S.A., M. Hoppus, J. Metzler, and S. Jin. 2005. Perspectives of Maine forest cover change from Landsat imagery and forest inventory analysis (FIA). Journal of Forestry 103: 299-303.

Sader, S.A., S. Jin, J.W. Metzler, and M. Hoppus. 2006. Exploratory analysis of forest harvest and regeneration pattern among multiple landowners. Forestry Chronicle 82: 203-210.

Sader, S.A., and Legaard, K.R. 2008. Inclusion of forest harvest legacies, forest type, and regeneration spatial patterns in updated forest maps: a comparison of mapping results. *Forest Ecology and Management* 255: 3846-3856.

Saunders, M.R, Fraver, S., and Wagner, R.G. 2011. Nutrient concentration of down woody debris in mixedwood forests in central Maine, USA. Silva Fennica 45(2): 197-210.

Schroeder, T.A., Cohen, W.B., Song, C., Canty, M.J., Yang, Z. 2006. Radiometric correction of multi-temporal Landsat data for characterization of early successional forest patterns in western Oregon. Remote Sensing of Environment 103: 16-26.

Seymour, R. S. 1992. The red spruce-balsam fir forest of Maine: Evolution of silvicultural practice in response to stand development patterns and disturbances. Ch. 12 (p. 217-244) In: Kelty, M. J., Larson, B. C. and Oliver, C. D., eds. *The Ecology and Silviculture of Mixed-species forests*. A festschrift for David M. Smith. Kluwer Publishers, Norwell, MA. 287 p.

Simons, E.M. 2009. Influences of past and future forest management on the spatiotemporal dynamics of habitat supply for American martens and Canada lynx in northern Maine. University of Maine, Thesis (Ph.D.)

Small Woodland Owners Association of Maine (SWOAM). 2005. Small woodland owner's handbook: a guide to owning and managing woodland in Maine, 2nd ed.. Augusta, ME: Small Woodland Owners Association of Maine.

Song, C., Schroeder, T.A., and Cohen, W.B. 2007. Predicting temperate conifer forest successional stage distributions with multitemporal Landsat Thematic Mapper imagery. Remote Sensing of Environment 106: 228-237.

Tinker, D.B., Resor, C.A.C, Beauvais, G.P., Kipfmuller, K.F., Fernandes, C.I., and Baker, W.L. 1998. Watershed analysis of forest fragmentation by clearcuts and roads in a Wyoming forest. Landscape Ecology 13: 149-165.

Thompson, J.R., and Spies, T.A. 2009. Vegetation and weather explain variation in crown damage within a large mixed-severity wildfire. Forest Ecology and Management 258: 1684-1694.

Tyrrell, L., Nowacki, G., Crow, T., Buckley, D., Nauertz, E., Niese, J., Rollinger, J., Zasada, J. 1998. Information about old growth for selected forest type groups in the eastern United States. GTR-NC-197. St. Paul, MN. USDA Forest Service NC Research Station. 507 pp.

Weyermann, D., Fassnacht, K., 2000. The Interagency Vegetation Mapping Project: estimating certain forest characteristics using Landsat TM data and forest inventory plot data. In: Greer, J.D. (Ed.), Remote Sensing and Geospatial Technologies for the New Millenium: Proceedings of the Eighth Forest Service Remote Sensing Applications Conference [CD-ROM], April 10-14, 2000, Albuquerque, NM. American Society of Photogrammetry and Remote Sensing, Bethesda, MD.

Whitman, A.A., and Hagan, J.M. 2007. An index to identify late-successional forest in temperate and boreal zones. Forest Ecology and Management 246: (144-154).

Wilson, E.H., Sader, S.A., 2002. Detection of forest harvest type using multiple dates of Landsat TM imagery. Remote Sensing of Environment 80: 385–396.

Woodcock, C. E., Collins, J. B., Gopal, S., Jakabhazy, V. D., Li, X., Macomber, S. A., et al. (1994). Mapping forest vegetation using Landsat TM imagery and a canopy reflectance model. Remote Sensing of Environment 50: 240−254.

Wulder, M.A, Niemann, K. O., & Goodenough, D. (2000). Local maximum filtering for the extraction of tree locations and basal area from high spatial resolution imagery. Remote Sensing of Environment 73: 103−111.

Wulder, M.A., White, J.C., Andrew, M.E, Seitz, N.E., Coops, N.C. 2009. Forest fragmentation, structure, and age characteristics as a legacy of forest management. Forest Ecology and Management 258: 1938–1949.

Yahner, R.H. 1988. Changes in wildlife communities near edges. Conservation Biology 2: 333-339.

APPENDIX A: DEFINITIONS OF FRAGMENTATION METRICS

Below are definitions for all metrics used in fragmentation analysis (Table 1.1). Definitions are from McGarigal et al. (2002).

Area/Density/Edge Metrics:

Area-weighted mean patch size (AREA_AM): AM (area-weighted mean) equals the sum, across all patches of the corresponding patch type, of the corresponding patch metric value multiplied by the proportional abundance of the patch [i.e., patch area (m^2) divided by the sum of patch areas]. The *area* of each patch comprising a landscape mosaic is perhaps the single most important and useful piece of information contained in the landscape. Not only is this information the basis for many of the patch, class, and landscape indices, but patch area has a great deal of ecological utility in its own right. Note that the choice of the 4-neighbor or 8-neighbor rule for delineating patches will have an impact on this metric. Also calculated as standard deviation of patch area (AREA_SD).

Patch Density (PD): the number of patches of the corresponding patch type divided by total landscape area (any internal background present). *Patch density* is a limited, but fundamental, aspect of landscape pattern. Patch density has the same basic utility as number of patches as an index, except that it expresses number of patches on a per unit area basis that facilitates comparisons among landscapes of varying size. Of course, if total landscape area is held constant, then patch density and number of patches convey the same information. Like number of patches, patch density often has limited interpretive value by itself because it conveys no information about the sizes and spatial distribution of patches. Note that the choice of the 4-neighbor or 8-neighbor rule for delineating patches will have an impact on this metric.

Edge Density (ED): the sum of the lengths of all edge segments involving the corresponding patch type divided by the total landscape area. User specifies proportion of internal background edge segments and landscape boundary segments (if not provided by presence of a landscape border) involving the corresponding patch type. *Edge density* at the class level has the same utility and limitations as Total Edge (see Total Edge description), except that edge density reports edge length on a per unit area basis that facilitates comparison among landscapes of varying size. *Total edge* at the class level is an absolute measure of total edge length of a particular patch type. However, when comparing landscapes of identical size, total edge and edge density are completely redundant.

Perimeter (PERIM): Patch *perimeter* is another fundamental piece of information available about a landscape and is the basis for many class and landscape metrics. Specifically, the perimeter of a patch is treated as an edge, and the intensity and distribution of edges constitutes a major aspect of landscape pattern. In addition, the relationship between patch perimeter and patch area is the basis for most shape indices.

Radius of gyration (GYRATE): GYRATE equals the mean distance (m) between each cell in the patch and the patch centroid. GYRATE = 0 when the patch consists of a single cell and increases without limit as the patch increases in extent (no limit on max value). GYRATE achieves its maximum value when the patch comprises the entire landscape.

Radius of gyration is a measure of patch extent; thus it is affected by both patch size and patch compaction. Calculated as area-weighted mean of radius of gyration (GYRATE_AM) and standard deviation of radius of gyration (GYRATE_SD).

Percentage of Landscape (PLAND): *Percentage of landscape* quantifies the proportional abundance of each patch type in the landscape. Like total class area, it is a measure of landscape composition important in many ecological applications. However, because PLAND is a relative measure, it may be a more appropriate measure of landscape composition than class area for comparing among landscapes of varying sizes.

Largest Patch Index (LPI): *Largest patch index* at the class level quantifies the percentage of total landscape area comprised by the largest patch. As such, it is a simple measure of dominance.

Shape Metrics:

Perimeter/Area Ratio (PARA): PARA equals the ratio of the patch perimeter (m) to area (m^2). *Perimeter-area ratio* is a simple measure of shape complexity, but without standardization to a simple Euclidean shape (e.g., square). A problem with this metric as a shape index is that it varies with the size of the patch. For example, holding shape constant, an increase in patch size will cause a decrease in the perimeter-area ratio. Range includes all numbers greater than 0. Calculated as standard deviation of perimeter-area ratio (PARA_SD) and perimeter-area ratio coefficient of variation (PARA_CV).

Fractal Dimension Index (FRAC): Corrects for raster bias in perimeter. A fractal dimension greater than 1 for a 2-dimensional patch indicates a departure from Euclidean geometry (i.e., an increase in shape complexity). FRAC approaches 1 for shapes with very simple perimeters such as squares, and approaches 2 for shapes with highly convoluted, plane-filling perimeters. *Fractal dimension index* is appealing because it reflects shape complexity across a range of spatial scales (patch sizes). Thus, like the shape index (SHAPE), it overcomes one of the major limitations of the straight perimeter-area ratio as a measure of shape complexity. Calculated as standard deviation of fractal dimension index (FRAC_SD) and fractal dimension index coefficient of variation (FRAC_CV).

Isolation/Proximity Metrics:

Euclidean Nearest Neighbor Distance (ENN): the distance to the nearest neighboring patch of the same type based on shortest edge to edge distance (cell center to cell center). *Euclidean nearest-neighbor distance* is perhaps the simplest measure of patch context and has been used extensively to quantify patch isolation. Here, nearest neighbor distance is defined using simple Euclidean geometry as the shortest straight-line distance between the focal patch and its nearest neighbor of the same class. This is difficult to interpret if landscape boundaries are present—within the landscape being analyzed, the nearest patch may be far away by ENN, but on the ground there may be a closer patch over the boundary.

Core Area Metrics:

Core area (CORE): the area within the patch that is further than the specified depth-of-edge distance from the patch perimeter. User can specify one fixed length for all patch types or provide a txt file with individual lengths between different types of patches. Calculated as area-weighted mean of core area (CORE_AM), standard deviation of core area (CORE_SD), and core area coefficient of variation (CORE_CV).

Core Area Percentage of Landscape: self explanatory; see PLAND above.

Core Area Index (CAI): *Core area index* is a relative index that quantifies core area as a percentage of patch area (i.e., the percentage of the patch that is comprised of core area). Calculated as standard deviation of core area index (CAI_SD).

Number of DCAs: *Number of disjunct core areas* is aggregated (summed) over all patches of the corresponding patch type. Number of disjunct core areas is an alternative to the number of patches when it makes sense to treat the core areas as functionally distinct patches.

Disjunct Core Area Density (DCAD): *Disjunct core area density*, like its counterpart, patch density (PD), expresses number of disjunct core areas on a per unit area basis that facilitates comparisons among landscapes of varying size. Of course, if total core area is held constant, then disjunct core area density and number of disjunct core areas convey the same information.

Interspersion/Contagion Metrics: These explain how the different patch types are distributed throughout the landscape. The three suggested are all subdivision metrics from Jaeger (2000).

Clumpiness Index (CLUMPY): Given any P_i , CLUMPY equals -1 when the focal patch type is maximally disaggregated; CLUMPY equals 0 when the focal patch type is distributed randomly, and approaches 1 when the patch type is maximally aggregated. *Clumpiness index* is calculated from the adjacency matrix, which shows the frequency with which different pairs of patch types (including like adjacencies between the same patch type) appear side-by-side on the map

Landscape Division Index (DIVISION: *Division* is based on the cumulative patch area distribution and is interpreted as the probability that two randomly chosen pixels in the landscape are not situated in the same patch. Note, DIVISION is redundant with effective mesh size (MESH), i.e., they are perfectly, but inversely, correlated, but both metrics are included because of differences in units and interpretation. DIVISION is interpreted as a probability, whereas MESH is given as an area.

Splitting Index (SPLIT): the total landscape area squared divided by the sum of patch area squared, summed across all patches in the landscape. *Split* is based on the cumulative patch area distribution and is interpreted as the effective mesh number, or number of patches with a constant patch size when the landscape is subdivided into S patches, where S is the value of the splitting index.

Effective Mesh Size (MESH): *Mesh* is based on the cumulative patch area distribution and is interpreted as the size of the patches when the landscape is subdivided into S patches, where S is the value of the splitting index. Note the similarity between MESH and area-weight mean patch size (AREA_AM). Conceptually and computationally, these two metrics are almost identical at the landscape level, and under most circumstances will return identical values. Specifically, AREA_AM gives the area-weight mean patch size, where the proportional area of each patch is based on total landscape area *excluding* any background (i.e., background is excluded from the total landscape area). MESH also gives the area-weighted mean patch size, but the proportional area of each patch is based on the total landscape area *including* any background. Thus, if there is no internal background, these metrics will return identical values.

BIOGRAPHY OF THE AUTHOR

Brianne Looze was born in Menomonie, Wisconsin on June 25, 1987. She was raised in La Crosse, WI with her six younger siblings. She knew she wanted to study forestry at 13 when she looked out over a mass expanse of the Black River State Forest in central Wisconsin and saw nothing but trees. She attended the University of Wisconsin-Superior on a full academic scholarship and earned her Bachelor of Science degree in Biology with a minor in Geographic Information Systems in 2009.

Brianne chose The University of Maine for her graduate studies because of Maine's vitally important forest legacy. Studying the forest via satellite imagery for three years sparked interests in land conservation and landscape ecology. She will begin a PhD program in Landscape Ecology at The University of Maine in September 2012, where she will study the landscape-level conditions of wild blueberry patches in Maine and their effects on native pollinators. Upon moving to Maine, Brianne's interests in hiking and cooking were renewed with vigor. Hiking allowed her to explore all parts of Maine in good weather, cooking kept her occupied inside when the weather was poor. She makes a really good Maine wild blueberry pie.

Brianne is a candidate for the Master of Science degree in Forest Resources from The University of Maine in May, 2012.